RICE UNIVERSITY

Improved Understanding of Apoptosis and Metabolism in Chinese Hamster Ovary Cell Culture

by

Ruiqiang Sun

A THESIS SUBMITTED
IN PARTIAL FULFILLMENT OF THE
REQUIREMENTS FOR THE DEGREE

Master of Science

APPROVED, THESIS COMMITTEE

Ramon Gonzalez, Chair
Willian W. Akers Assistant Professor
inChemical and Biomolecular Engineering

Laura Segatori
T.N. Law Assistant Professor in Chemical
and Biomolecular Engineering

Ka-Yiu San
E. Dell Butcher Professor in
Bioengineering

HOUSTON, TEXAS
April 2011

Abstract

Improved Understanding of Apoptosis and Metabolism in Chinese Hamster Ovary Cell Culture

by

Ruiqiang

Mammalian cell culture has gained importance in biotechnology for the development of therapeutic and diagnostic agents. Among them, Chinese hamster ovary (CHO) cells are regarded as the mammalian cell "workhorse". The use of CHO cell line for the production of recombinant proteins used in human therapy has reached a level of industrial production. However, a major problem encountered in *in vitro* cultures is cell death via apoptosis. Since apoptosis leads to the loss of viability of mammalian cells *in vitro*, especially in serum-free media. This is important and necessary to prevent the activation of apoptosis cascade and increase their cell viability and enhance their cellular robustness. The overall goal of this study is to improve our understanding of the cellular and physiological determinants of apoptosis and its relationship with other cellular functions.

Apoptosis is a result of a very complex network of signaling pathways triggered from both inside and outside of the cell and a highly regulated pathway by both pro-apoptotic and anti-apoptotic proteins that promote cell survival or cell death. Although many causes of apoptotic process in mammalian cell cultures had been researched in the past and have been discussed in recent years, a lot need to be explored. In order to bring novel strategies to understand apoptosis in mammalian cell cultures, our study was not only focused on the apoptotic pathway but also expand to metabolic network to set up a link between cell growth and apoptosis. In our project, we applied systems biology methods in a mammalian cell line (CHO TF 70R), to understand the relationship between cellular metabolism and apoptosis in

a typical serum free culture medium. After establishing the basic culture platform, the effects of culture conditions on initiating apoptosis will be evaluated. Healthy and apoptotic cell samples were identified and isolated using Fluorescence Activated Cell Sorting (FACS) and Magnetic Activated Cell Sorting (MACS), respectively. A comprehensive study of CHO cellular metabolism was made using a metabolic flux network to compare and analyze by metabolic flux analysis (MFA) to get more information on cell metabolism and apoptotic behavior. Furthermore, 2-NBDG combined with Annexin V-PE was also successfully applied to estimate the glucose uptake rate in real early apoptotic cells.

In summary, we used the integration of the data generated by MFA to understand apoptotic behavior and establish a correlation between cell regulation and apoptosis. It will help us to identify the changes during the onset of apoptosis process will be studied by using proteomics tools to analyze the protein up-regulation or down-regulation in different cell status in the future.

Acknowledgments

I wish to thank my advisor, Dr. Ramon Gonzalez for his intellectual support, encouragement and advice on my research. I would also like to thank Dr. Laura Segatori and Dr. Ka-Yiu San for agreeing to participate on my thesis committee and providing me with their valuable advice.

I want to thank Dr. Claudia Altamirano group, our collaborative group, from Escuela de Ingeniería Bioquímica, Pontificia Universidad Católica de Valparaíso at Chile for their kind assistance on cell line and technique help during this work. I would specially like to thank Dr. Julio Berrios and Silvana Becerra for their training and discussions.

I would like to thank Dr. Qin Sun in Medical Genetics Laboratory at Baylor College of Medical for his help of amino acid analysis.

I would also like to acknowledge our group members: Venetia Rigou, Yandi Dharmadi, Abhishek Murarka, Ashutosh Gupta, Guyton Durnin, Clementina Dellomonaco, James Clomburg, John Park, Maria Rodriguez-Moya, Anagela Cintolesi, Dr. Syed Shams Yazdani, Dr. Suman Mazumdar, Dr. M. Blankschien, and Dr. Elliot Miller for their assistance and help during these years. I would specially like to thank Dr. Suman Mazumdar for his suggestions and discussions.

Finally, I want to thank my family and friends for the understanding and support which makes me this far. Their support and love are always encouraging me, no matter where I am.

Contents

Abstract ii

Acknowledgments iv

Contents v

List of Figures viii

List of Tables x

Introduction 1

1.1. Motivation 1

1.2. Thesis Organization 4

Literature Review 6

2.1. Mammalian Cell Culture Technology 6

2.2. Metabolism of Mammalian Cell Lines 8

2.2.1. Energy source metabolism 11

2.2.1.1. Glucose Metabolism 11

2.2.1.2. Glutamine/glutamate metabolism 13

2.2.1.3. The metabolism of other amino acids 15

2.2.1.4. Effect of lactate and ammonium in Mammalian cell Metabolism 16

2.3. Apoptosis in Mammalian Cell Culture 18

2.3.1. Apoptotic pathways 20

2.3.2. Apoptosis vs. Necrosis 22

2.3.3. Apoptosis in Mammalian Cell 24

2.3.4. Methods for apoptosis inhibition 27

2.3.4.1. Media supplementation 27

2.3.4.2. Genetic strategies 30

2.3.5. Methods of apoptosis Detection 31

2.4. Cell Separation 37

2.4.1. Aqueous Two Phase Systems (ATPSs) 39

2.4.2. Magnetic Activated Cell Sorting (MACS) 41

2.5. Metabolic Flux Analysis of Mammalian Cells 43

2.5.1. Introduction 43

2.5.2. c-MFA 44
2.5.3. Identifiability of fluxes 46
2.5.4. Consistency of data 47
2.5.5. Sensitivity Analysis 48
Materials and Methods 49
3.1. Cell Culture 49
3.2. Analytical Methods 50
3.2.1. Determination of Cell Density and Viability 50
3.2.2. Metabolite determinations 52
3.2.2.1. Analysis of sample composition using HPLC 52
3.2.3. Protein sample preparation 53
3.3. Quantification of Apoptosis 54
3.3.1. Imaging study 54
3.3.2. FACS analysis 55
3.4. Cell Separation 55
3.4.1. Aqueous Two-Phase Partition System (ATPS) 55
3.4.2. Magnetic Associated Cell Sorting (MACS) 56
3.4.3. Ficoll gradient centrifugation 56
3.5. Metabolic Flux Analysis 57
Investigation into Cell Growth and Apoptosis 58
4.1. Introduction 58
4.2. Results 60
4.2.1. Investigation into Cell Growth Characteristics 60
4.2.2. Fluorescence Image 65
4.3. Discussion 68
Apoptotic and Non-apoptotic Cell Partition 71
5.1. Introduction 71
5.2. Results 74
5.2.1. Effect of concentration of binding beads 74
5.2.2. Separation performance in different cell status 77
5.2.3. Effect of mobile phase on cell separation 80

5.2.4. Comparison of MACS and other separation methods 82
5.2.4.1. ATPSs 83
5.2.4.2. Ficoll gradient centrifugation 84
5.3. Discussion 85
Estimation of Specific Glucose Uptake Rates in Early-apoptotic State in Culture of CHO Cells 88
6.1. Introduction 88
6.2. Theory 90
6.3. Results 91
6.3.1. Effect of 2-NBDG incubation time on MFI 91
6.3.2. Fluorescent density (D) has a linear relationship with the intracellular concentration of 2-NBDG 93
6.3.3. Development of an assay to measure glucose uptake rates of healthy and apoptotic cells simultaneously 94
6.4. Discussion 97
MFA of CHO Cells Metabolism in the Apoptotic and Healthy Phase 99
7.1. Introduction 99
7.2. Results 103
7.2.1. Metabolic investigations on CHO cells between healthy and early apoptotic cells 103
7.3. Discussion 113
Conclusions and Future Work 117
References 2
Appendix A. Model Development for Flux Analysis 20
Appendix B Biomass Composition 27

List of Figures

Figure 1The demand for mammalian cell culture products[5] **2**

Figure 2.Central Metabolism of Mammalian Cells **9**

Figure 3 Interaction of the metabolism of the amino acids in central metabolism **16**

Figure 4 an overview of the intrinsic and extrinsic pathways[42] **20**

Figure 5 the process of Apoptosis and necrosis. Apoptosis includes cellular shrinking, chromatin condensation and margination at the nuclear periphery with the eventual formation of membrane-bound apoptotic bodies that contain organelles, cytosol and nuclear fragments and are phagocytosed without triggering inflammatory processes. The necrotic cell swells, becomes leaky and finally is disrupted and releases its contents into the surrounding tissue resulting in inflammation. Modified from [32] **23**

Figure 6 Healthy and apoptotic CHO cells stained with acridine orange and ethidium bromide[16] **25**

Figure 7 Schematic representation of the loss of membrane lipid asymmetry during apoptosis[79] **35**

Figure 8 Bivariate PI/Annexin V analysis of rat thymocyte cells. Region R1 contains viable cell population (Annexin V-/PI-), R2 contains the early apoptotic cells (Annexin V+/PI-), R3 contains late apoptotic cells (Annexin V+/PI+) and R4 is necrotic cells (Annexin V-/PI+)[79] **36**

Figure 9 TUNEL staining of formalin fixed, paraffin embedded skin. Note nuclear staining of apoptosis cells (green). Counterstain-PI (red) **37**

Figure 10 Schematic flowchart of MACS using MicroBeads, MACS columns, and MACS separators. A mixture of magnetically labeled and unlabeled cells is loaded onto a ferromagnetic matrix. Magnetized cells are retained on the column while unlabeled cells pass through. Labeled cells are recovered after demagnetization of the column. **42**

Figure 11 Time courses of viable and dead cell number in batch culture **61**

Figure 12 Time courses of early and dead late apoptotic ratios in batch culture 62

Figure 13 Specific apoptotic rates as a function of time. Exponetial prediction (-) compared to experimental data for early apoptotic cells (A) and late apoptotic cells (B) 64

Figure 14 Imaging of viable, early and late apoptotic cells stained with Annexin V-FITC and PI under 40× objective (fluorescent images were enhanced by Adobe Photoshop CS software) 67

Figure 15 MACS separation performance in different labeling bead concentrations for samples from stationary phase. 75

Figure 16 MACS separation performance in different labeling bead concentrations for samples from exponential growth phase (apoptotic deletion only) 76

Figure 17 MACS results 79

Figure 18 flow cytometry analysis after MACS separation using two different mobile phases. (a) unlabeled partition, (b) labeled partition 81

Figure 19 Time course of 2-NBDG uptake by CHO cells at various treatments 92

Figure 20 Lineweaver-Burk plots of 1[A] against 1rA 94

Figure 21 FACS dot plots staining with 2-NBDG and Annexin V-PE..... 95

Figure 22 Time course of glucose uptake rates for healthy cells (A) and early apoptotic cells (B) 96

Figure 23 MFA Model A) Glucose metabolism and B) Amino acid metabolism 103

Figure 24 Profiles of glucose consumption and lactate formation 105

Figure 25 Comparison of flux trends in (A) healthy cells (B) early apoptotic cells 114

List of Tables

Table 1 Effects of lactate concentrations on cell growth at constant pH 16

Table 2 Effect of ammonium on cell growth and productivity 18

Table 3 Differential features and significance of apoptosis and necrosis 23

Table 4 Media supplementation in multiple cells 27

Table 5 Methods for Detection of Apoptosis 31

Table 6 Methods of cell separation 37

Table 7 separation results of density gradient centrifugation under different treatment 84

Table 8 Calculated specific uptake rates in healthy and early apoptotic cells 107

Table 9 Calculated intracellular fluxes via c-MFA 108

Table 10 distribution of metabolic fluxes around pyruvate and glutamate-- α-ketoglutarate 111

Table 11 extracellular fluxes (normalized to glutamate uptake, mol/mol glutamate) 113

Introduction

Although mammalian cell lines are important hosts for the production of biopharmaceuticals, they have met some severe problems in bioreactors, especially cell death during culture processing is an inherent problem in current high density, serum free mammalian cell culture. Our work focuses on mammalian cell culture, specifically on addressing issues arising from their culture in bioreactors. A mass of research has been conducted in this area. In this chapter, we briefly introduce the basic research motivation, project proposal goals and the outline of the thesis.

1.1. Motivation

Mammalian cells are widely used in the manufacturing of therapeutic proteins: human and veterinary vaccines, interferon, monoclonal antibodies and genetically engineered products[1] Mammalian cell cultures were developed just a century ago by embryologists Ross Harrison[2] , who published his findings on the growth of frog embryo nerve fibers in *vitro*. Since the first trial for human viral vaccines in the 1950s, mammalian cell culture has been accelerated to develop and become a mature technology with rapid expansion. *Escherichia coli* and mammalian

cell lines are the workhorses of biopharmaceutical production. Although mammalian cell cultures are more technically complex, slow, and expensive compared to *E. coli* cultures, they satisfy the requirement of post translational modification of proteins for full bioactivity and native conformation. Thus, since the first human therapeutic protein, recombinant insulin, was licensed in 1982, more and more biopharmaceutical proteins produced form mammalian cell culture have been approved[3]. By 2003, 17 of the 32 therapeutic proteins approved are produced by mammalian cell lines. Recently, the number of approved biopharmaceutical by *E. coli* has decreased, which leads to the trend that the rate of biopharmaceutical approval has leveled off, while the approved proteins produced by mammalian cell increased, which bodes well for the future[4]. Figure.1 shows the increase in the amount of biopharmaceuticals approved from mammalian cell culture from 1986 to 2006. Starting in 2000, there has been a substantial increase in the manufacturing capacity to satisfy the demand[5].

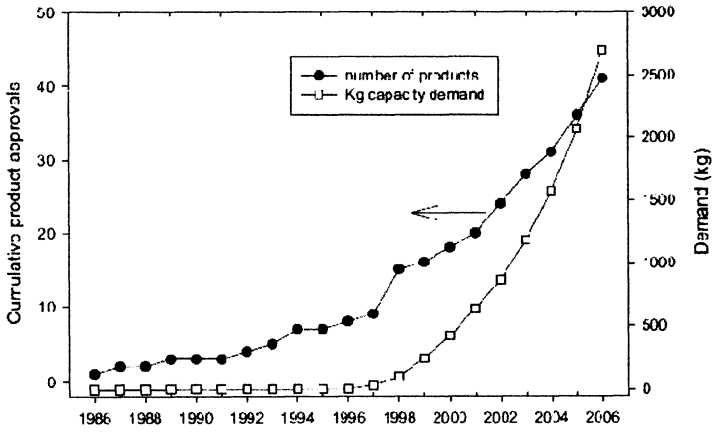

Figure 1The demand for mammalian cell culture products[5]

CHO cell lines, which were first isolated by Puck et al. in University of Colorado Medical Center in 1957 [6], have been extensively used in the production of antibodies and recombinant glycoproteins such as Tissue Plasminogen Activator(tPA), Erythropioetin(EPO), factor III and Interferon- ɣ (IFN- ɣ)[7]. Since they can be adapted to suspension culture in serum free media, which satisfies the requirement of modern industry and of stringent safety, CHO cell lines have become the most important mammalian cell. Based on the data collected by/from several sources (http://www.fda.gov, http://www.eudra.org/en_home.htm, http://www.phrma.org) [4], 24 biopharmaceuticals produced by CHO cells have approved in US or Europe since 1987, the time at which the first tPA produced in CHO cells was approved in US.

However, a major problem faced by *in vitro* mammalian cell culture is cell death, which is caused by various factors. Apoptosis – programmed cell death – is a mode of cell death essential to the homeostasis of multi-cellular organisms and has been shown to occur in cultured mammalian cells. Apoptosis is frequently a barrier to maintaining viability and high cell densities. However, most mammalian cell death in culture has been attributed to apoptosis. Strategies to prevent apoptosis in mammalian cell culture can be broadly placed into two methods: manipulation of the culture environment or genetic manipulation Given that the onset of apoptosis is often triggered by conditions outside of the cells, one important strategy to inhibit cell death is to alter the physicochemical environment[8]. Nutrient feeding provides a potential solution for enhancements of culture longevity to inhibit apoptosis. On the other hand, from the point of view of preventing the apoptotic signaling cascade

from within the cell, chemical and genetic strategies are also used as effective methods. Chemical strategies targeting caspases, the downstream effectors of apoptosis, prevent these proteins from executing the cell death program and lead to sustained viability in mammalian cell bioreactors[9] Genetic strategies have also targeted caspases. The exogenous expression of gene effectively suppresses apoptotic signaling, limits cell death and maintains viability, such as Bcl-2 and Bcl-x_L preventing the release of cytochrome c from the mitochondria [10]. In some sense, the most successful strategy will consider both metabolic engineering techniques and media formulations in combination with current bioreactor technology.

The objective of this thesis is to develop methods for quantitative physiological studies for CHO cells in apoptotic process. In this regard, it is important to adopt and modify current methods and ideas in mammalian cell culture, and relevant biotechniques to achieve an improved understanding of apoptosis.

1.2. Thesis Organization

The thesis is organized into three major parts as follows:

1. Quantitative characterization of defined apoptotic and healthy behaviors in a CHO cell. Cell heterogeneity almost undoubtedly exists within cell culture system. Quantitative characterization of apoptotic and healthy cells during cell culture was used to understand cultured mammalian cell behavior with respect to metabolic flux distribution, population survival heterogeneity and cell death. This

included using cell separation techniques such as FACS and fluorescence imaging technique to observe and detect apoptosis in CHO cell cultures.

2. Experimental investigation and validation of healthy and apoptotic models in a "natural culture". This work is divided into two main parts: analysis of metabolites and metabolic flux analysis (MFA). The conventional experimental approaches entail the genetic and biochemical techniques to detect the activities of postulated metabolic events in apoptotic and healthy status to monitor the physiological states in combination with other parameters. The impact of specific metabolic pathways of key metabolites was evaluated via MFA to show the significant difference between healthy and apoptotic cells under a certain cultured condition.

Chapter 2

Literature Review

In this chapter, an overview of research system and tools is given. We briefly introduce mammalian cell culture and its metabolic behavior, apoptosis *in vitro,* cell separation technology, and metabolic flux analysis.

2.1. Mammalian Cell Culture Technology

Although prokaryotic cells are ideal host for expression of proteins because of their simplicity, ease of genetic manipulation and rapid growth, the synthesis of eukaryotic proteins presents a significant challenge due to their inability to carry out necessary post-translational modifications such as glycosylation and phosphorylation. In comparison to bacteria, mammalian cells are much more complex in structure and components and have more biological functionality[11] . That is why they have long been used as the hosts for production of glycosylated therapeutic proteins that require precise post translational modification in order to

support their biological function. Then continuous cell lines, such as Chinese hamster ovary, CHO, baby hamster kidney, BHK, myeloma cells, NS0 and SP2/0, and human embryo kidney, HEK-293, were obtained and approved by regulatory agencies for industrial manufacture. Of these, CHO cells are a popular host for the production of recombinant proteins. CHO cell was first isolated in 1958 by Puck[6]. Since that time, cell cells have been widely used for producing recombinant proteins and many glycoprotein productions in CHO cells are approved. CHO cells provide an efficient host for the reliable synthesis and the expression of recombinant proteins including: tPA[12], EPO[13], Factor VIII[14], human growth hormone (hGH), humanized antibody (hAb), erythroid differentiation factor (EDF)[15]

Mammalian cell culture is a hybrid technology that combines many different disciplines such as biochemistry, cell biology, genetic engineering, protein chemistry and chemical engineering. It is a technology that has been applied to produce biopharmaceuticals. It has been developed during the last three decades and become an essential part of biotechnology. Medicines from mammalian cell culture focus on the use of cell culture to produce human and veterinary vaccines, interferon, monoclonal antibodies and genetically engineered products. Most of these cell lines can be cultured in suspension culture as opposed to an anchorage-dependent mode, make large scale cultivation achievable in sparged, stirred tank bioreactors.

A typical upstream cell culture process development can be described as following. First, a number of high-producing cell clones are obtained by state-of-the-

art transfection, amplification, and selection methods. Then cell culture medium is customized to support the growth of various cell clones. The medium normally contains more than 60 synthetic ingredients with well-defined concentrations, including carbon sources, amino acids, salts, vitamins, lipids, growth factors, and buffers. Because of the disadvantages of batch variation and vulnerability to contamination, serum and other animal components are required to be eliminated from medium formulation. Finally, bioreactor operation parameters are optimized in order to achieve consistent product quality and high protein expression level. Small scale bioreactors are used to determine acceptable range of pH, DO, temperature, and inoculation density. Then the cell culture process is scaled-up to production levels of 20,000 L, or greater. Overall, the improvement of host cell line engineering, media optimization, and bioreactor operation in last two decades resulted in a dramatic increase of product titer to the range of grams per liter.

2.2. Metabolism of Mammalian Cell Lines

Mammalian cell lines are used to produce therapeutic proteins, so the characterization and understanding of their basic metabolism are needed to improve cell lines' performance in culture systems. Metabolic profile is the simultaneous assessment among major metabolic pathways of macromolecule synthesis and energy production under growth phases and physiological conditions. Metabolic pathways of central importance include glycolysis, tricarboxylic acid (TCA) cycle, pentose phosphate pathway (PPP), oxidative phosphorylation,

glutaminolysis, the metabolism of other amino acids and biosynthetic pathways.[7]

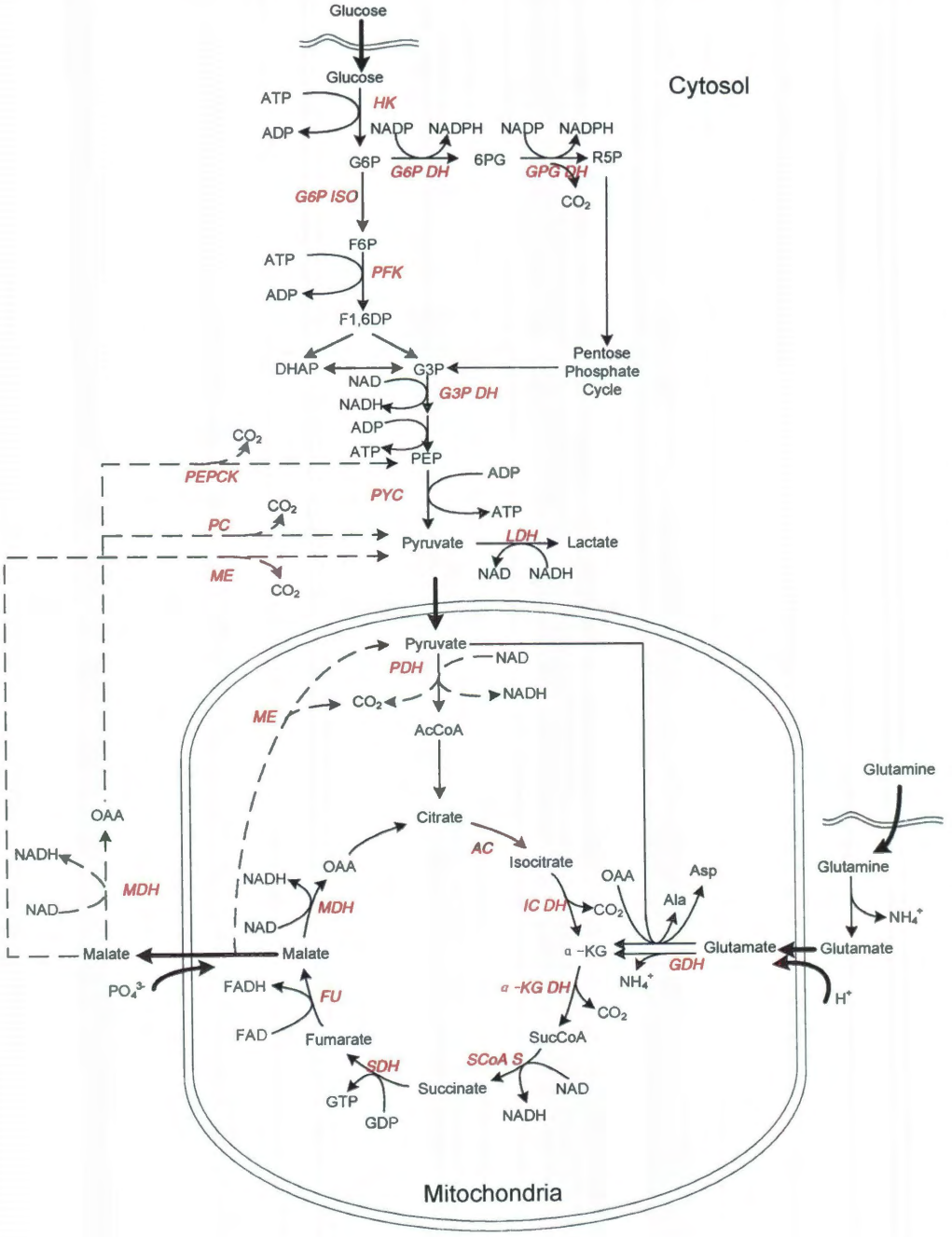

Figure 2.Central Metabolism of Mammalian Cells

Figure 2 shows the outline of important pathways for mammalian cell metabolism. The central metabolic pathways are of key importance from the perspective of metabolic engineering because they are including common pathways from which fluxes are distributed to different branches. In these pathways, carbon sources are catabolized to produce energy, reducing equivalents and the precursors for biosynthesis. Since central metabolic pathways are very import points of intervention, in this study the focus is on these parts. In contrast to bacterial and plant cells, mammalian cell lines cultured *in vitro* exhibit a highly deregulated metabolism in central metabolic pathways, which is characterized by a very high and inefficient consumption of the main energy sources, leading to the accumulation of lactate and ammonium ions in the culture media. From the analysis of glucose and glutamine utilization, products rates and glycolytic flux and measurement of the maximal activities of some key enzymes of glycolysis, glutaminolysis and TCA cycle, most of glucose, about 70% to 99.8% [16], was found to be oxidized to pyruvate and finally to lactate. This causes acidification of cell medium. And it is show a very low flux of glucose via TCA cycle and no or very low activities of the key enzymes connecting glycolysis with the TCA cycle [1, 17]. However, in general, an active TCA cycle is prerequisite for efficient growth. Thus, to satisfy the energy requirements, mammalian cells consume more glutamine, which will lead to the generation of more ammonia. So in this case, glutamine or glutamate is also the main energy source in mammalian cells. Thus glutamine or glutamate oxidation drives carbon entering TCA cycle through glutaminolysis.

2.2.1. Energy source metabolism

Glucose and glutamine are the main compounds. The significant point is the metabolism of glucose and glutamine generate more lactate and ammonium. Figure 2 shows metabolic energy network of glucose and glutamine degradation, which include glycolysis, TCA cycle and glutaminolysis. Arrows with dashed line indicate that the respective metabolic pathway does not exist or its activity is very low in cultured mammalian cells.

2.2.1.1. Glucose Metabolism

The first step in metabolism of a substrate is its transport across the cell membrane. The cytoplasmatic membrane is impermeable to polar molecules such as glucose, and the uptake of glucose through membrane is the work of the transport proteins located in the plasmatic membrane. Most researches were focused on glucose transport. Several kinds of factors control this system. A family of related proteins is responsible for this transport activity in mammalian cells such as GLUT 1 and GLUT 4 glucose transporters[18]. In addition to the facilitated diffusion by GLUT series, glucose transfer can also happen through sodium symport process [19]. After the substrate is transported into the cell, it is fed to the bioreaction network.

Once entering the cytosol, glucose will be converted by two main pathways: glycolysis and PPP. Once glucose is phosphorylated by hexokinase, glucose 6-phosphate (G6P) is formed. There are two enzymes determining the pathways of

G6P, G6P isomerase and G6P dehydrogenase. G6P isomerase channels G6P to glycolysis and G6P dehydrogenase to PPP. In glycolysis, G6P is converted to pyruvate, generating a lot of intermediates for biosynthesis, two ATP and two NADH. However, glycolysis is deregulated in cultured mammalian cells, which is highly linked to the generation of large amount of lactate that we have mentioned ahead, that indicates that a low percentage of pyruvate is incorporated into the TCA cycle. This is because of the lack of these specific enzyme activities, such as pyruvate dehydrogenase complex (PDHC), phosphoenolpyruvate carboxykinase (PEPCK) or pyruvate carboxylase (PC), directly causing this imbalance rate between glycolysis and TCA cycle. Other biosynthesis precursors provided by glycolysis pathways are: fructose 6-phosphate (F6P) for the synthesis of amino sugars; dihydroxyacetone phosphate (DHAP) for lipid synthesis; and glycerate 3-phosphate, precursor for synthesis of serine and glycine[7].

As discussed previously, low level glucose is transferred into TCA cycle. However, TCA cycle is still a major pathway in the central metabolism, which provides metabolic energy and biosynthesis precursors. The TCA cycle is directly relevant to metabolic energy generation in the form of ATP based on the respiratory system. It is also very important to balance the rate of glycolysis and glutaminolysis [7]. The pyruvate node is the juncture between glycolysis and TCA cycle. Pyruvate is first transported into the mitochondria and further dissimilated into Acetyl coenzyme A (AcCoA). In mammalian cells, some enzymes lacking activities are just in this node, which directly causes an imbalance between glycolysis and TCA cycle and leads to ample lactate. Paredes *et al* analyzed the flux from pyruvate to AcCoA

through PDHC in a hybridoma cell line, the values was less than 1% [20-21] AcCoA enters the cycle reacting with oxaloacetate to form citrate. Citrate then undergoes a series of reaction to generate CO_2, NADPH and α-ketoglutarate in this cycle. However, at this point, a flux of citrate leaves the TCA cycle and is exported to cytosol for lipid formation[7]. Thus, both the low incorporation of AcCoA into TCA cycle and the outflow of citrate towards lipid reduce the flux in the TCA cycle. So in order fulfill the energy generation, glutamine becomes the replenisher at the point of α-ketoglutarate. Mancuso A *et al* found that the flux from citrate to α-ketoglutarate was only about 10% of the flux through citrate synthase in hybridoma cells[22]. Because of the high uptake of glutamine and the anaplerotic reaction of α-ketoglutarate, the flux from succinate to malate is higher than the flux from oxaloacetate to citrate. Thus extra malate leaves TCA cycle and further is converted to pyruvate via malate shunt[7].

2.2.1.2. Glutamine/glutamate metabolism

Glutamine/glutamate is the second major component and the source of most of the ammonium generated. In addition to the important role as an energy source via TCA replenishment as mentioned previously, glutamine is also a nitrogen source for first use in synthesis of prydine, purine, amino sugars, NAD and asparagines, and also second necessary for the synthesis of praline and ornithine[7].

Glutamine or glutamate transport is through principal amino acid transport systems, just as many other amino acids' movements to cell membrane. Na^+ dependent and Na^+ independent appear to mediate amino acid uptake[23]. In Na^+

dependent system, glutamine or glutamate is cotransported with Na^+ against their concentration gradient by Na^+/K^+-ATPase[7]. In Na^+ independent system, it facilitates the selective movement of amino acids across the membrane by catalyzing exchange rather than net uptake[23]. In addition to the transport from media to cytosol, transport mechanism around the mitochondria is very important, since most of the glutamine metabolism inside of the mitochondria. An important enzyme, phosphate activated glutaminase (PAG) is located either in the mitochondrial membrane or matrix. It can cause the deamination of glutamine to form glutamate, which can be transported into the mitochondria by glutamate-aspartate exchanger or the proton symport system[7].

Once glutamate is transported, its fate is determined by glutamate dehydrogenase (GDH) or transaminases. GDH deaminates glutamate to α–ketoglutarate and channels it towards TCA cycle. Transaminases, such as alaTA and aspTA channel glutamate towards transamination (TA) reactions. The role of glutamine metabolism in the generation of oxaloacetate has been highlighted previously, since the anaplerotic reaction of TCA cycle. In this cycle, it can be completely oxidized to CO_2, for energetic yield (up to 27 ATP per glutamine)[7]. In TA pathway, glutamate reacts with oxaloacetate to form aspartate or with pyruvate to form alanine, while glutamate itself is also converted into α–ketoglutarate. Aspartate and alanine can be further converted into purine, pyrimidine and asparagine. So the released ammonium from glutamate to α–ketoglutarate is

transferred. Thus the TA pathways balance ammonium overflow due to the rapid glutamine consumption in mammalian cell culture.

2.2.1.3. The metabolism of other amino acids

Unlike prokaryotic cells, cultured mammalian cells cannot synthesize the branched chains or ring systems in amino acids. Thus, these kinds of amino acids are essential, which includes arginine, histidine, isoleucine, leucine, lysine, methionine, phenylalanine, threonine, tryptophan and valine. However, in cultured mammalian cells, alanine, asparagine, aspartate, cysteine, glutamate, glutamine, glycine, proline, serine, and tyrosine can be synthesized. Among these nonessential amino acids, glutamine or glutamate is required in high quantities duo to the role of energy source in mammalian cells. Alanine is the greatest amino acid product of glutamine metabolism and about 40% of the glutamine can be converted to alanine as end product[7]. Asparagine is produced by the amidation of aspartate which comes from TA reaction between glutamate and oxaloacetate. Proline is formed directly form glutamate accumulation. The amounts of these amino acids are changed due to the cell physiological states. However, the amounts of some amino acids such as threonine, arginine, phenylalanine, serine histidine, methionine and glycine keep constant or are consumed in very fair amounts. All of these amino acids can be connected by TCA cycle (figure 3). So, the amounts of these amino acids must be appropriately balanced. Amino acids must be supplied form the media to ensure the metabolic functions of mammalian cells and supply the required amounts in a

balanced state. The absence of any of these amino acids would trigger the onset of cell death.[7, 11, 17]

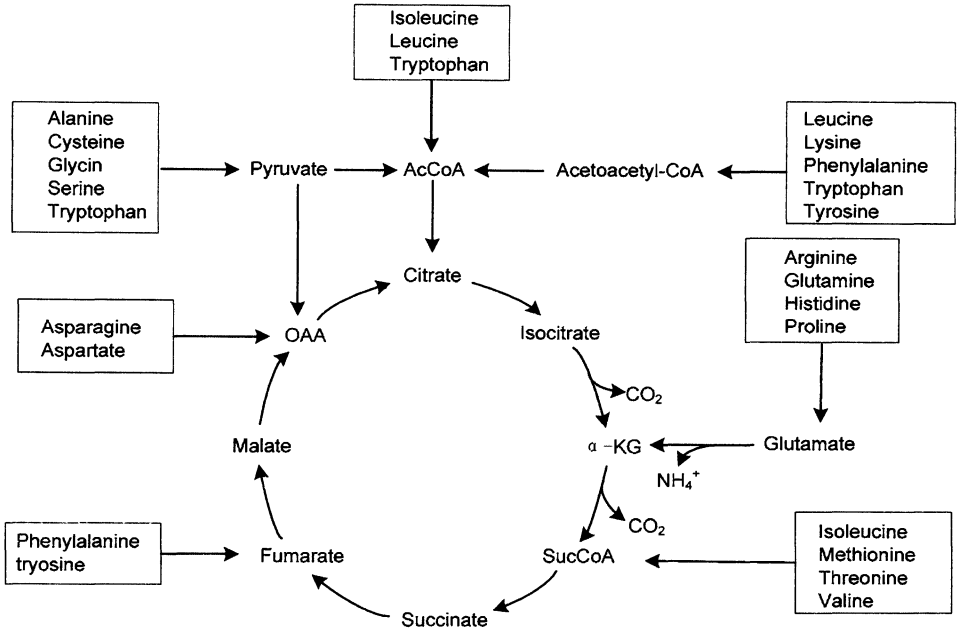

Figure 3 Interaction of the metabolism of the amino acids in central metabolism.

2.2.1.4. Effect of lactate and ammonium in Mammalian cell Metabolism

Lactate and ammonium are main end products of mammalian cell metabolism. As mentioned previously, the accumulation of lactate and ammonium derive from the high glucose and glutamine consumption. Both of them have inhibitory effect on cell growth. However, generally, the direct inhibition of ammonium is much more serious than that of lactate.

Lactate generation by mammalian cells has been mentioned in glucose metabolism. The large amounts of lactate have great effect on mammalian cell growth (Table 1). If a critical concentration is exceeded, lactate can become inhibitory to cell growth. Generally, lactate concentration below 20 mmol/L has not any negative effective effects[11].

Table 1 Effects of lactate concentrations on cell growth at constant pH

Lactate concentration(mmol/L)	Growth	Productivity	Reference
<20	No effect	No effect	Wagner[24], Miler[25]
20-40	No effect	Inhibition	Glacken[26]
40-60	Slight inhibition	Inhibition	Glacken[26]
>60	Inhibition	Inhibition	Glacken[26]

Ammonium can inhibit growth and productivity. Ammonium ions compete with potassium ions for inward transport via potassium transport proteins such as the Na^+/K^+-ATPase[7]. McQueen[27] *et al* assumed an effect of ammonium by a reduction of the intercellular pH value. Some key enzyme such as PFK can be inactivated by the increase of the ammonium concentration. Moreover, cells can be adapted to ammonium concentrations up to 5 mmol/L (Table 2). In some report, cell were tolerant up to maximum values of around 30mmol/L[28]

Table 2 Effect of ammonium on cell growth and productivity

Ammonium concentration(mmol/L)	Growth	Productivity	Reference
<2	No effect	No effect	Glacken[26]
2-5	Inhibition	No effect	Glacken[26] McQueen[27]
>5	Inhibition	Inhibition	Glacken[26]

It should be considered that although most attention has been given to the potential toxic effect of lactate and ammonium, there is experimental evidence that other substances may also cause negative effects on cellular behavior[29]

2.3. Apoptosis in Mammalian Cell Culture

In mammalian cell culture, cell death is an ineluctable phenomenon that is different from bacteria. No matter what kind of culture, *in vivo* or *in vitro*, cell death is part of the normal development and it is the result of many response patterns. For every cell, there is a time to live and a time to die. Cell death can occur by either of two distinct mechanisms, necrosis or apoptosis. Though it is now extensive thought that the failure of cell death, especially apoptosis (also known as programmed cell death) may be very important in the development of cancer, viral infection and autoimmune disorders[30]. Recent research findings show that it is also an important mechanism in mammalian cell lines *in vitro* [7, 31-33] Apoptosis is the regulated form of cell death, which is a complex process defined by a set of characteristic morphological and biochemical features. Although apoptosis,

involving many different pathways and signals, is a very complex process in eukaryotic cells and not fully understood at present, To date, approximately 14 mammalian caspases have been identified and can be roughly divided into three functional groups: apoptosis initiator (including caspase-2, -9, -8, -10), apoptosis effector (including caspase-3, -6, -7), and cytokine maturation (including caspase-1, -4, -5, -11, -12, -13, -14)[31, 34-35].Two main pathways predominate the whole program[36-37].In mammalian cells, the apoptotic response is mediated through either the intrinsic or the extrinsic pathway [38]. The extrinsic pathway is induced by the ligation of plasma membrane death receptors and the intrinsic pathway is caused by a change in the mitochondria due to a perturbation of intracellular homeostasis. Both pathways finally converge on the proteolytic activation of downstream effector caspases[39].

Kroemer *et al* divided apoptosis into three stages[40]:

1) Signaling phase: cell receives an internal or external signal to activate signal transduction pathways.
2) Effector phase: in this phase, various pathways influence the cell to further commit to apoptosis. The relative levels of both pro-apoptotic and anti-apoptotic proteins are critically involved in this phase.
3) Degradation phase: essential proteins will degrade in this phase. And most of the morphological features of apoptosis are found to occur.

2.3.1. Apoptotic pathways

As mentioned previously, there are two characterized apoptotic pathways, intrinsic and extrinsic pathways (figure 4)[41]. Both pathways lead to activation of caspase-3 and give rise to apoptosis.

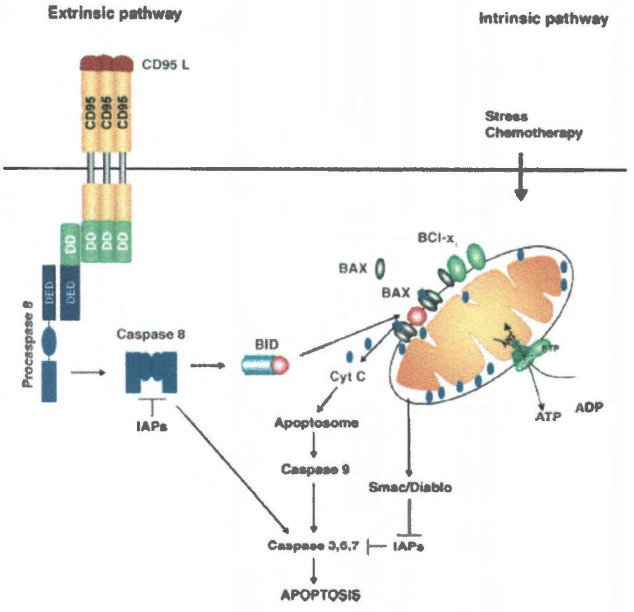

Figure 4 an overview of the intrinsic and extrinsic pathways[42]

The intrinsic pathway is triggered by death stimuli which are generated inside of the cell, such as oncogene activation, DNA damage and ER stress[43]. The intrinsic pathway is mediated by mitochondria and regulated by *Bcl-2* family that can either promote survival or apoptosis, playing a pivotal role in this process[31, 43]. In the intrinsic mitochondria-mediated pathway, apoptosis is initiated by the

release of cytochrome c into the cytosol. In the presence of an apoptotic stress as serum deprivation, heat shock and chemical toxins, cytochrome c will be released from the mitochondria. *Bcl-2* family modulates cytochrome c release. The cytochrome c, released from the mitochondrial intermembrane space to cytoplasm, works together with the other two cytosolic protein factors, apoptotic protease activating factor-1(Apaf-1) and procaspase-9, to promote the assembly of a caspase-activating complex termed the apoptosome, which in return induces activation of caspase-9 and thereby initiates the apoptotic caspase cascade [44-45].

The extrinsic pathway is triggered on the cell surface via binding extracellular death ligand like FasL, tumor necrosis factor α (TNFα) and apo3-ligand, to the death receptors, such as Fas and death receptor(DR) 3, 4, 5, or 6[45-46]on the surface of the cell receive death signals and the result is that procaspase-8 is auto catalytically cleaved into its active form, which results in apoptosis execution[43, 46]. Generally, death receptors has an extracellular region containing cysteine-rich domains[47] for ligand binding, and an intracellular region with a death domain (DD) motif, which can trigger homotypic protein-protein interactions. Adapter molecules like FADD or TRADD themselves possess their own DDs by which they are recruited to the DDs of the activated death receptor. These homotypic interactions lead to form death-inducing signaling complex (DISC), which can trigger procaspase-8 cleavage. Then the active caspase-8 triggers the release of mitochondrial proteins that results in apoptosis [47]. At the point of active caspase-8, the extrinsic apoptosis pathway forks here. Type I is a direct pathway that downstream effecter caspases such as caspases-3, -6 and -7 are activated by active

caspase-8. In type II, there are lower levels of active caspase-8[48]. Thus, the signal needs to be amplified via mitochondria-dependent apoptotic pathways. This type is the link between extrinsic and intrinsic pathways by the Bcl-2 family member Bid. Bid is cleaved by active caspase-8 to form truncated Bid (tBID), which induces the release of cytochrome c. Type II induced apoptosis is block by Bcl-2 over-expression, while type I is not[47].

2.3.2. Apoptosis vs. Necrosis

Cell death is reported to occur by two different and alternative modes: apoptosis, an active, programmed cell death of autonomous cellular dismantling and necrosis a passive, unordered and accidental cell dying resulting from environmental perturbations with uncontrolled release of inflammatory cellular contents. There are many observable morphological and biochemical differences between apoptosis and necrosis [49-52].

Apoptosis includes cellular shrinking, chromatin condensation and margination at the nuclear periphery with the eventual formation of membrane-bound apoptotic bodies that contain organelles, cytosol and nuclear fragments and are phagocytosed without triggering inflammatory processes. The necrotic cell swells, becomes leaky and finally is disrupted and releases its contents into the surrounding tissue resulting in inflammation. Figure 5 is the sketch of the processes of two kinds of cell death[53].

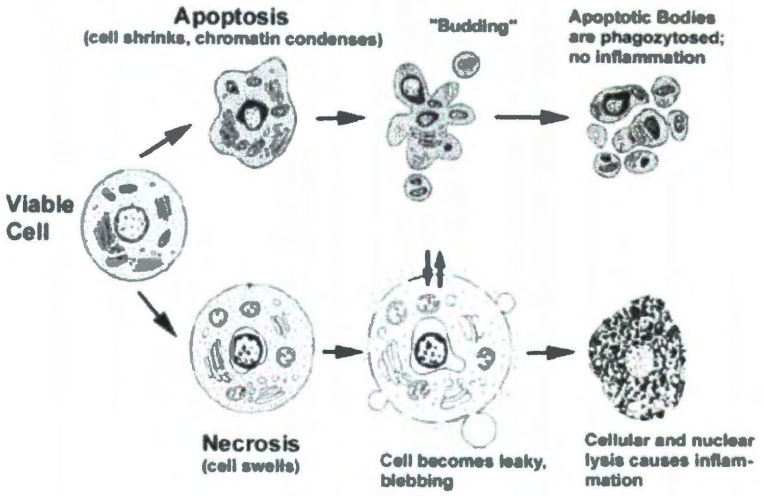

Figure 5 the process of Apoptosis and necrosis. Apoptosis includes cellular shrinking, chromatin condensation and margination at the nuclear periphery with the eventual formation of membrane-bound apoptotic bodies that contain organelles, cytosol and nuclear fragments and are phagocytosed without triggering inflammatory processes. The necrotic cell swells, becomes leaky and finally is disrupted and releases its contents into the surrounding tissue resulting in inflammation. Modified from [32].

Morphological, biochemical, and physiological differences are listed in Table 3[50, 53].

Table 3 Differential features and significance of apoptosis and necrosis

Apoptosis	Necrosis
Morphological features	
Membrane blebbing, but membrane integrity maintained	Membrane integrity lost
Aggregation of chromatin at the nuclear	

membrane	
Begins with shrinking of cytoplasm and condensation of nucleus	Begins with swelling of cytoplasm and mitochondria
Ends with fragmentation of cell into smaller bodies	Ends with total cell lysis
Apoptotic bodies form	No vesicle formation, complete lysis
Biochemical features	
Tightly regulated process	Loss of regulation of ion homeostasis
DNA cleavage	No DNA cleavage
Energy dependent	Energy independent
Physiological significance	
Affects individual cells	Affects groups of contiguous cells
Induced by physiological stimuli	Evoked by non-physiological disturbances
No inflammatory response	Significant inflammatory response

2.3.3. Apoptosis in Mammalian Cell

Though apoptosis is widely developed in cancer and AIDS[47], a bundle of evidence shows it is also an important mechanism during the *in vi*tro mammalian culture[54], especially in serum free suspension culture, which makes the cell more susceptible to death[16, 54]. Evidenced by condensed chromatin and the appearance of a characteristic DNA ladder, 60-90% of total cells die via apoptosis[17, 55], and the exact ratio depends on the type of mammalian cell line, mode of culture and cultivations conditions. Healthy and apoptotic CHO cells in bioreactor are distinguished by acridine orange and ethidium bromide staining (Figure 6). Although apoptotic bodies can be phagocytosed *in vivo*, in vitro they might break apart or accumulate during the cell culture process. Mammalian cells

are prone to apoptosis when cultured in large scale for production of biopharmaceuticals. And this will reduce production duration and results in high cost of production. Apoptosis is triggered by various factors, and delicately regulated by a set of genes [16, 31].

To understand apoptosis in mammalian cell culture, it is necessary to consider the insults that may initiate apoptosis. In spite of best efforts to maintain an optimal environment, cells are constantly changing conditions. Non-optimal conditions can produce cell death. It also has been shown that the accumulation of toxic byproducts, ammonia and lactate, can cause apoptosis[25, 56]. In high-density cell cultures, apoptosis is often induced by the depletion of glucose and glutamine. Wong et al [38] found some up-regulation of apoptosis genes such as FasL, Rip1, Bak, Caspase-8, and -9 occurred at the stationary phase in CHO batch culture, which coincided with the depletion of glucose and glutamine.

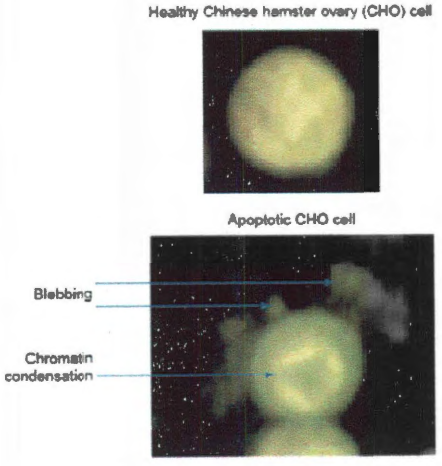

Figure 6 Healthy and apoptotic CHO cells stained with acridine orange and ethidium bromide[16]

The generation of reactive oxygen species (ROS) during culture, either as a result of oxygen sparging or cellular metabolism, may trigger apoptosis. Atsumi et al[57] found that the potent phophatidylserine (PS) externalization and loss of the potential of mitochondria appeared to be mediated by ROS generation, which showed the relationship between early apoptosis and the induction of ROS generation. Stephanopoulous et al [58] found that free fatty acid-induced ROS generation and apoptosis are accompanied by the decoupling of glycolysis and TCA cycle leading to abnormal cytosolic redox states. Thus, antioxidants such as N-acetylcysteine have been used in mammalian cell culture to prevent apoptosis[59].

Recent evidence has shown NAD(P) is essential to mediate cell signaling processes[60] in addition to its role in basic metabolism. The depletion of the cytosolic NAD^+ pool makes the cells unable to utilize glucose, which leads to apoptosis. Ying et al[61] analyzed the functions of cytosolic NAD+ in supporting the flux of glucose and reducing equivalents to the mitochondria and suggested that a sequence of events in which NAD^+ depletion plays an essential role of linking metabolic impairment and apoptosis.

Mitochondria play a complex role in the control of apoptosis and they participate directly in the apoptotic pathway as the site of action of Bcl-2 and caspase activity and interaction[43, 47, 61]. Intracellular signals that induce mitochondrial membrane permeability transition leads to release of cytochrome c. On the other hand, mitochondrial ATP generation seems to be required for apoptosis to proceed [43, 47]. Mitochondria are not only the key regulatory centers

for the genesis of apoptosis, but are also the metabolic centers that provide energy. It is believed that mitochondrial dysfunction, and consequently alterations in energy metabolism, is an important event during apoptosis.

Generally, numerous insults present in the bioreactor environment that may promote cell death via apoptosis. Changes in the intracellular environment resulting from metabolic stress also have a significant impact on induction of apoptosis. Identification of the metabolic changes and the apoptotic pathways should lead to an enhanced ability to understand apoptosis during mammalian cell culture.

2.3.4. Methods for apoptosis inhibition

Because the induction of apoptosis can lead to the loss of viability in bioreactors, it is of considerable value to be able to prevent or inhibit apoptosis in mammalian cell culture in order to extend the time span of high cell viability. Several methods have been developed and evaluated to limit the activation of apoptosis. Normally, there are two kinds of strategies that have been applied to inhibit or slow the onset of apoptosis in bioreactors: the alteration of the external environment via media supplementation and genetic manipulations.

2.3.4.1. Media supplementation

Because the external environment often triggers the onset of apoptosis *in vitro*, altering the conditions of media can be an effective approach to enhance cell robustness.

The most common strategy is the utilization of a fed batch mode of cultivation, which we have mentioned above. Fed batch not only control the concentration of nutrient, but also regulate some critical parameters such as dissolved oxygen and pH and reduce toxic byproduct as well as lactate and ammonia concentration. In high-density cell cultures, apoptosis is often induced by the depletion of glucose and glutamine. Wong et al [38] found some up-regulation of apoptosis genes such as FasL, Rip1, Bak, Caspase-8, and -9 occurred at the stationary phase in CHO batch culture, which coincided with the depletion of glucose and glutamine. Thus, appropriate feeding strategies can delay onset of apoptosis in culture. In some sense, fed batch is a simple and good strategy to delay apoptosis. However, since apoptosis is induced by conditions other than depletion of nutrients, cell death in fed batch is not due to nutrient limitation and will also appear in the end of culture.

Although serum is known to contain unidentified anti-apoptotic chemicals that can provide protection of cell viability during all stages in culture[62], cell growth in serum free medium is often a requirement for current industrial condition. Therefore, some supplements have been considered as independent anti-apoptotic factors. Zanghi *et al* [63] found that suramin, which is drug used for treatment of human sleeping sickness and onchocerciasis caused by trypanosomes, protects CHO cells in serum free culture from apoptosis during exponential growth phase but does not work in death phase as an active site-directed, reversible and tight-binding inhibitor of protein tyrosine phosphatases[64]. Similarly, other specific inhibitors are available to suppress apoptosis such as transferring or insulin

growth factor, which can replace insulin as a mitogen and inhibit apoptosis[16]. Silkworm hemolymph may decrease cell detachment from an adhering surface and then inhibits apoptosis in mammalian cell culture[65]. Heat shock proteins of the hsp70[66] family protects cell against various cytotoxic agents and apoptotic stimuli (Table 4). However, not all of them are appropriate to large-scale culture because of the expense of these supplements.

Another approach for inhibition of apoptosis is to supplement with additives that can block events within the apoptosis cascade. The addition of the caspase inhibitors (Ac-DEVD-cho and z-VAD-fmk) suppresses the apoptotic program in hybridoma cells deprived of glutamine[67]. However, Caspase inhibition does not appear to provide complete cytoprotection from the apoptotic process because mitochondrial dysfunction, phosphatidylserine exposure, plasma membrane permeabilization and loss of clonogenic potential are still observed[68]

Table 4 Media supplementation in multiple cells

Cell line	Manipulation
CHO	Suramin[63]
CHO	Transferrin and insulin like growth factor I receptor [69]
Hybridoma	High mitochondrial membrane potential selection [70]
Hybridoma	Rapamycin [71]
Hela	Silkworm hemolymph [65]
NS0	Hsp70[38, 66]

2.3.4.2. Genetic strategies

Genetic strategies have proven successful in delay apoptosis in mammalian cell culture. Over-expression of anti-apoptotic genes towards delaying the onset of apoptosis has been attempted in animal cell culture[16, 31].

The Bcl-2 was the first to be recognized as an anti-apoptotic gene and protein it produces to enhance cellular robustness: in *C. elegans*, ced-3 and ced-4 were identified as genes essential for programmed cell death, while ced-9 was found to be a regulator of cell death by preventing apoptosis. The first mammalian homolog for ced-3 was described in 1988 as Bcl-2 which is involved in B-cell lymphomas[36-37]. The bcl-2 proteins are a family of proteins involved in the response to apoptosis. Some of these proteins (such as Bcl-2 and Bcl-X_L) are anti-apoptotic, while others (such as Bad or Bax) are pro-apoptotic [31, 38, 43, 46-47]. The sensitivity of cells to apoptotic stimuli can depend on the balance of pro- and anti-apoptotic bcl-2 proteins. When there is an excess of pro-apoptotic proteins the cells are more sensitive to apoptosis, when there is an excess of anti-apoptotic proteins the cells will tend to be more resistant.

In mammalian cell culture, Bcl-2 is the best studied of the anti-apoptotic genes, since it is demonstrated to suppress apoptosis in a wide range of cell types in response to numerous inducing agents, including growth factor withdrawal, cytotoxic drugs, and exposure to ionizing radiation[72].Bcl-2 resides on the cytoplasmic face of the mitochondrial outer membrane, the nuclear envelop, and the endoplasmic reticulum. There are a number of theories concerning how the Bcl-2

gene family exerts their pro- or anti-apoptotic effect. An important one states that this is achieved by activation or inactivation of an inner mitochondrial permeability transition pore, which is involved in the regulation of matrix Ca^{2+}, pH, and voltage. It is also thought that some Bcl-2 family proteins can induce or inhibit the release of cytochrome c in to the cytosol which, once there, activates caspase-9 and caspase-3, leading to apoptosis[36-37]. This interaction between pro- and anti-apoptotic proteins disrupts the normal function of the anti-apoptotic Bcl-2 proteins and can lead to the formation of pores in the mitochondria and the release of cytochrome C and other pro-apoptotic molecules from the intermembrane space. This in turn leads to the formation of the apoptosome and the activation of the caspase cascade. Except Bcl-2, other two anti-apoptosis proteins (Bcl-X_L and XIAP) have also been compared with their wild type counterparts and show remarked effects on cell viability.

2.3.5. Methods of apoptosis Detection

Rapid and accurate apoptosis assay is essential requirements in our research. Cell death typically follows one of two distinct paths, apoptosis or necrosis. Cells undergoing apoptosis display distinct morphological and biochemical changes. Just because of these characteristics, apoptotic cells can be distinguished from healthy and necrotic cells. Thus, based on these changes, such as morphological changes, DNA fragmentation, exposure of phosphatidylerine (PS) at the outer plasma membrane and caspase activation, detection techniques were developed. Normally, apoptosis is analyzed either by flow cytometry or fluorescence microscopy.

During apoptosis, mitochondria are well preserved; however, nuclei have chromatin condensation. On the other side, during necrosis, cells undergo swollen mitochondria and nuclear flocculation. These differences among viable, apoptotic and necrotic cells can be detected some morphological assessment methods:

1) Morphological Assessment of Apoptosis: One of the classic features of apoptosis is the cleavage of the DNA into fragments. So much work has been performed on the analysis of apoptotic events on DNA fragmentation. However, DNA fragmentation also occurs in certain stages of necrosis [73], and this is not a definitive test for apoptotic cell death. Nevertheless, it is a useful feature in characterizing the cell death in any case.
2) Detection of DNA Fragmentation: This phenomenon is easily visualized by agarose gel electrophoresis. This method is often tedious and time-consuming and provides qualitative rather than quantitative data.[74] Quantification of DNA fragmentation can be done by labeling DNA (FACS analysis) or DNA ends (TUNEL).
3) Biochemical Analysis of Apoptosis: During apoptosis, members of caspases are activated and then orchestrate the apoptotic events. Assessment of caspase activation is a good tool that can be applied to analyze a variety of apoptotic systems[75].

Short comparisons and comments are listed in Table 5 as follows:

Table 5 Methods for Detection of Apoptosis

Method	Convenience	Notes
	Morphological Assessment of Apoptosis	
AO/EB staining[76]	Very rapid Cannot be stored	Gives information on early vs. late apoptosis, necrosis Somewhat subjective but definitive
Hoechst 33258 staining [77]	Very rapid Cannot be stored	Somewhat subjective but definitive
Electron microscopy[76]	Expensive and time-consuming	Definitive Only small area can be observed
Annexin V [77]	Rapid, simple and cell can be fixed	Measures an event of known significance Not all cells expose PS prior to loss of membrane integrity Hard differentiation between bate apoptosis and necrosis
	DNA Fragmentation	
Gel electrophoresis [74]	Fairly rapid and cheap	Qualitative Can not define apoptosis exactly Does not occur in some cells
TUNEL [73]	Often used Expensive and time-consuming	Quantitative and sensitive Somewhat definitive False-positive staining of necrotic cells
	Biochemical Analysis of Apoptosis	
Caspase activation [75]	Expensive	Allows identification of specific caspases activated

All the methods were developed in 1990's, and each method has its advantages and disadvantages. At present, TUNEL and Annexin V are commonly in use, because both TUNEL and Annexin V methods are sensitive and specific and produced similar data in all measurements. Among them, the TUNEL method appears to be the most specific method. Annexin V method is limited only by successive loss of membrane integrity of the apoptotic cells. Only staining by Annexin V cannot distinguish between apoptotic cells and cells that suffered from accidental cell death[78]. It needs double stain technique to improve the ability to distinguish different cell stages. For double-labeling, Annexin V/PI and Annexin V/anti-Lamin B2 are recommended [79-80]. On the other hand, using the Annexin V method in suspension systems, the number of apoptotic cells can be detected in a relatively fast, simple and sensitive way [79]. As far as AO/EB staining method, this method can give information on early vs. late apoptosis. This is a very fast method comparing to other assays. However, since we need to distinguish not only the colors but also the morphological criteria, it is somewhat more subjective than TUNEL and Annexin V methods. Normally, this method has been the dye of choice for many years for many researchers, and currently it is preferred to combine AO/EB staining with Annexin V or TUNEL together to detect apoptosis qualitatively and quantitatively.

Annexin V

In healthy cells, the phospholipids of the plasma membrane are distributed asymmetrically over the two leaflets of the bilayer. Phosphatidylcholine and sphingomyelin are predominant in the outer membrane and phosphatidylerine (PS)

is in the inner membrane leaflet. In the early apoptotic stage, PS is externalized to the outer membrane. Surface exposed PS can be detected by its affinity for Annexin V, which is a phospholipid binding protein. As showed in figure 7[78], hapten-labeled Annexin V binds in the presence of millimolar Ca^{2+} to PS residues that are exposed in the outer membrane of apoptotic cells. As far as dead cells, since the integrity of the plasma membrane is lost, Annexin V can also bind PS in the inner membrane. To distinguish dead and apoptotic cells, Propidium Iodide (PI), a membrane impermeable DNA stain, is added at the same time. Thus, viable, apoptotic and dead cells can be distinguished bye the double labeling for Annexin V and PI, which can be detected by flow cytometry or fluorescence microscopy. Thus, this method can be used to distinguish between viable cells (Annexin V-/PI-), early apoptotic cells (Annexin V+/PI-), late apoptotic/secondary necrotic cells (Annexin V+/PI+), and necrotic cells (Annexin V-/PI+) (Figure 8).

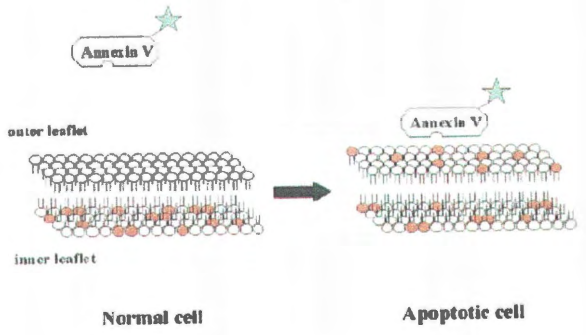

Figure 7 Schematic representation of the loss of membrane lipid asymmetry during apoptosis[79]

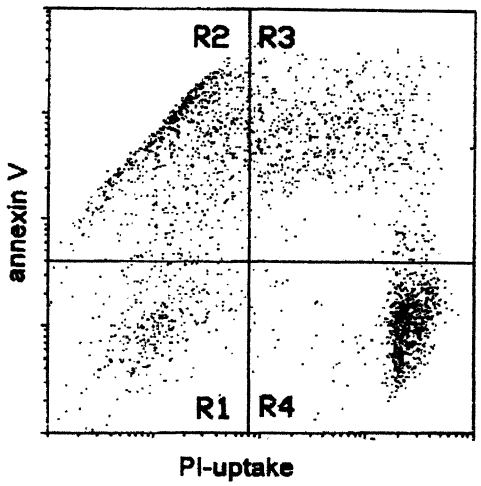

Figure 8 Bivariate PI/Annexin V analysis of rat thymocyte cells. Region R1 contains viable cell population (Annexin V-/PI-), R2 contains the early apoptotic cells (Annexin V+/PI-), R3 contains late apoptotic cells (Annexin V+/PI+) and R4 is necrotic cells (Annexin V-/PI+)[79]

TUNEL

Terminal uridine deoxynucleotidyl transferase dUTP nick end labeling (TUNEL) is a common method for detecting DNA fragmentation that results from apoptotic signaling cascades. The assay relies on the presence of nicks in the DNA which can be identified by terminal deoxynucleotidyl transferase, an enzyme that will catalyze the addition of dUTPs that are secondarily labeled with a marker. The biotin-labeled cleavage sites are then detected by reaction with HRP conjugated streptavidin and visualized by DAB showing brown color. Recently, more methods for the detection of apoptotic cells and specific parts of the apoptotic pathway are also available such as the detection of caspase activity (specifically caspase-3), Fas-

ligand and Annexin V, etc. It is also important to use TUNEL in conjunction with other methods especially morphology, immunohistochemistry and electron microscopy.

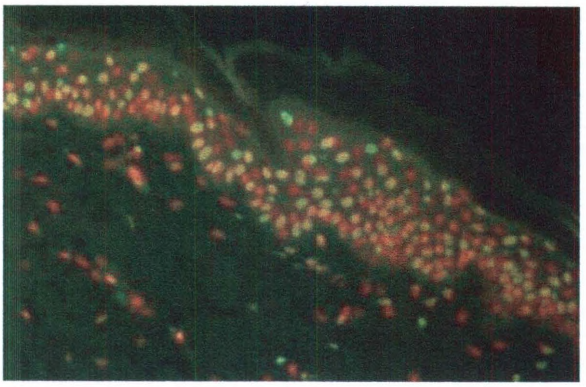

Figure 9 TUNEL staining of formalin fixed, paraffin embedded skin. Note nuclear staining of apoptosis cells (green). Counterstain-PI (red)

2.4. Cell Separation

Cell separation, which obtains defined cell populations or isolate rare cell types to high purity, plays a major role in a variety of biological and biomedical applications. The history of cell separation can be tracked back to 1960s. Isolation of cell subpopulations has been a major goal in the research on cell biology, disease diagnostics, therapeutics and as well as industrial application. The potential applications of cell separation can be divided into: removal of specific cell types; purification of cell mixtures for diagnostic tests; tracking tumor cells in the body; isolation and detection of various cells[81].

Table 6 Methods of cell separation

Using physical properties		
Principle	Technique	Application
Density	Ficoll-Paque density gradient medium	Isolation of mononuclear cells from blood Removal of dead cells
Density	Percoll density	Fractionation of leukocyte substes
Density, cell size	Elutriation	Separation of cells according to their cell cycle
Cell shape, surface properties	Aqueous Two Phase Systems (ATPSs)	Isolation of hematopoietic cells, Separation of viable cells
Using immunological parameters		
Cell-cell interaction antibody-mediated	Rosseting	Depletion of specific leukocyte subsets
Specific lysis of antibody coated cells	Complement lysis	Depletion of an specific cell type
Antibody specificity, fluorescence	Fluorescence activated cell sorting (FACS)	Fluorescent dyes to specific cellular target or antibodies
Antibody specificity, magnetism	Magnetic activated cell sorting (MACS)	Applicable to any cell suspension with known specific surface markers.

The current cell separation methodologies can be divided into two main groups. The first is based on physical criteria like size, shape and density differences using filtration and centrifugation techniques. Another technique comprises of

affinity methods that are based on biochemical cell surface characteristics and biophysical criteria[82-83]. Cell separation technologies can be cataloged according to their separation principle. Those include cell separation based on physical principles, biological characteristics, biochemical characteristics or a combination of one of more of the above. Table 6 summarizes some of the current techniques used in cell separation.

Because of t specificity and high affinity of antibody-antigen interaction, usually more purified cell population is expected from the immunological separation. At the same time, the cost associated with immunological separation is usually higher compared to other physical separation methods.

2.4.1. Aqueous Two Phase Systems (ATPSs)

An aqueous two phase system (ATPS) essentially consists of two immiscible aqueous solutions of different polymers. Generally, ATPSs are formed by the incompatibility of two aqueous polymer solutions such as polyethylene glycol (PEG) and dextran, or one polymer and one low molecular weight solute, such as potassium phosphate. ATPSs have been used for the isolation and characterization of different types of cells, which is conventional technique and can separate cells easily and effectively without using antibodies. It is well known extraction technique for the separation of fragile biomaterials such as proteins, biological membranes, and cells[84]. Separation is dependent on the properties of the polymers, additives, pH and temperature. The basis of cell separation in ATPSs is the selective distribution of substances between the two phases due to the sensitivity to cell

surface properties such as surface charge and lipid composition, and the presence of specific components depending on the cell type. ATPS is one of the few techniques that separate cells on the basis of surface properties[85]. The partition coefficient K of a cell in an ATPS can be described as $K = {C_{top}}/{C_{bottom}}$ and be expressed as a function of several variables in an empirical formula

$$\ln K = \ln K^{\circ} + \ln K_{electrochemical} + \ln K_{hydrophobic} + \ln K_{Biospecific} + \ln K_{size} + \ldots$$

where K^0 includes other surrounding environmental factors. This formula considers the contributions are both from the cell properties and from the ATPS physical conditions[86].

Haematopoietic cells were first separated and characterized by ATPSs. Walter[87] studied the effects of the relative percentages of phosphatidylcholine and sphingomyelin of the cellular membrane on the partition coefficient and showed the importance of membrane lipid composition on erythrocyte cell separation. Recently microfluidic devices were used to separate animal and human blood cells continuously[88-89]. Continuous cell partitioning in microfluidic devices can create a stable aqueous two phase laminar flow and large interface to perform partitioning, without diffusive mixing. Viable and dead CHO-K1 cells were successfully separated by this continuous flow extraction method with high purity.

2.4.2. Magnetic Activated Cell Sorting (MACS)

Magnetic cell separation is a widely used method for isolating many different types of cells, which uses magnetic particles conjugated to proteins or antibodies to tag cells of interest. Compared with FACS, magnetic cell separation is based on the difference in cell's magnetism between target cells and other cells in the mixture. To differentiate cells in their magnetism, target cells are labeled specifically with magnetic labels via antibody-antigen interaction or other bioaffinity interactions. The specific cells to be sorted are labeled with antibodies to the cell surface antigen. Cell mixture containing labeled and non-labeled cells pass a column with magnetic field. The magnetically labeled cells are retained on the column, while unlabeled cells pass through. These cells can be collected as the unlabeled fraction. The retained cells are eluted from the column after removal from the magnet there is no harsh physical and chemical treatment required to obtain the targeted cells, which are suitable for the further use. They separate cells based on the distances they travel under the magnetic energy gradient, which are directly related to the cell's magnetism after labeling. These systems can provide higher or comparable throughput compared to FACS. Figure 10 shows schematic flowchart of MACS.

To label cells, many types of magnetic microbeads and nanobead have been developed. Dynaead magnetic particles (Invitrogen, Carlsbad, CA) and MicroBeads (Miltenyi Biotec GmbH, Bergisch Gladbach, Germany) are commercially used. Dynabeads were the first magnetic particles used for clinical cell separation applications, in particular, bone marrow purging of gliomas prior to

transplantation[90]. Due to their relatively large size (from 1 mm to 4.5 mm) the preferred applications of Dynabeads is negative cell selection, where the cells targeted by the magnetic label are discarded, and only the unlabeled cells are used In comparison to micrometer-sized magnetic particles, the use of colloidal magnetic particles as labeling reagents offers advantages in forming stable suspensions and fast reaction kinetics, similar to immunofluorescence labels and positive cell selection. Small magnetic particles (MACS), with diameters ranging from 50 nm to 150 nm, produce a paramagnetic moment and therefore require the use of high-gradient magnetic separation fields, such as those produced by thin wires of a ferromagnetic material immersed in the cell suspension. [91]

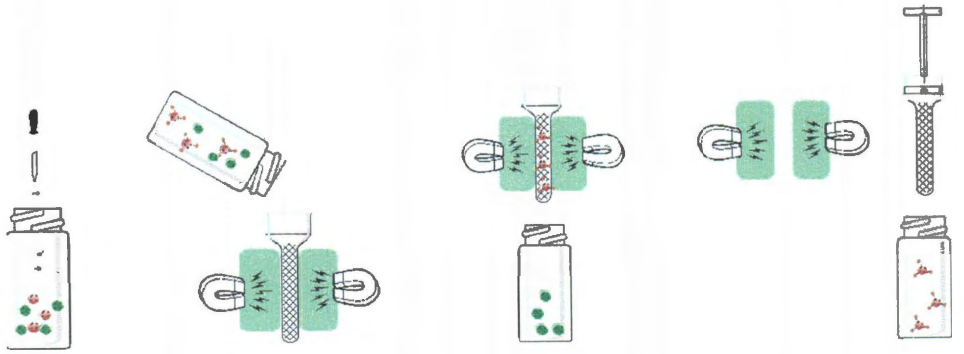

Figure 10 Schematic flowchart of MACS using MicroBeads, MACS columns, and MACS separators. A mixture of magnetically labeled and unlabeled cells is loaded onto a ferromagnetic matrix. Magnetized cells are retained on the column while unlabeled cells pass through. Labeled cells are recovered after demagnetization of the column.

Magnetic microbeads coupled with the use of specific antibodies can effectively separate cells. Therefore, the successful application of MACS relies mainly on the selection of specific antibody and an appropriate labeling strategy.

Based on the antibody used, there are multiple applications for the MACS technology such as sperm improvement[92], cancer cell detection[93] and rare cell selection[94]

2.5. Metabolic Flux Analysis of Mammalian Cells

2.5.1. Introduction

Metabolic flux analysis (MFA) has become a standard tool for analyzing metabolism and optimizing bioprocesses. It uses a metabolic reaction network in combination with extra cellular measurements and mass balance to calculate flux distributions in metabolism[95].

As mentioned previously, the metabolism of mammalian cells is very complex. These metabolic pathways determine the fate of any carbon and nitrogen sources in mammalian cells under different environmental or genetic background. However, their metabolism takes place not only in cytosol but also in mitochondria. Also the cells require a complex medium. MFA can be a useful tool to reduce these complexities and get a better understanding of mammalian cells[96].

MFA is a popular tool for the modeling of metabolic networks containing metabolites and reactions. The metabolites are the network nodes and the metabolic reactions represent the edges of the network. With the help of a metabolic network and the flux measurements, it is possible to find the values of the fluxes.

Most studies on MFA use the stoichiometric approach or the isotope tracer approach to estimate intracellular fluxes: conventional metabolic flux analysis (c-MFA) or labeling-based metabolic flux analysis (l-MFA). The metabolic fluxes are computed by analysis of nutrient and metabolite levels or isotopic tracer concentrations.

2.5.2. c-MFA

c-MFA uses the information obtained from determination of measurable fluxes and a steady state assumption for the intracellular metabolites to calculate the metabolic fluxes in a given metabolic network[97]. Thus the first step is the development of stoichiometric model of the metabolic network. Next mass balances are written for all compounds present in the metabolic network as follows:

$$\frac{dX_{met}}{dt} = r_{met} - \mu X_{met} \tag{1}$$

Where X_{met} is the concentration vector of the metabolites, r_{met} is the production rate and μ is the specific growth rate of cells at time t. assuming no accumulation of intracellular metabolites, that is the metabolites are at a pseudo-steady state, the left side of equation (1) becomes zero. Also, since the concentration of the intracellular metabolites is very low, μX_{met} can be neglected and equation (1) can be simplified to

$$0 = r_{met} \tag{2}$$

The rate of formation and consumption of a metabolite is determined by the stoichiometric reaction network and the fluxes through each reaction. Supposing there are J reactions and K metabolites, the rate of formation of the i^{th} metabolite is given by:

$$r_i = \sum_{j=1}^{J} \alpha_{ij} v_j \tag{3}$$

where α_{ij} is the stoichiometric coefficient of the i^{th} metabolite in the j^{th} reaction, and v_j is the rate of the j^{th} reaction. Then equation (3) can be written in matrix notation as follows

$$r_{met} = G^T v \tag{4}$$

where G^T is the matrix of stoichiometric coefficients. Further, we have

$$G^T v = 0 \tag{5}$$

The matrix G^T and the rate vector v can be divided into two parts: the extracellular measured parts (G_m and v_m) and the calculated parts (G_c and v_c). Then equation (5) can be constructed to :

$$G_m^T v_m + G_c^T v_c = 0 \tag{6}$$

Calculate v_c and get:

$$v_c = -\left(G_c^T\right)^{-1} G_m^T v_m \tag{7}$$

Equation (7) is for the matrix G_c^T invertible, that is the system should be exactly determined. If not, a pseudo-inverse of the matrix G_c^T will be replaced by:

$$\left(G_c^T\right)^{\#} = \left(G_c G_c^T\right)^{-1} G_c \tag{8}$$

Then ν_c can then be calculated as follows:

$$\nu_c = -\left(G_c^T\right)^{\#} \left(G_m^T \nu_m\right) \tag{9}$$

This equation is for the system is redundant and singular[97].

However, c-MFA requires an identified metabolic network. This requires detailed knowledge, on which enzymes may be expressed, the reactions they catalyze and even their localization in cells. This will result in very large networks. To simplify this network, serial reactions in linear pathways can be lumped into a single overall reaction and biomass components which have the same biosynthetic pathway can be lumped into a single component with an average composition. This simplification might lead to identifiability of fluxes and c-MFA might be used.

2.5.3. Identifiability of fluxes

One of the important issues using MFA to solve the system of equations for calculating unknown fluxes should be identifiable. As discussed in above paragraphs, this equation has a solution only if the system is exactly determined, If it has full rank, which means rank of this matrix is equal to the number of metabolite balances, this condition could be easily evaluated by calculating the rank of the

matrix, and if it is equal to the number of balances, the matrix is invertible. Calculation of rank of matrix G_c^T helps in identifying any redundant equations in the system of reactions and removing such equations from the system helps in solving it. However, in some cases, an analysis of the reaction network may show that some of the balances are redundant and this system is underdetermined, then it is solved by applying constraints and optimization routines. Thus, reducing the complexity of reaction network by lumping some of the reaction or removing them, might lead to identifiability of fluxes, facilitating c-MFA analysis.

2.5.4. Consistency of data

Since MFA is a very useful tool in the decision making for the cellular pathway manipulation or for the studying cellular physiology, it is noted that the importance of confidence on MFA results obtained from this analysis. It depends on the accuracy of the model being used to calculate the fluxes for intracellular metabolites as well as on the extracellular measurements. Therefore, other type of balances such as elemental balances can be used to check the consistency of the data. One of the popular elemental balances is around carbon, where number of carbon atoms going into the system through substrate is balanced against the number of carbon atoms coming through the extracellular products. But similar information is often not available about the carbon atoms going into the biomass and hence it is very difficult to perform accurate carbon balances. Same arguments cam also be made for other elemental balances such as nitrogen, oxygen, sulfur and hydrogen. Another method, which can be used to check the consistency of the data,

is the redox balance analysis. In this case, sum of the multiplications of the products moles into their oxidation states should be equal to the multiplication of moles of substrate into its oxidation state.

2.5.5. Sensitivity Analysis

The sensitivity analysis is performed to provide a certain confidence of interval for each flux parameter based on the measurement errors and ensure that the stoichiometric metrix developed is well posed. It can be checked by condition number and solution matrix.

Chapter 3

Materials and Methods

3.1. Cell Culture

The cell line CHO TF 70R that produces tPA was kindly provided by Professor Claudia Altamirano (Pontificia Universidad Católica de Valparaíso, Chile) Recombinant CHO TF 70R was original from CHO DG 44, which is a dihydrofolate reductase-deficient(dhfr-) cell line, by transferring a DHFR(+)-tPA plasmid. T75 flasks (Corning, USA) were used for the preliminary work for subculture. Seed was prepared in a proprietary serum-free medium HyClone SFM4CHO (Thermo Scientific, UT). The medium was supplemented with 20 mmol of glucose and 6 mmol of glutamate. The cell culture experiments were selected cells from the mid exponential phase of growth at a cell concentration of 10^6 cells/ml. Cell culture experiments with selected medium were carried out in spinner flasks (Techne, NY) with working volume of 100mL and stirred at 50rpm in a CO_2 incubator at 37°C and

5 % CO_2. During the incubation period, about 600µl samples were taken on time for analysis.

The cells for cryopreservation were chosen in exponential growth phase with viability above 90%. The cells were centrifuged at 1000g for 5 minutes and the supernatant was removed. The cells with the concentration of about 8×10^6 cells/ml were then resuspended in 80% DMEM/F12 medium, 10% serum and 10% dimethyl sulfoxide (DMSO). The cells were transferred to 2 ml sterile cryovials (Nalge Nunc, NY) freezing container. The container was kept at -80 °C overnight and then transfer to the liquid nitrogen tank with the model of XC33/22 (CBS, MI) for long term cryopreservation.

3.2. Analytical Methods

3.2.1. Determination of Cell Density and Viability

Cell number was estimated using a hemacytometer (Neubauer improved, Hausser Scientific, PA) and counting was under a normal light inverted microscope (AE 31, Matic, Canada). Cell viability was determined through the method of Trypan Blue Exclusion. The trypan blue exclusion method was outlined by Patterson. Viable cells with membranes will exclude trypan blue. Cell sample was removed from cell suspension. An equivalent volume of 0.2% Trypan blue (1:1 mixture of Trypan Blue Solution (0.4%) (Sigma, MO) and PBS buffer (v/v)) was added to the cell sample. Cell/Trypan mixture was mixed by pipet gently for approximately 10 times. Allow to stand for 1 to 2 minutes at room temperature to permit dye uptake. The stained

sample (about 15mL) was transpired onto a hemacytometer. The total number of cells and the number of unstained cells were counted under the inverted microscope (10× objective) in all of the (4+4) of the major sections of the counting chamber (1mm x 1mm). Viable cells and cells in early stages of apoptosis exclude trypan blue; cells in the late stages of apoptosis and necrotic cells take up the dye and appear as blue cells[1].

The counting rule was: count all the cell in the $1mm^2$ squares of A, B, C and D and delete both the maximum and minimum of viable cells and non-viable cells. Sum the two rest numbers of viable cells and get the total viable cells. Sum the two rest numbers of non-viable cells and get the total non-viable cells.

The formula to derive the concentration of cell sample was:

$$c = \frac{n}{2}\frac{1mm^3}{1mm \times 1mm \times 0.10mm}\frac{1000mL}{1mm^3} \times 2 = n \times 10^4 (cells/mL) \qquad (10)$$

where c is the cell concentration (cells/mL) and n is the number of cells counted. (Note: the first 2 in the denominator is 2 squares of counting areas we sum, and the second 2 in the numerator is we dilute cell sample by equivalent volume of trypan blue solution). The average of two counts was used as the calculating result, and the percentage of viable cells and total cells was used to calculate the cell viability.

Specific cell growth rate (μ), specific nutriments consumption rates, specific byproduct rates and tPA production rate are estimated by plotting the

concentrations of total cell, nutriments consumption, byproducts and tPA versus the integral of viable cells (IVC).

3.2.2. Metabolite determinations

3.2.2.1. Analysis of sample composition using HPLC

Metabolite composition of the samples was mostly measured by HPLC (high performance liquid chromatography) such as glucose, lactate and amino acids. At each measurement point, samples were drawn from the spinner flask and were centrifuged as described previously and store at -20 ºC. VP series HPLC system by Shimadzu Scientific Instruments (Columbia, MD) was used in our study. The data was analyzed by the software, VP Class developed by Shimadzu, for calculating area under the peak for each compound.

Sugars and lactate

Samples were run through the organic acid column Aminex HPX-87H from Bio-Rad Laboratories (Hercules, CA) under optimum conditions determined by the optimization routine developed from our group for effective separation of glucose and lactate. Deionized water for the mobile phase and needle wash was purified using a Nanopure II system (Barnstead, Dubuque, IA) to a conductivity of 18 MΩ-cm and filtered through a 0.22μ membrane (Millipore, Billerica, MA). Isocratic elution for all runs was executed at flow rate = 0.3 ml/min using 5 mM H_2SO_4 solutions as mobile phase at column temperature 42 °C[98].

Amino acids

Amino acids were analyzed via a reversed phase HPLC with pre-column derivatization by orthophthalaldehyde (OPA). Samples were centrifuged at 1000g for 5 minute to remove the cells and the supernatant was filtered through a 0.22μ membrane. The prepared samples were sent to Medical Genetics Laboratory at Baylor College of Medical (Houston, TX) for further analysis.

3.2.2.2 Glucose Uptake assay

Cells were plated at 5×10^5 cells/well in 24-well plates with various concentrations of 2-NBDG (10-80μM). After incubation in at 37°C and 5 % CO_2 for a certain period of time as described in each experiment, the 2-NBDG uptake reaction is stopped by removing the incubation. After centrifugation, samples (1×10^5 cells) were washed with ice-cold PBS buffer and then diluted with 500μl of buffer to the final analysis solution. Samples were analyzed in a FACSCanto II (BD Biosciences, San Jose, CA) with 10,000 cells counted per event. 2-NBDG shows intense fluorescence at 542nm when excited at 467nm.

3.2.3. Protein sample preparation

Samples are collected from spinning flasks. Cell pellets are centrifuged at 1000g for 10 minutes and are washed by ice cold PBS twice and then stored at -80°C. When preparing protein extracts, frozen cell pellets are thawed and resuspended in lysis buffer containing 7 M urea, 2M thiourea, 30mM Tris-Cl, 5mM magnesium acetate, 4% 3-[(3-Cholamidopropyl) dimethylammonio]-1-propanesulfonate (CHAPS) with the amount about 1 ml per 5×10^7 cells [99-102]. The mixture is homogenized carefully by 20 gauge needle five times. Samples are

left on a plate shaker at room temperature for 1 hour to allow extraction and then centrifuged at 14000 rpm at room temperature for 15 minutes. The supernatant is removed and samples are stored at -80℃ for use. Concentrated proteins are resuspended in the DIGE labeling buffer (8M urea, 4% w/v CHAPS, 30mM Tris pH 8.0) and concentration is measured by Bradford protein assay (Bio-Rad, UK).[103]

3.3. Quantification of Apoptosis

Apoptosis will be evaluated by the CytoGLO™ Annexin V-FITC Apoptosis Detection Kit (IMGENEX Co., CA). 0ne hundred µl of samples at a concentration of 106 cells/ml are washed twice with 1000µl of PBS (pH 7.4) and then resuspended by 100 µL of binding buffer (10mM Heps/NaOH, 140mM NaCl, 2.5 mM CaCl2, pH 7.4). The reaction solution is added with 5µl of Annexin V-FITC and 5µl of PI and is incubated at room temperature in the dark for 15 minutes.

3.3.1. Imaging study

After incubation, the stained sample (about 15µl) was transpired onto a hemacytometer (Neubauer improved, Hausser Scientific, PA) for observation. Samples were observed by fluorescence microscope with 10×, 20×, 40× objectives (Olympus, San Jose, CA). Images are taken and determined numerically using Compix Imaging software (Hamamatsu Photonics Management Co, Sewickly, PA). The images captured were gray-scale images and needed to be processed to colorize via software Image-J (National Institutes of Health, USA).

3.3.2. FACS analysis

For FACS analysis, samples are diluted with 400µl of binding buffer to the final analysis solution. Samples should be analyzed as soon as possible within 1 hour, since apoptosis is a rapid and dynamic process. Samples are analyzed via BD FACSCanto II (BD Biosciences, San Jose, CA), and the instrument settings is as follows: FSC= 275, SSC= 359, FITC: FL1=381, PI: FL2=391; Threshold FSC 15000; Compensation: PI to FITC: 0; FITC to PI: 0.53. The data are evaluated using the software FACSDiVa 6.2.

3.4. Cell Separation

3.4.1. Aqueous Two-Phase Partition System (ATPS)

10% (w/w) Dextran T500 and 8% Polyethylene glycol 8000 (PEG 8000) in 10mM sodium-potassium phosphate buffer at pH 7.4 were prepared as stock solutions. Phase systems were prepared by weight (1:1) from the stock solutions. The systems must be mixed well, left in a separatory funnel for 6 hours to equilibrate at room temperature. Samples with total cell number at approximate 10^8 were washed twice with 10ml of PBS (pH 7.4) and then resuspended with 50 ml of working phase solution. After around 30 minutes of setting. 70µl of result samples in each phase were collected for apoptosis and viability assay.

3.4.2. Magnetic Associated Cell Sorting (MACS)

Magnetic cell isolation uses MiniMACS kit (Miltenyi Biotec, Bergisch gladbach, Germany). The samples are centrifuged at 150g for 5 minutes at 37℃ and the cells collected are washed twice by PBS buffer (pH 7.4). The cell pellets are resuspended by 80μl of binding buffer and 20μl of MACS Annexin V MicroBeads per 10^7 total cells. The suspension is mixed well and incubated for 15 minutes at 8℃. After incubation, the suspension is passed through MS column kept in magnetic field. The column is washed with the equal volume of buffer three times. The unlabeled cells passing through in the effluent are collected. Then the magnetic field is removed. Equal volume of buffer is applied onto the MS column to flush the labeled cells out. Also, the column is washed with the equal volume of buffer three times to remove the remaining labeled cells.

3.4.3. Ficoll gradient centrifugation

Samples were diluted by 4× PBS buffer. Each 35mL of diluted cell suspension was carefully layered over 15mL of Ficoll-Paque Plus (GE healthcare, NJ), drop by drop. Mixture was centrifuged at 400×g for 30 minutes at 20ºC in the swinging bucket rotor without brake. After centrifuge, the upper layer was aspirated and the target cells at the interphase were obtained.

3.5. Metabolic Flux Analysis

From the experimental data of extracellular concentrations, the stoichiometric model described in appendix was divided into measured (G_m^T) and calculated (G_c^T) matrices and the intracellular fluxes (v_c) were calculated from measured fluxes (v_m) using equation in chapter 2.

Chapter 4

Investigation into Cell Growth and Apoptosis

4.1. Introduction

Cell death via apoptosis is an essential process in the life of mammalian cells in serum-free batch culture[32, 54]. Although cell cultures are sometimes treated as a homogeneous mixture of identical cells, cell heterogeneity almost undoubtedly exists within cell culture system. The fact is that individual cells exhibit heterogeneity as a result of small differences in their cellular metabolism dynamics. Throughout the course of a cell culture cycle, cells run the risk of encountering numerous stresses or insults and each individual cell may or may not commit apoptosis.

From an industrial point of view, the goal of study on apoptosis during cell growth is to prolong cell growth as much as possible in the cultivation, thus giving a

higher concentration of targeted protein. Classical descriptions of cell growth rarely include death via apoptosis, but only viability. In the research of cell culture, Trypan blue dye exclusion test was normally applied to characterize the total population of cells as either viable or dead. However, this is just a rough description to distinguish cell stages, moribund through apoptosis. In order to improve our understanding of apoptosis in mammalian cell culture, specific cell phases during culture need to be detected and characterized. The changes from these phases such as apoptotic and non-apoptotic, should bring more information of apoptosis, which can help us better understand this process.

Our research is conducted in an effort to understand cultured mammalian cell behavior. So, it is imperative to identify healthy and apoptotic cells during cell culture using prior knowledge and current techniques. The method of apoptosis assay using dual staining with Annexin V-FITC and PI can distinguish viable non-apoptotic cells, early phase, late phase of apoptotic cells and necrotic cells based on membrane integrity and DNA fragmentation[104]. Each stage of the cell life cycle exhibits characteristic morphology. It has been documented that cell morphology may be used to infer the cell status. Flow cytometry and fluorescence microscopy can be used to detect several of the morphological changes characteristic of apoptotic cells. In particular, flow cytomery can be used to calculate the percentage of apoptotic cells present in a cell population and fluorescence microscopy can describe briefly the different morphological features of cell undergoing apoptosis. Fluorescence imaging provides the means of identifying the different stages of cell growth and death[105]. To fully understand apoptosis, one should investigate not

only at single cell level, but also at the population level to compare the percentage of apoptotic cells within the population. Due to the capacity to analyze and isolate simultaneously a large number of singe cells for different parameters and requirements, FACS has changed our understanding of the behavior of cells in culture. Investigation into apoptosis during the course of a cell culture cycle can help us provide the checkpoints for the future research.

4.2. Results

4.2.1. Investigation into Cell Growth Characteristics

Both kinetics of cell growth and metabolism are desired for a better understanding of cell physiology and program of apoptosis. For these reasons, the first consideration was to describe the kinetics of CHO cell growth. Growth characteristics of CHO cell culture had been studied in batch culture. Spinner flasks with 50mL working volume were used in this small-scale culture system to describe the time profile of the concentration of cells, nutrients and metabolites. Both the viable cell number and the specific growth rate reach a maximum and decline afterwards. The cell growth curve in SFM4CHO medium with 20mM glucose and 6 mM glutamic acid in batch culture is given in Figure 11. Figure 11 shows that the growth curve for batch run had been broadly divided into three phases: lag, exponential and post exponential. The specific growth rate was $\mu_{avg} = 0.6718 / day$ during the exponential phase and maximum specific rate occurred in the late exponential growth before cell concentration reached its peak. The maximum cell

concentration achieved was 4.37×10^6 cells/mL, as well as the cells keeping high viability (over 90%) as determined by Trypan blue dye on day 7. Cell death was also minimal during this time.

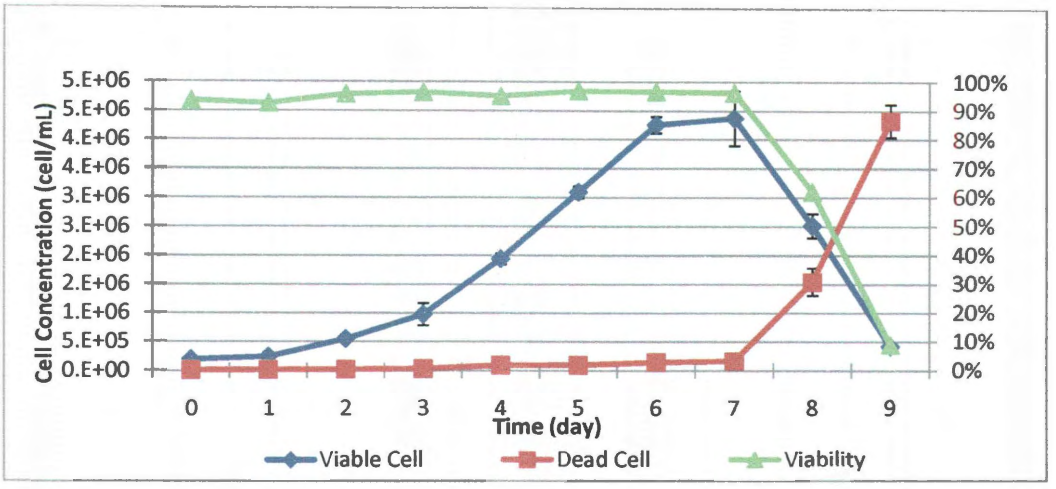

Figure 11 Time courses of viable and dead cell number in batch culture

To further confirm this observation and quantitatively investigate the cell growth behavior, FACS was applied as a tool to detect and monitor the transition of apoptotic cells and estimate subpopulations in batch culture. Cells stained with Annexin V-FITC and PI can be distinguished into subpopulation between viable, early apoptotic, and late apoptotic, and can help us examine the kinetics of apoptosis. Equivalent experiments were performed. During the exponential phase, the conditions of growth were more stable, the samples were analyzed every 24 hours. However, samples were analyzed every 4 hours at the end of exponential phase and every 2 hours post exponential phase because apoptosis is a relatively fast and dynamics bioprocess [106].

In comparison to the samples in exponential growth phase, the Annexin V-FITC fluorescence was significantly shifted to higher intensities very quickly in the post exponential phase.

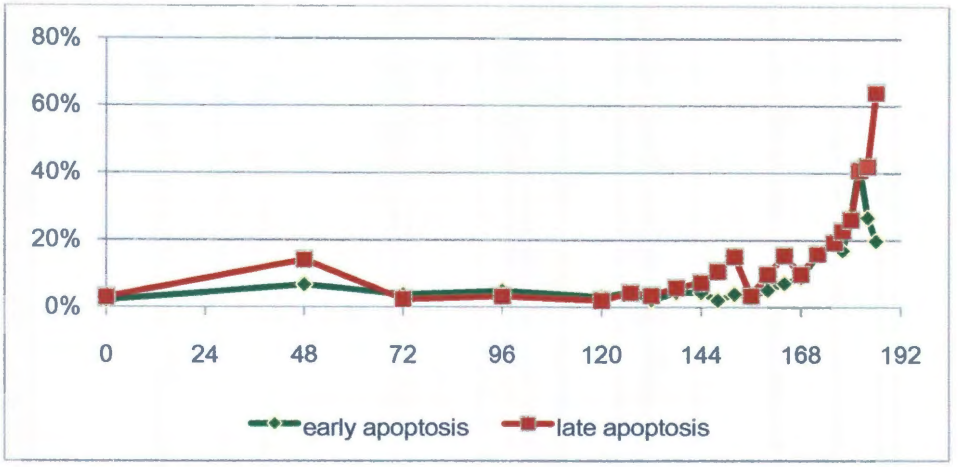

Figure 12 Time courses of early and dead late apoptotic ratios in batch culture

The results are described in figure 12. Initially, in the lag phase, both the early and late apoptotic ratios were higher than those in exponential growth phase due to the cell growth adaption. It was noted that apoptotic ratio in lag phase was approximately two-fold higher than that in cell growth exponential phase. During the lag phase, cells were preparing for reproduction, but no increase in cell number. It is possible because that certain amount of cells underwent apoptotic while there was no cell growing. Moreover a significant increase of ratio of late apoptotic cell but no increase of death ratio was observed. When cells entered exponential growth phase, stable apoptotic rates were found with early apoptotic ratio at (3.61±1.10) %

and late apoptotic ratio at (3.17±0.81) %. The apoptotic ratios and dead ratio were compared. A significant apoptotic death was found between day 6 and 7 (144 to 168 hours) due to the nutrient depletion. Early apoptotic ratio stayed constant up to 160 hours, while late apoptotic ratio up to 144 hours. But death ratio remained at (4.67±1.59) % for more than 168 hours (day 7). It is possible that late apoptotic ratio is significantly more sensitive than viability at quantifying cell status. In contract, comparison of stabilities between early and late apoptotic ratio from lag to exponential growth phase indicates that cells from early to late apoptotic status are more sensitive to environmental changes and the active phase of late apoptotic might be relatively shorter. With the nutrient depletion, cells tend to display exponential apoptotic death ratio. After cell concentration reached its peak, the total cell number was supposed to be constant and apoptotic ratios were applied to fit the data. The expressions of $\mu_e = \frac{1}{X_v}\frac{dX_e}{dt}$ and $\mu_l = \frac{1}{X_e}\frac{dX_l}{dt}$ were considered, where μ_e and μ_l represent the specific apoptotic rates for early and late apoptotic cells respectively, and X_v, X_e, and X_l are the viable, early apoptotic and late apoptotic population respectively. Specific rates of apoptotic ratios were calculated and the experimental data in cell post exponential growth phase were analyzed by nonlinear regression. Specific rates of early apoptotic ratio were found to follow exponential equation as $\mu_e = \mu_{e0}e^{k(t-t_0)}$, where μ_{e0} is the constant of specific apoptotic rate, t_0 is the time point where stable early apoptotic rates are expired, and kis a kinetic constant. The calculated result was

$$\mu_e = 0.003e^{1.56(t-160)} \ (R^2 = 0.943)$$

In contrast, the specific late apoptotic rate did not follow the exponential model and instead exhibited a constant at (0.0914±0.0176) hr^{-1}. The calculated results are shown in figure 13.

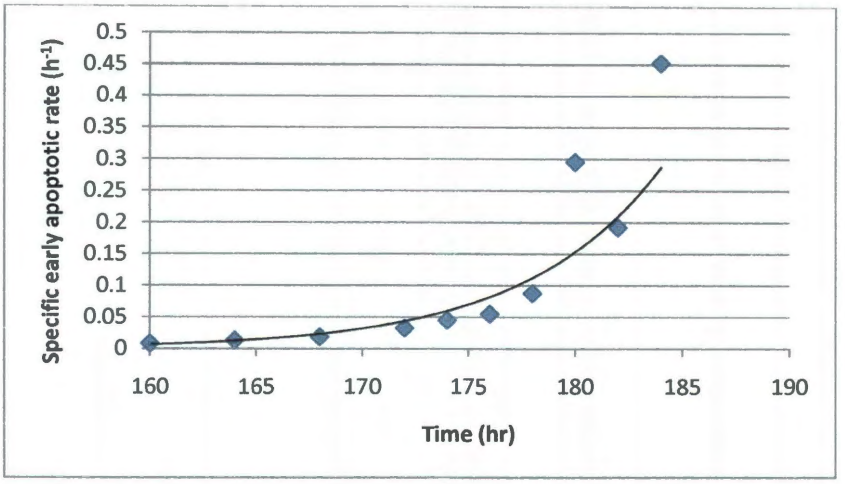

(A)

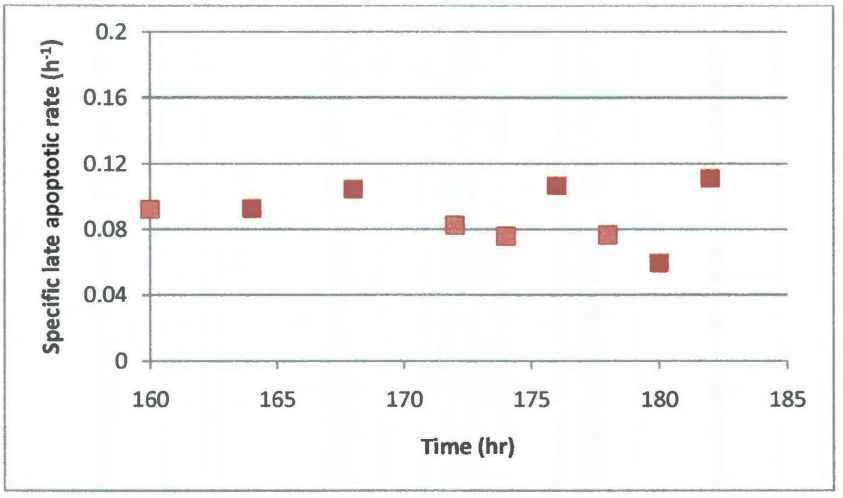

(B)

Figure 13 Specific apoptotic rates as a function of time. Exponetial prediction (-) compared to experimental data for early apoptotic cells (A) and late apoptotic cells (B)

Similar calculations were done for the exponential growth phase with the consideration of all viable, early apoptotic and late apoptotic cells. The specific early apoptotic rate was (0.0324±0.0189) hr^{-1} and the specific late apoptotic rate was (0.0677±0.0221) hr^{-1}, respectively, close to the calculated data above in post exponential growth phase. Overall these data well described the kinetic apoptotic behavior throughout the course of a cell culture cycle.

4.2.2. Fluorescence Image

Images shown in this report were obtained in experiments for batch culture in spinning flasks. 10×, 20×, or 40× were used to observe and characterize the overall population into viable, early apoptotic, late apoptotic and dead cells for a total duration of 9-day culture (figure 14 showed the images during and after exponential phage (day 3 and day 8)). The cell morphology was observed from day 2, the late of lag phase. On day 2, in BF (bright filed) image, some cells still lost the intact structure, and they did exhibit clearly week green in FTIC, however, they exhibited bright red in TXRED. This demonstrated that there were no obvious early apoptotic cells, only late apoptotic cells except viable cells. The week green signal could be observed under the eyepiece, but hard to be captured by camera due to the long exposure time and photo bleaching. This is in good agreement with what we measured by FITC, as the late apoptotic ratio was significantly high. From day 2 to day 7, during the exponential growth phase, apoptotic cells were observed, but viable cells were dominant. On day 3 and 4, most of apoptotic cells were in early stage (Annexin V+/PI-) and were still maintaining an intact structure. Also there

was visible chromatin condensation in some of the cells with no loss of nuclear integrity, which is the typical early apoptotic cell morphology. From day 5, the ratio of apoptotic cell to viable cells was increasing sharply and some of the cells progressed to the late apoptotic stage where the cellular membrane exhibit permeability and stained red by PI as time went on. The trend continued subsequently with some cells receding into late apoptotic stage. During the observation of the whole culture process, the number of apoptotic death cells increased continuously and dominated the total dead cells at the end of the culture. As far as PI positive signals, although Annexin V-FITC and non-vital dye PI could not allow the discrimination of necrotic cells and debris which are both Annexin negative and PI positive, most of the PI positive cells were also Annexin V positive at the end of our culture. These results demonstrate that apoptosis is the prevailing death mechanism in our cell line and culture conditions. From these trends, it seems that the kinetics of transition from early apoptosis to late apoptosis and then to dead cells is much faster than the kinetics of apoptosis induction.

Also fluorescent images taken from experiments indicated that death of the CHO cells is primarily through apoptosis, since red stained number were observed after green stained number. In exponential growth phase, green stained cells were first found and then red ones. That indicates that cell death is via the process from viable, early apoptotic, late apoptotic stages and then to apoptotic bodies.

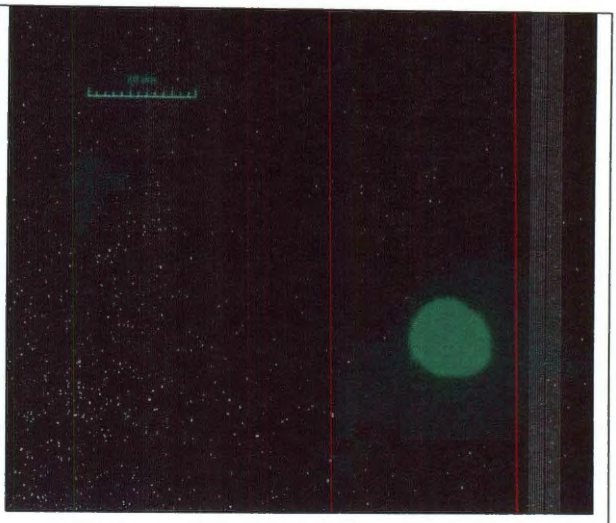

Bright Field (left two: viable; right: early apoptotic)	Fluorescent
Imaging during exponential phase (day 3)	

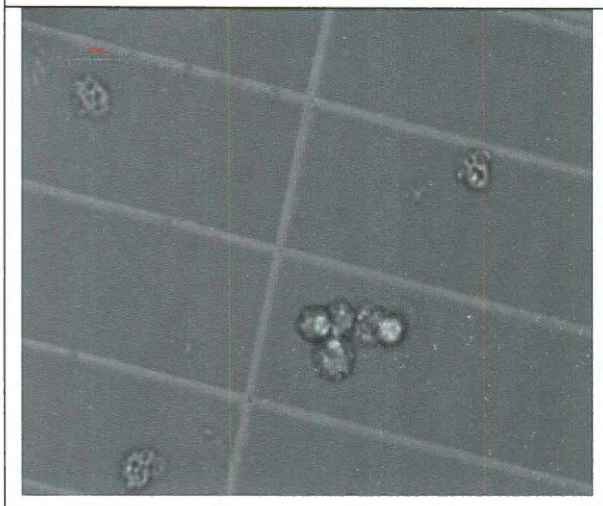

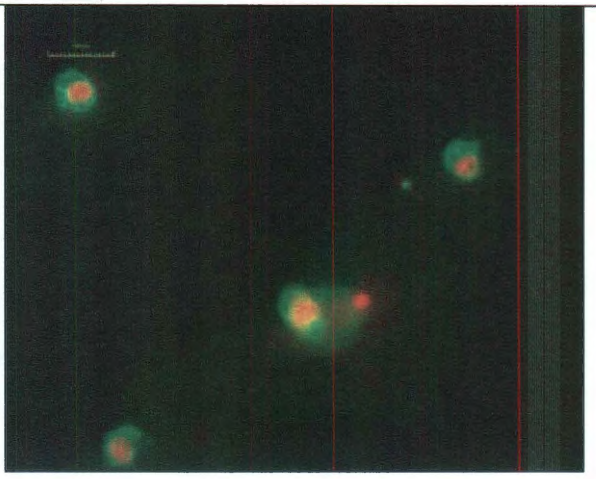

Bright Field (most of them were in late apoptotic stage and lost the intact structures)	Fluorescent
Imaging after exponential phase (day 8)	

Figure 14 Imaging of viable, early and late apoptotic cells stained with Annexin V-FITC and PI under 40× objective (fluorescent images were enhanced by Adobe Photoshop CS software)

4.3. Discussion

Preliminary data from fluorescence imaging used as a tool to capture the changes in cell morphology along the course of batch culture showed the transition from healthy to apoptotic cells. This study led to interesting insights into how apoptosis is executed at single cell level, but included no population heterogeneity. While population measurement emphasizes characterization of overall cell population into subpopulations based on differences throughout the course of a cell culture cycle, it failed to take into account intracellular details. From this point of view, the combination of the fluorescence imaging of single cell and population measurement may help us understand apoptosis during cell culture.

Fluorescence microscope works for our observation as a tool to capture the changes in cellular morphology along the course of cell culture. From the images, dramatic morphological changes, such as chromatin condensation, structure and others were observed. Initially, the integrity of the cell membrane remains intact. The organelles inside of viable cells were distributed evenly (Imaging during exponential phase in bright field). It began to condense to form aggregates at the nuclear periphery in the early apoptotic stage (Imaging during exponential phase in bright field). However, in late apoptotic cells, the chromatin further condensed into discrete parts, and then formed apoptotic bodies (Imaging after exponential phase in bright field). Besides the late apoptotic cells were both Annexin V and PI positive, comparison between early and late apoptotic cells in fluorescent field also showed that fluorescence intensity of late apoptotic cells was significantly higher.

Concomitant with subcellular alterations during apoptosis, cell underwent changes in shape as well as changes in the proximity and spacing of cells within colonies. Viable and early apoptotic cells were round and detached to each other. However, late apoptotic cells showed irregular shapes as well as clustering status of the cell population, indicating significant changes of cell surface during apoptosis. Cell attachment is influenced by cell structures, surface charge characteristics, and hydrophobicity. As is evident from literature available[107-108], apoptosis makes the surface negative charge increased due to the exposure and enrichment of PS on the outer surface of the plasma membrane. The cell surface charges of healthy and apoptotic cells were measured by Zeta Potential analyzer. Results showed that viable cells had surface charge close to neutral (1.1±11.97)mV, while late apoptotic cells had surface negative charge (-17.8±7.45)mV. Although it could not express why late apoptotic cells adhered together, it showed a significant change of membrane during apoptotic.

By combination Annexin V-FITC with PI staining via FACS had been found to give good correlation with the levels of apoptosis throughout the course of a CHO cell culture cycle, during which apoptosis accounted for the major of cell death with constant specific apoptotic rates for early and late stage during the cell exponential phase. And in the post exponential growth phase, early apoptotic cells generated from non-apoptotic cells had an exponential expression on its specific apoptotic rate, while cells from early to apoptotic were still following the rate as similar as that in cell exponential phase. These findings validated those obtained in the fluorescence studies demonstrates that late apoptotic cells are already isolated from

the environmental condition and they just follow a certain rate to finish the whole apoptotic rate. In contract, early apoptotic cells still keep a relationship to environmental condition, indicating that they are still having biological activity.

On the other hand, since the whole process of apoptosis is too complex and many causes can trigger apoptosis in cell culture, only one kind of apoptosis assay cannot fulfill the understanding of apoptosis process, it is important to use the combination of apoptosis analysis methods. Multiple assays will give us a multi-dimensional view of apoptosis, by analyzing more than one apoptotic characteristic simultaneously. This may be very informative about the nature of the apoptotic pathway and may give us convincing confirmation that apoptosis is occurring during cell culture. With the availability of FACS, we have a wide variety of instruments, single and multiple laser, flow and imaging, to observe and characterize apoptosis. TUNEL, caspase analysis and DNA ladder will be applied for elucidating the complex progression of apoptotic death. It is proposed to use this multiple approach to analyzing apoptosis in cell culture to provide information in multiple early, intermediate, and late apoptotic stages.

Chapter 5

Apoptotic and Non-apoptotic Cell Partition

5.1. Introduction

The long-term goal of our studies is to identify metabolic differences between apoptotic and healthy cells using functional genomics approaches. In order to reduce the effects from a vast number of extracellular factors, we want to observe and characterize apoptotic and healthy behavior in the same "natural culture" condition. In our work, no extreme conditions but only metabolic stresses will be investigated for the aim. In order to obtain the apoptotic cell population from the cell culture, different cell separation techniques were used as part of sample preparation. Cell separation is increasingly used in biotechnology to isolate a specific cell population from a heterogeneous mixture of cells. Magnetic Associated

Cell Sorting (MACS) and other systems such as, aqueous Two-Phase Systems (ATPSs) and gradient centrifugation were compared.

MACS developed rapidly in the past decade. The interaction of a cell with a magnetic field is usually mediated by a magnetic particle conjugated to antibodies or a chemical reagent, which binds specifically with the targeted cell population. FACS provides a method that allows us to analyze quantitatively several fluorescence parameters of individuals and purify them. However, what we need is bulk sorting for the future analysis. For example, in order to fulfill the requirement of proteomics, we would need to separate different samples on the order of 10^7 cells to detect expressed proteins, from a total starting population of $\sim 10^8$ harvested cells. Even if we use a common high-speed cell sorter (BD FACS Vantage SE), which sorts cells at rates up to 25,000 cells/second, the translation time is at least 4,000 second. This does not take into account cell losses due to sample preparation and handling or time losses due to technical issues. Also, cross contamination becomes a problem at the highest sorting rate. However, apoptosis is a rapid and dynamic process [106], and normally, apoptosis detection using flow cytometer should be completed within 1 hour after cells are labeled. Moreover, during the sorting process, cells are exposed to conditions that might bring about changes in gene and protein expression. Preliminary research in our group on cell viability and apoptotic status in buffer solutions has shown that all the separation should be finished in 2 hours. Therefore, it is important that isolated cells retain their viability and biological function after the separation process, which means that traditional FACS based methods do not satisfy our requirements. In order to separate cells, the effective

method needs also the drive to separate the targeted cells. Compared to FACS, MACS uses magnetic field as force, which is more powerful, efficient and less time-consuming. Several examples of magnetic separation systems have been reported in recent years with good purity (>95%) and high throughput (~10^{11} cells/hour)[82].

The selection of healthy and apoptotic cells is a prerequisite for comparing different subpopulations. In this study we applied commercially available Annexin-V directed against cell surface activation sites for selection of apoptotic cells under high throughput conditions. The system consists of a column filled with polymer-coated steel beads that when placed inside a magnetic field creates a high magnetic gradient capable of retaining magnetically labeled cells. Magnetic cell sorting using annexin-V microbeads can effectively separate apoptotic and non-apoptotic cells.

A previous study by Nam *et al*[88] determined the conditions and requirements for viable and dead CHO cell partition using ATPSs of PEG 8000 (4%) and dextran T500 (5%) in 10mM sodium-potassium phosphate buffer. The ability of Percoll density gradient centrifugation to remove spermatozoa with PS translocation of membrane fraction was studied to select non-apoptotic spermatozoa[109] and apoptotic thymocytes were enriched via density gradient centrifugation[110]. We then compared different separation technologies to achieve separation of apoptotic and non-apoptotic cells. Our results proved that the MACS technology surpasses the results achieved by other systems.

5.2. Results

5.2.1. Effect of concentration of binding beads

The ideal concentration of antibody beads leads to label the target cells without or with the least possible unspecific staining of non-target cells. Although commercial device MiniMACS system was used, the optimal concentration of antibody beads was only designed for the depletion strategy. The concentration of magnetic beads depends on the target on the cell surface receptor as well as on the affinity of the antibody and a Langmuir type saturation relationship was reported when binding the appropriate cell receptor[111]. It is important to note that the amount of apoptotic surface marker, the exposure of phosphatidylserine (PS), at the outer plasma membrane, depends on the apoptotic stages. Considering the classical antigen-ligand interaction theory, the amount of binding beads influences the separation results. The recommended concentration was 200μL/10^8 total cells. To determine the effect of labeling bead concentration, cells stained with four different concentrations of magnetic beads were tested: 50, 100, 200, and 400μL/10^7 target cells. After labeling, the fluorescence intensities were measured via FACS (only FITC intensity was considered). Figure 15 shows the separation performance versus labeling bead concentration.

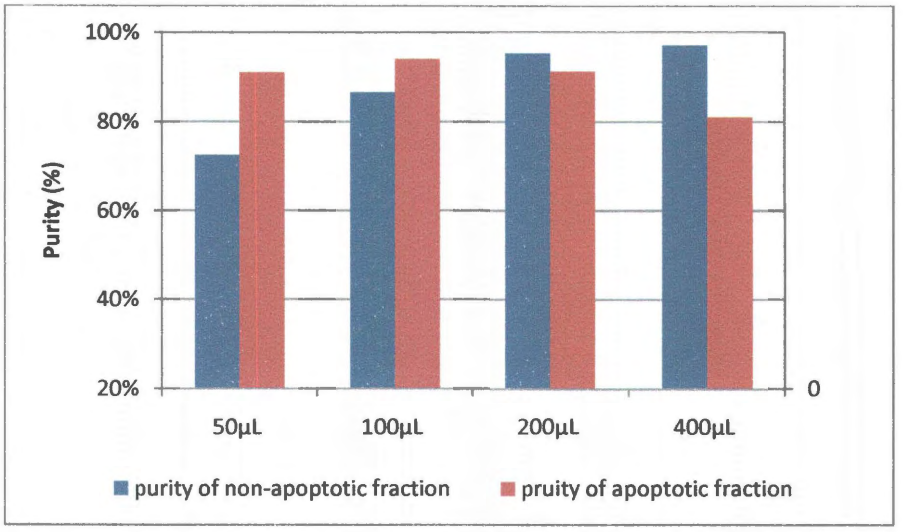

Figure 15 MACS separation performance in different labeling bead concentrations for samples from stationary phase.

The same test was applied for samples from exponential growth phase (Figure 16). Only the negative selection (non-apoptotic fraction) was considered due to the very low apoptotic ratio during exponential growth. The histogram of purity did not show obvious differences under each treatment, except the result from the test of 50μL/10^7 target cells. It has been demonstrated that during exponential growth, the average amount of PS externalization is less than that in stationary phase, resulting in less binding positions. Saturated binding could then be reached using a concentration of magnetic beads of 100μL/10^7 target cells. Comparison between the two figures shows that the binding saturation is related to the property of cells and antibody conjugates, not to the relative amount of antibodies.

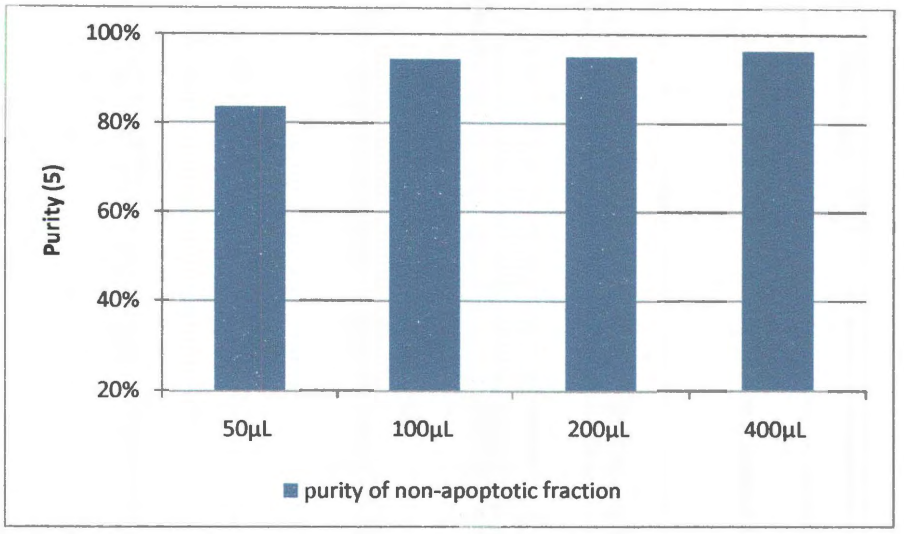

Figure 16 MACS separation performance in different labeling bead concentrations for samples from exponential growth phase (apoptotic deletion only)

It is important to note that when the labeling bead concentration was too high or too low, the results were not good. Too high concentrations of antibody beads (400µL/10^7 target cells) might lead to unspecific labeling of non-apoptotic cells. This would reduce the purity of the selected fraction, which led to lower purity of apoptotic fraction than the other treatments. Too low concentration of antibody beads (50µL/10^7 target cells) might lead to an insufficient labeling of apoptotic cells, resulting in a reduced purity of the annexin negative fraction. Therefore 100 and 200µL/10^7 target cells were regarded as the optimal concentration and were used in subsequent experiments (100µL/10^7 and 200µL/10^7 target cells were used for samples in exponential growth phase and samples in stationary phase, respectively).

5.2.2. Separation performance in different cell status

Several values are commonly used in evaluating the performance of cell separation processes, such as recovery, final purity, enrichment, and throughput rate. However, purity and recovery depend on the objective of the separation, the starting cell mixture characteristics, and the method used for isolation. To evaluate the performance of MACS, raw cell samples (approximate 2 to 5×10^7 total cells) were carried out from middle and end of growth exponential phase (day 4 and day 6.5), respectively. Data in Figure 17 are representative flow cytometry plots before and after separation.

No matter whether apoptotic cells were in low (5~10% of all in our tests during exponential phase) or high percentage (more than 30% in cell transition phase), after separation, the annexin-V negative fraction prepared by MACS had a low apoptotic ratio, less than 2% of total cells, while the annexin-V positive fraction, which was labeled, was retained in the column. The retained fraction eluted from the column after removal of the magnetic field had a rather high apoptotic ratio more than 80%, which represents about 10-fold enrichment. Similar sorts have been done with the apoptotic ratio at 85% to 97%, depending on the initial apoptotic rate and loading amount. Comparing the results of purity in different phases, the percentage of healthy cells collected in the annexin negative fraction was significantly higher during exponential growth, and less debris was generated during passing through the column. However, samples from the transition phase between cell growth exponential and stationary phase had high levels of debris in

annexin negative fraction after separation due to the mechanical damage caused by matrix material during passing through the column. It is possible that this was caused by the increased sensitivity to mechanical damage due to nutrient limitation in stationary phase.

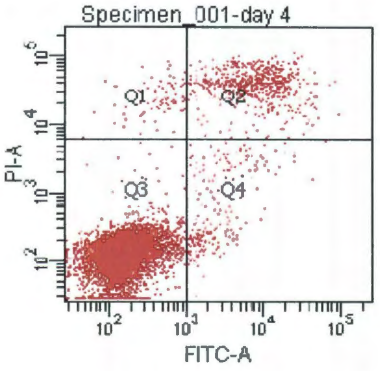

Before MACS

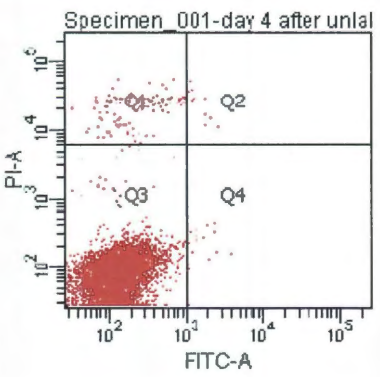

Unlabeled partition after MACS

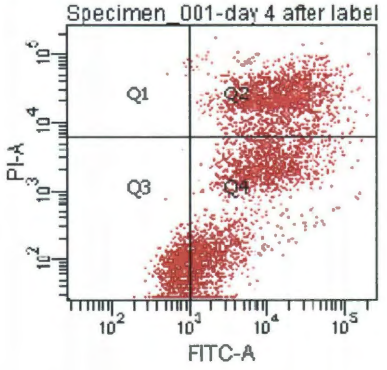

Labeled partition after MACS

	Healthy Q3	Early apoptotic Q4	Late apoptotic Q2	Debris Q1
Before MACS	90.1%	2.4%	6.6%	1.0%
Unlabeled	98.4%	0.2%	0.1%	1.3%
labeled	18.0%	45.8%	36.2%	0.1%

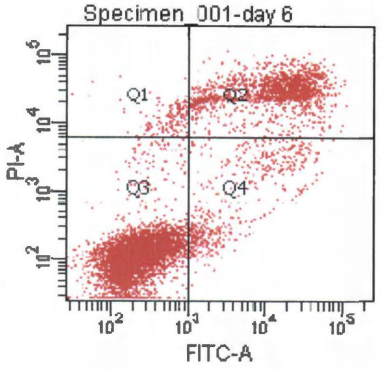

Before MACS

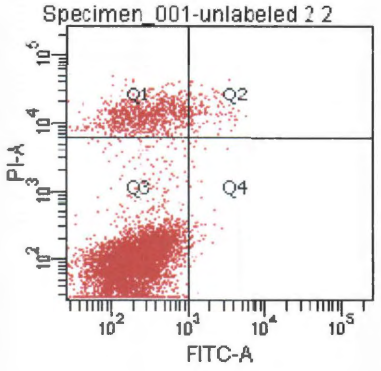

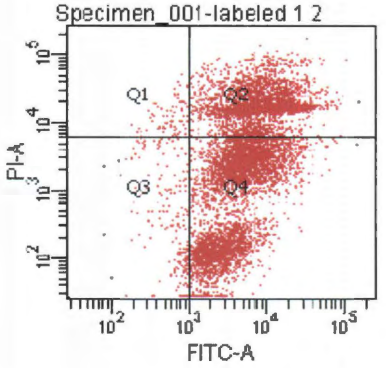

Unlabeled partition after MACS | Labeled partition after MACS

	Healthy Q3	Early apoptotic Q4	Late apoptotic Q2	Debris Q1
Before MACS	68.1%	6.7%	23.5%	1.7%
Unlabeled	88.5%	0.6%	1.4%	9.5%
labeled	2.4%	56.9%	39.9%	0.8%

Figure 17 MACS results

The recovery of separation was calculated by dividing total number of target cells in each fraction by the initial count of cells. In unlabeled partition, the recovery (72%) of samples from cell exponentially growing cells was much higher than the recovery (53%) from stationary phase samples. It is possible that the debris generation led to low recovery. However, in both cases cell recoveries in labeled partition are not in good agreement with the expected values, since the overall recovery is only around 40%. It is possible that when the magnetic field was removed a certain amount of labeled cells were still retained in the column. A modified separation process for labeled fraction with more flush was also tried, but still with lower separation recovery. These results suggest that more studies need to be done to have a better understanding of the process.

5.2.3. Effect of mobile phase on cell separation

As can be found out in the flow cytometry data, a significant population of debris still exits after separation. Due to the fact that cells will be easy damaged under the condition without nutrients, it is necessary to determine how to protect cells from mechanical damage during MACS process. After taking from medium, cells will be washed by PBS buffer and be incubated in PBS buffer or binding buffer at room temperature or at 4℃. Only pH value and osmolarity are close approximations to the normal medium without any protective factors. In cell culture technology, although serum-free formulations are required and developed in both the research and the industrial communities, serum is also used in some tough conditions, such as cryopreservation, to protect cell survival. In order to reduce the sensitivity to mechanical damage during cell separation through the column and minimize the debris in annexin negative fraction, serum was tested because serum can protect cells from shear induced by mechanical agitation[110]. Cell separation was carried

out using two different mobile buffers during passing the columns. Samples were collected in stationary phase. Using the optimized operating conditions for the first steps and after incubation with magnetic beads, binding buffer and medium with 10% serum were used as mobile phase to elute the column, respectively.

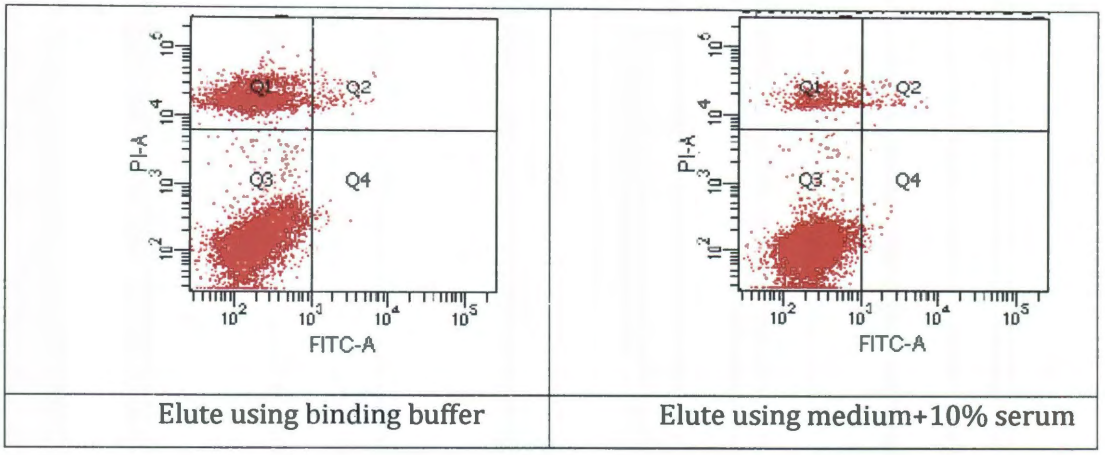

(a)

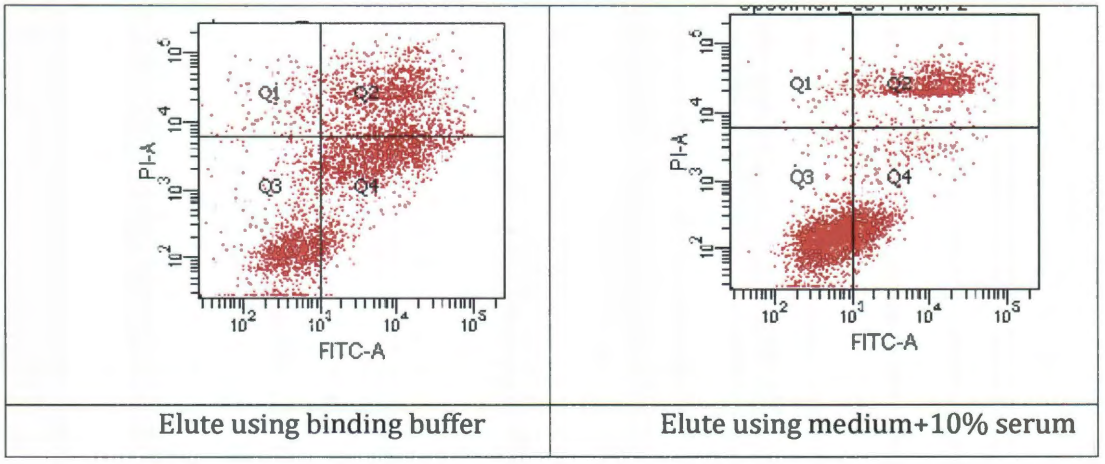

(b)

Figure 18 flow cytometry analysis after MACS separation using two different mobile phases. (a) unlabeled partition, (b) labeled partition

Figure 18 presents the flow cytometry analysis after MACS separation for both treatments. A remarkable decrease in the debris ratio in the annexin negative fraction was obtained under the treatment with the medium with 10% serum to elute the column, about 23- 70% reduced, depending on the initial cell status and loading amount. Comparing the result to the raw sample from middle growth phase, although medium with 10% serum as mobile phase could not prevent the occurrence of debris generation during passing the column, it significantly reduced the total number of the debris in the annexin negative fraction. It demonstrates that serum can act as a shear protecting agent in hard condition during cell separation. However, the labeled, annexin positive, fraction contained a considerable percentage of unlabeled cells using medium with 10% serum as mobile phase. It is possible that some components in serum, such as fibronectin, promote attachment of cells to the substrate. Separation theory for MACS system indicates that all non-magnetically labeled cells should elute from column. In this case, target labeled cells as well as non-target cells could be clumped and a certain amount of the undesired cells were retained on the column. This made the very high unlabeled cell contamination in apoptotic fraction, resulting in a reduced purity.

5.2.4. Comparison of MACS and other separation methods

To further enrich for healthy or early apoptotic cells, other separation techniques, such as ATPSs and density gradient centrifugation were performed. Preliminary results under fluorescence microscope show that though the apoptotic cell population contains varying degrees of early and late apoptotic cells, it is

interesting to note that early and late apoptotic cells have some differences in morphology as well as viable and dead cells have physical differences like size, shape and density.

5.2.4.1. ATPSs

ATPSs have been used for the isolation and characterization of different types of cells. This is a conventional technique that can separate cells easily and effectively without using antibodies. The studies completed by Nam *et al*[88] determined a favorable condition to separate CHO cells. The optimum pH for the fractionation was 6.6, however the pH for our experiments is 7.4. The value of pH affects both surface charge and hydrophobicity[113]. Therefore, the surface properties of mammalian cells have a significant effect on fractionation efficiency using ATPSs. To test the fractionation efficiency of viable and dead CHO cells partitioned at pH 7.4, viable and dead cells were mixed at a ratio of viable to dead cells around 2:1 for test. After cell separation, viable cells were distributed to the PEG-rich top phase with a fractionation efficiency of 80~88%. With the increasing of settling time, the cells were distributed on the interface by sedimentation. A modified ATPS process using centrifugation during phase separation was investigated to accelerate the process and improve separation efficiency. However, although the viability was improved, when we checked apoptotic ratio, a significant population of apoptotic cells still existed before and after ATPS.

Previous research on cell separation using MACS and ATPS respectively shows that there is a gap on loading capacity to combine MACS and ATPS due to the

working concentration. MACS has a high loading capacity is around 2×10^8 cells/ml. However, one-step of ATPS is approximate 2×10^5 cells/ml, much lower than MACS. Generally, centrifugation can narrow the gap. However, the total initial cells number is $\sim10^8$ to make sure get enough enriched apoptotic cells. That means approximate 500mL of ATPS working solution needed to satisfy the heavy work. In order to reduce the workload of ATPS, a high loading concentration was tested. In general, loading capacity and working volume are important factors to consider when evaluating cell separation processes. However, the test of high initial loading concentrations in one-step of ATPS has suggested that separation is not efficient. Concerns about its limited loading capacity have led us to develop and optimize a one-step of ATPS device. We propose to test multiple-step of ATPS instead of one-step to increase the purity. Additional experiments will be developed to optimize separation, recovery and to maintain cell status.

5.2.4.2. Ficoll gradient centrifugation

Apoptosis is accompanied by water loss, cellular shrinkage and chromatin condensation in the early phase[30, 32, 54]. Viable CHO cells with density of 1.051g/mL were reported[114] and the density of apoptotic cells was found to be higher, 1.082-1.095g/mL[115]. We exploited these physical characteristics to develop our method to isolate apoptotic and non-apoptotic fraction, which is based on the evaluation of cell size, density, and surface details. Commercial product, Ficoll-Paque Plus containing 5.7% (w/v) ficoll 400 (GE healthcare, NJ), and modified formula using Ficoll-400(Sigma, MO) and FBS were tested. Samples were taken

from the late exponential phase with an apoptotic ratio of 19.1%. Centrifugation caused non-apoptotic cells to accumulate at the interface between the density gradient material and culture medium overlay and the apoptotic cells were enriched in the bottom phase. The results are presented in Table 7.

Table 7 separation results of density gradient centrifugation under different treatment

Material	Density (g/mL)	non-apoptosis		Apoptosis	
		Purity	Recovery	Purity	Recovery
Ficoll-Paque Plus	1.077±0.005	86.4%	48%	66.9%	19%
10% Ficoll-400	1.049±0.010	83.6%	33%	51.8%	31%
20% Ficoll-400	1.024±0.018	89.1%	24%	34.2%	16%

From the data above, the density gradient centrifugation process proved to be working with the healthy enrichment rates at around 4-fold and apoptotic enrichment rates at 2 to 3-fold. It performed lower efficiency than MACS, and more debris were generated due to the centrifugal force and interfacial tension. It then appears that apoptotic cell density and morphology were not high selectable markers. The recoveries were rather low due to samples taking form interface between layers.

5.3. Discussion

Our target is to realize fast isolation of apoptotic and non-apoptotic cell population with good purity and high throughout. Results derived from the application of MACS to obtain two different subpopulations, healthy and apoptotic

cells, present encouraging results. While previous reports had focused on apoptotic depletion, such as immunomagnetic separation of membrane-intact and non-apoptotic spermatozoa[109, 116], in our study we attempted to evaluate the performance of the modified separation technology to obtain the two selections together.

It was shown that using the modified procedure we achieved higher separation efficiency compared to what we obtain from the standard procedure suggested by the vendor. This can be because the standard procedure is designed for depletion strategy (negative selection). The standard procedure uses the magnetic beads over its saturation value to ensure that the maximum binding equilibrium is reached. The supersaturation would reduce the purity of positive selection as we discussed previously. To increase the separation efficiency of positive selection, different amounts of binding beads were applied in different cell status, exponential growth and stationary phase, respectively.

A debris-reduced fraction can be obtained by modifying the mobile phase. We attempted to evaluate the effect of growth medium with serum instead of normal binding buffer from the standard procedure. When the separation process during passing column was applied, the separation column could be viewed as an affinity chromatography, the binding interactions on apoptotic cells dependent on the strength of antibody-antigen interaction.

Growth medium with serum would reduce the mechanical damage as well as the binding strength. Using this strategy, we could only obtain enriched viable cells

in non-apoptotic fraction at the expense of recovery for the samples from the stationary phase. However, for apoptotic fraction, to obtain higher purity, higher binding level was required, standard binding buffer was used as the mobile phase.

From the brief comparison among MACS, ATPS and density gradient centrifugation, it is clear that MACS is the best method to obtain non-apoptotic and apoptotic fraction with high purity and throughout. Even with a modified ATPS process, we haven't achieved stable and high separation efficiency. Similar results were obtained with gradient centrifugation. This can be because both ATPSs and gradient centrifugation depend on cell's physical criteria, unlike MACS, which is based on affinity. Although other separation systems are not as good as MACS using annexin V, many morphological as well as biochemical differences between apoptosis and non-apoptosis are observed.

In conclusion, it has been experimentally demonstrated that it is possible to obtain high purity apoptotic (less than 10% of contamination by others) and healthy fractions (less than 3% of contamination by apoptotic cells), which provides samples for further analysis, such as metabolic flux and proteomic analysis.

Chapter 6

Estimation of Specific Glucose Uptake Rates in Early-apoptotic State in Culture of CHO Cells

6.1. Introduction

Assimilation of glucose reflects the physiological state of the cell culture. The uptake rate of glucose will also help in determining the importance of metabolic regulation. Evaluation of glucose uptake ability in cells plays a fundamental role in glucose metabolism. Glucose is essential for the survival of cells, and the levels of glucose uptake are dynamic and regulated, which can be seen as cells display increased glucose uptake during growth and decrease glucose uptake when cells undergo apoptosis. The early apoptosis is regulated by the rate of glucose transport [106, 117-118]. But it has not been reported how much the glucose uptake rate decreases from healthy to early apoptotic state. The fluorescent glucose analog, 2-

[N-(7-introbenz-2-oxa-1,3-diazol-4-yl)amino]-2-deoxyglucose (2-NBDG)[119] may provide an indicator for the rate of glucose uptake. It is rapidly uptaken by cells and hence accumulates in cells to a quasi steady state. 2-NBDG was reported to be transported intracellularly by mammalian cells via glucose transporters (GLUTs), the same as glucose [120-121], and also to be phosphorylated by hexokinase at C-6 position as the final accumulation to give fluorescent 2-NBDG-6-phosphate.

If the healthy and apoptotic population will be monitored in the same culture, one difficulty with the measurement and characterization of the glucose uptake for different populations is the fact that only the apparent uptake rate of total cells can be measured in the same pool using common methods. In this research, we developed and implemented a fluorometric method to directly evaluate glucose uptake rates of healthy and apoptotic cells combining a fluorescent glucose analog with an apoptosis dye, annexin V-PE, at the same condition without separating cells. In addition, since it is hard to measure the intracellular 2-NBDG concentration accurately, there has been no report previously to quantitatively characterize the glucose uptake rate by acquiring the fluorescent density. We applied Michaelis-menten Kinetics equation to obtain the quantitative relationship between measured mean fluorescence intensity (MFI) and intracellular 2-NBDG concentration (C_A). Our results clearly demonstrate that combination of 2-NBDG and annexin V-PE can be used to accurately and reproducibly measure and distinguish glucose uptake rates between apoptotic and healthy cells. .

6.2. Theory

Considering cells taking up glucose and 2-NBDG using a protein-mediated specific system, which can be described by Michaelis-Menten Kinetics as[122]

$$r_G = \rho_T A_C k_{cat} \frac{[G]}{K_G+[G]} = r_{Gmax} \frac{[G]}{K_G+[G]} \tag{11}$$

And

$$r_A = \rho_T A_C k_{cat} \frac{[A]}{K_{GA}+[A]} = r_{Amax} \frac{[A]}{K_A+[A]} \tag{12}$$

Where ρ_T is the glucose transporter density on the cell membrane, A_C is the cell membrane area, k_{cat} represents the constant rate, [G] and [A] are the extracellular concentration of glucose and analog, 2-NBDG, respectively, and K_G and K_A are the half saturation constant, respectively.

Apply the competitive inhibition mechanism due to 2-NBDG is a the competitive inhibitior of glucose for uptake

$$r_A = \rho_T A_C k_{catA} \frac{[A]}{K_A(1+\frac{[G]}{K_G})+[A]} \tag{13}$$

And

$$r_G = \rho_T A_C k_{catG} \frac{[G]}{K_G(1+\frac{[A]}{K_A})+[G]} \tag{14}$$

Then, the relationship between r_A and r_G could be described as

$$r_G = \frac{k_{catG}}{k_{catA}} \left(\frac{\frac{[G]}{K_G(1+\frac{[A]}{K_A})+[G]}}{\frac{[A]}{K_A(1+\frac{[G]}{K_G})+[A]}} \right) r_A \tag{15}$$

Under a given condition, assuming that all the factors are constant, the glucose uptake rate is directly proportional to the 2-NBDG uptake rate.

In addition, 2-NBDG uptake rate can be estimated from the steady state distributions of intracellular 2-NBDG concentration. The degradation of 2-NBDG-6-phosphate to a nonfluorescent metabolite was assumed as a first-order process[120-121]. Then the accumulation of intracellular 2-NBDG (C_A) can be described as

$$\frac{dC_A}{dt} = r_A - r_{deg} = r_A - k_d C_A \quad (16)$$

Where k_d is the kinetic constant of degradation.

Ingrating with the boundary condition (t=0, $C_A = 0$), the expression becomes

$$C_A(t) = \frac{r_A}{k_d}\left(1 - e^{-k_d t}\right) \quad (17)$$

At steady state, r_A is directly proportional to the intracellular 2-NBDG concentration (C_A).

6.3. Results

6.3.1. Effect of 2-NBDG incubation time on MFI

To obtain the optimal incubation time to reach steady state, cells were treated with 2-NBDG (10, 20, and 40μM) for 10, 20, 30, 40 and 60 minutes, then washed with PBS and fluorescent intensities were measured. The time course of uptake of 2-NBDG is shown in Figure 19. The dynamics of 2-NBDG uptakes were

similar in different treatments. Uptake followed a hyperbolic pattern with a fast initial uptake in the first 10 to 20 minutes, followed by a slower uptake approaching steady states values at approximate 30 to 40 minutes. An incubation time of 40 minutes was selected for the analysis.

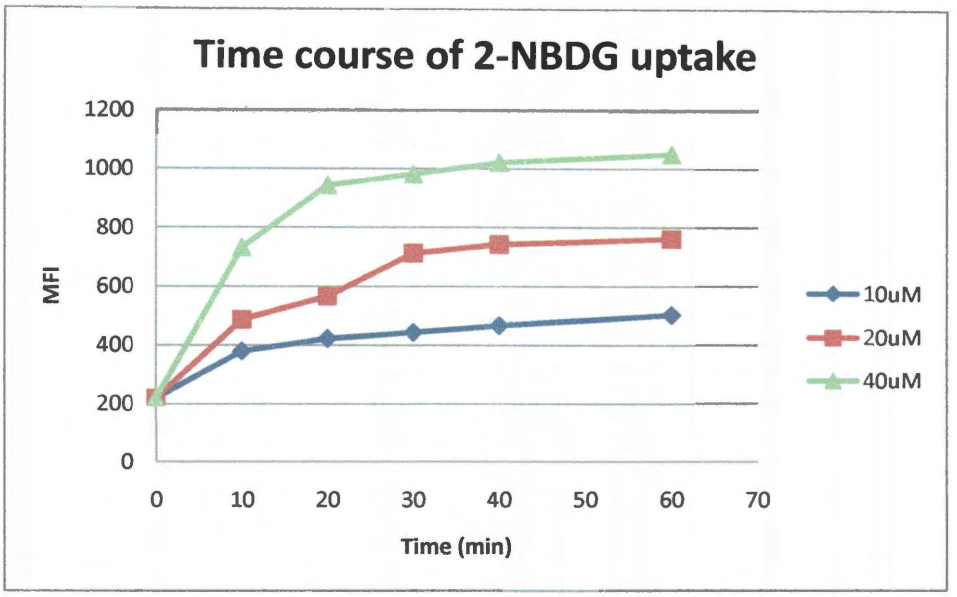

Figure 19 Time course of 2-NBDG uptake by CHO cells at various treatments

Uptake levels of 2-NBDG were fairly low and slow to reach steady state at low concentrations of extracellular 2-NBDG. In addition, at the given extracellular glucose concentration, the competitive inhibition uptake was observed in figure 19 as 2-NBDG is mainly transported by facilitative diffusion via GLUTs, consistent with previously published papers[122, 124]. In order to obtained rapid and high levels of uptake, high incubation concentrations of 2-NBDG would be applied (20, 40, and 80μM).

6.3.2. Fluorescent density (D) has a linear relationship with the intracellular concentration of 2-NBDG

The observed 2-NDBG signal value (V) may be considered to result from the contributions of fluorescent density (D) accumulated in the single cell, background (B) and noise (N), contributions. That is

$$V_{MFI} = D_{2-NBDG} + B + N \quad (18)$$

As a general rule, negative unstained background is at minimally about 10 times noise, thus the noise N is not dominated, which can be considered together with background B. The measured signal value V without any dye can be considered as the sum of N and B. Thus, the fluorescent density of 2-NBDG in cells can be expressed from the difference of V-B-N and $D \approx V - B$. To address the relationship between fluorescent density and intracellular concentration of 2-NBDG, the extracellular 2-NBDG concentration ([A]) was considered, since at steady state, r_A is directly proportional to the intracellular 2-NBDG concentration (C_A) and r_A can be described by [A] via Michaelis-Menten kinetics. Assuming that extracellular 2-NBDG concentration ([A]) keeps constant for a short incubation time, the independent variables $\frac{1}{[A]}$ and the dependent variable $\frac{1}{D}$, by fitting the regression line in least-squares approach. Various concentrations of 2-NBDG (10, 20, 40, and 80 μM) were tested and the results were plotted as $\frac{1}{D}$ versus $\frac{1}{[A]}$ according to the Lineweaver-Burk equation $\frac{1}{r_A} = \frac{K_A}{r_{max}}\frac{1}{[A]} + \frac{1}{r_{max}}$ in figure 20. The results satisfied Michaelis-Menten

kinetics and revealed fluorescent density (D) is directly proportional to the intracellular 2-NBDG concentration (C_A).

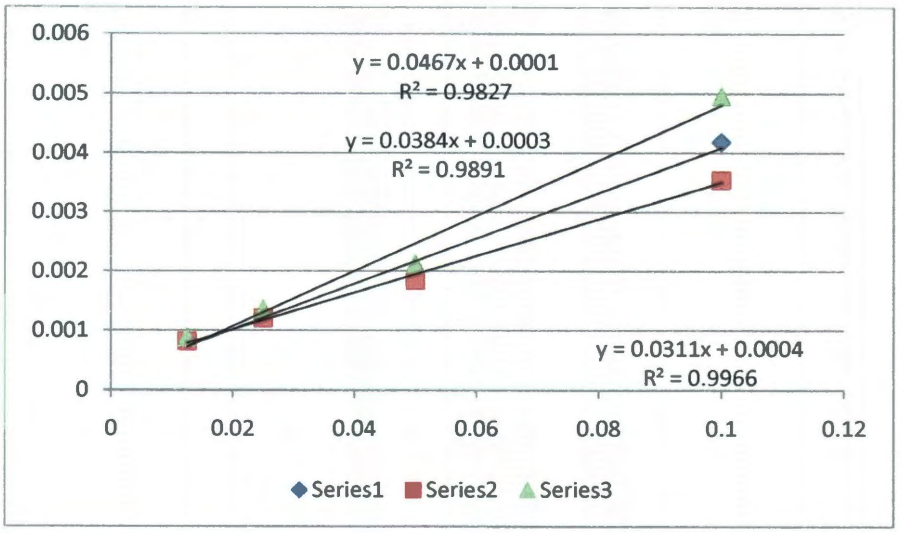

Figure 20 Lineweaver-Burk plots of $\frac{1}{[A]}$ against $\frac{1}{r_A}$

6.3.3. Development of an assay to measure glucose uptake rates of healthy and apoptotic cells simultaneously

In the flow cytometer FACSCanto II, 2-NBDG and PE shares the same blue laser but can be distinguished via different filters. Therefore, the healthy and apoptotic cells can be determined by annexin V-PE staining and their glucose uptake rates can be estimated from the 2-NBDG fluorescent intensity. Cells were treated with 2-NBDG (20, 40, and 80μM) for 40 minutes and then were stained with Annexin V-PE. Under this treatment, the 2-NBDG fluorescent intensity in PE positive population represented the glucose uptake rate of healthy cells, whereas glucose uptake rate of apoptotic cells was obtained from the 2-NBDG fluorescent intensity in

PE negative fraction. Uptake ratio of healthy to apoptotic cells was obtained from the ratio of 2-NBDG fluorescent intensities. From the scatter plots, with the treatment of 2-NBDG and Annexin V-PE together, cells were separated into two populations (Figure 21): the major population with Annexin V-PE negative was healthy cells has higher fluorescent intensity of 2-NBDG, while the minor population with Annexin V-PE positive was apoptotic cells and has lower fluorescent intensity of 2-NBDG. This demonstrates that glucose uptake rate decreased significantly in the early apoptotic cells, to values lower than healthy cells. In addition, it was found that only healthy and early apoptotic cells (Annexin V-PE positive, and PI negative) took up 2-NBDG, while late apoptotic cells (Annexin V-PE positive, and PI positive) revealed to be 2-NBDG negative and the fluorescent intensity of 2-NBDG was as low as the background, consistent with the previous studies using 2-NBDG for the assessment of cell viability[125-126]. Thus, deducting the late apoptotic background from Annexin V-PE positive fraction, the 2-NBDG uptake rate can be calculated.

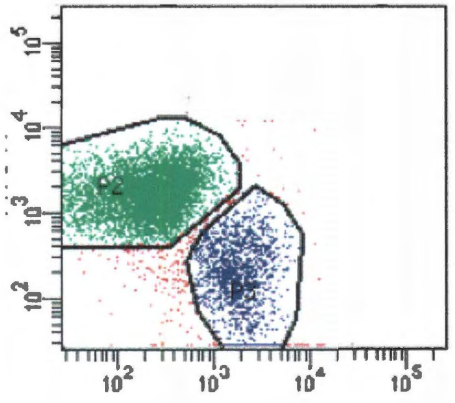

Figure 21 FACS dot plots staining with 2-NBDG and Annexin V-PE

Specific glucose uptake rates were calculated and the experimental data in cell exponential growth phase were analyzed by nonlinear regression.

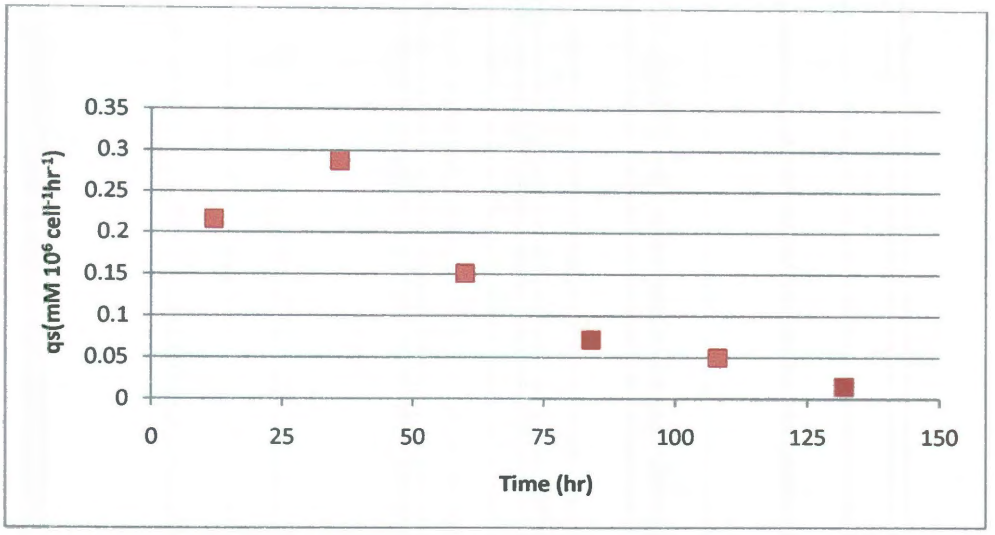

(A)

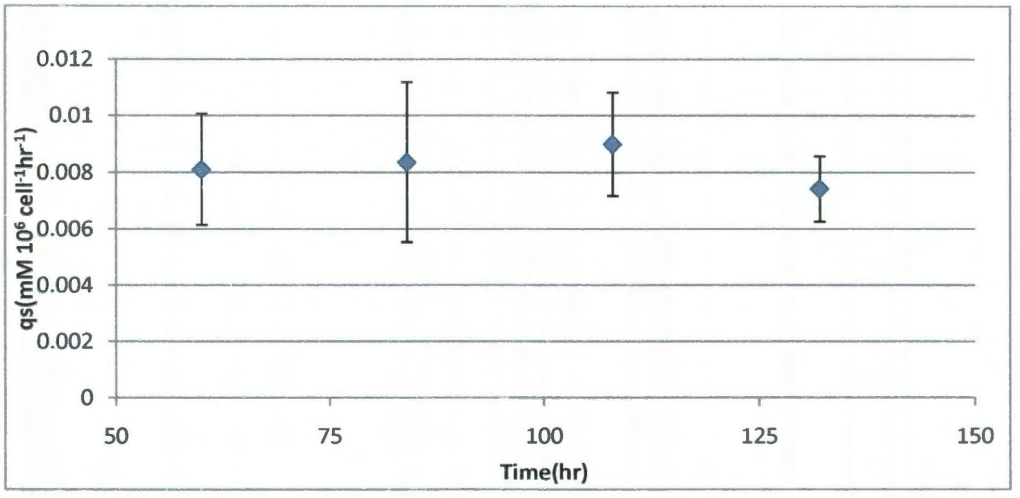

(B)

Figure 22 Time course of glucose uptake rates for healthy cells (A) and early apoptotic cells (B)

Specific glucose uptake rate of healthy cells were much higher than early apoptotic cells in cell exponential growth phase, and it strongly depends on the medium condition. In contrast, the specific glucose uptake rate of early apoptotic cells exhibited a constant at 8.2×10-9 mM cell-1hr^{-1}(Figure 22). The specific glucose uptake rate in healthy was approximate 10 to 20-fold higher than early apoptotic cells in cell exponential growth phase. And, this ratio was much higher in the early cell growth phase after 24 hours. This demonstrated that the growth of healthy cell was somehow substrate limited, while once cells turned to apoptosis, a certain amount of glucose was required to trigger and maintain the apoptotic process. In the previous papers, apoptosis occurs as the result of glucose depletione in batch culture [38, 118, 120, 126, 129], however, it was found that although healthy cells mainly grew and kept its viability, apoptosis was activated in a small fraction of cells, even in rich medium. At the end of the cell growth phase, glucose depletion occurred and intracellular 2-NBDG concentrations reflected 2-NBDG uptake behaviors directly.

6.4. Discussion

Glucose uptake and metabolism play a key role in apoptosis, with the established paradigm involving decreased glucose transport [106]. In this study, 2-NBDG was used as a glucose metabolism indicator. Using the glucose analog 2-NBDG, healthy and early apoptotic cells were found to take up glucose but late apoptotic cells did not. The same observation has been reported in variety of cell types to determine cell viability as well as to compare glucose uptake rates [119,

125, 130]. Previous studies [124, 130]of 2-NBDG in cancer cell lines have shown rapid uptake with a peak uptake within 15 minutes of incubation. Our result in CHO cells show the similar uptake kinetics and reach maximum constat after around 30 minutes. As shown in figure 20, a Lineweaver-Burk plot reveals the linear relationship between fluorescent intensity of 2-NBDG and its intracellular concentration. Therefore, we validated NBDG as an accurate indicator to measure glucose uptake.

After evaluating 2-NBDG's validity as a quantitative measuring tool, we assessed the utility of 2-NBDG and annexin V-PE simultaneously to quantitavely compare the glucose uptake rates between healthy and early apoptotic cells. In conclusion, our study provides an evaluation of the potential of 2-NBDG in apoptotic cells. Healthy and early apoptotic cells have different glucose uptake rates. Glucose uptake is a key step in cell metabolism to control the rate of glucose utilization. Our data indicated early apoptotic cells have rather low glucose utilization. This measurement supports the ability of 2-NBDG to highlight the understanding of metabolic activities between healthy and apoptotic cells.

Chapter 7

MFA of CHO Cells Metabolism in the Apoptotic and Healthy Phase

7.1. Introduction

Metabolic Flux Analysis (MFA) has been become an important tool in metabolic engineering as part of in depth physiological studies for optimizing bioprocess. Using a metabolic reaction network in combination with cellular measurements and mass balances to calculate flux profiles can be used to understand cell metabolism. These metabolic pathways containing pathways contain glycolysis, tricarboxylic acid (TCA) cycle, pentose phosphate pathway (PPP), oxidative phosphorylation, glutaminolysis, the metabolism of other amino acids and biosynthetic pathways determine the fate of any carbon and nitrogen sources in mammalian cells under different environmental or genetic background. However, their metabolism takes place not only in the cytosol but also in the mitochondrion.

On the other hand, cell growth requires a complex medium. Although the metabolism of mammalian cells is very complex, MFA has been applied frequently in mammalian cell cultures. The first application was to use MFA and linear optimization to analyze hybridoma metabolism[131-132] . Subsequently, MFA was used for medium optimization. The effects of medium, supplements and toxins were studied via metabolic balancing, such as dissolved oxygen concentration on the metabolism of hybridoma cell line[133], the effect of replacing glutamine by glutamate on the metabolism of CHO cells[134]. On the other hand, the phenomenon of multiple steady states in continuous cultures of mammalian cells[135] was also investigated via metabolic flux analysis techniques.

The above are only few of many examples for the applications of metabolic balancing to determine intracellular fluxes of mammalian cells during cell growth. Quantification of intracellular fluxes can help to determine the extracellular control parameters for cell culture technology. However, biopharmaceutical production in CHO cells is often decoupled from cell growth [136]. The coupling of cell growth and product formation indicates that the evaluation of the metabolic fluxes in non-growth phase, such as apoptotic phase, can help in understanding cellular metabolism throughout the course of a cell culture cycle. The metabolic behavior of CHO cells at the healthy and apoptotic stage will be different due to the cell fate. The metabolic networks for each stage are in accordance with the general metabolism of mammalian cells and the specific pattern of consumption or excretion of metabolites during the specific stage. Inspired from Agnes' work [137]and the model between apoptosis and cell growth, our research was aiming at connecting

cell fate and metabolic state to build a model that covers central carbon metabolism and amino acid biosynthesis. A great deal of data has been gathered for the various biochemical pathways that are involved in the control and execution of apoptosis[32, 43-44, 57, 59]. This shows that the network of pro- and anti-apoptotic signals is very complex. A simplified metabolic pathway was proposed to show proliferation-apoptosis transition in CHO cell culture via MFA to link cell proliferation and cell death with metabolic behavior. Based on our results from MFA, we would try to explain the basis of variation in apoptotic and non-apoptotic cultures.

CHO cell metabolism consists of thousands of enzymatic reactions. MFA can be a useful tool to reduce these complexities and get a better understanding of mammalian cells[96]. In this chapter strategies and methodologies are developed for quantifying the metabolic fluxes in early apoptotic CHO cells. A simplified metabolic network is shown in figure 23. The individual flux reactions corresponding to the metabolic pathway are listed in the appendix. Two compartments, cytosol and mitochondrion, are considered to represent the presence of the same metabolite in distinct pools as well as mitochondrion/cytosol transfer reactions. The biomass composition of CHO cells is taken from Altamirano result[134], which are similar to typical values found in the literature. The model consists of glycolysis, the pentose phosphate pathway (PPP), anaplerotic reactions, the tricarboxylic acid (TCA) cycle, amino acid metabolism, energy metabolism, and biomass formation. Some linear reaction sequences have been lumped to reduce the number of balance equations. The metabolism of amino acid is lumped into one

reaction until reaching a metabolite in the central carbon metabolism, which is derived from [138] and curated using primary literature.

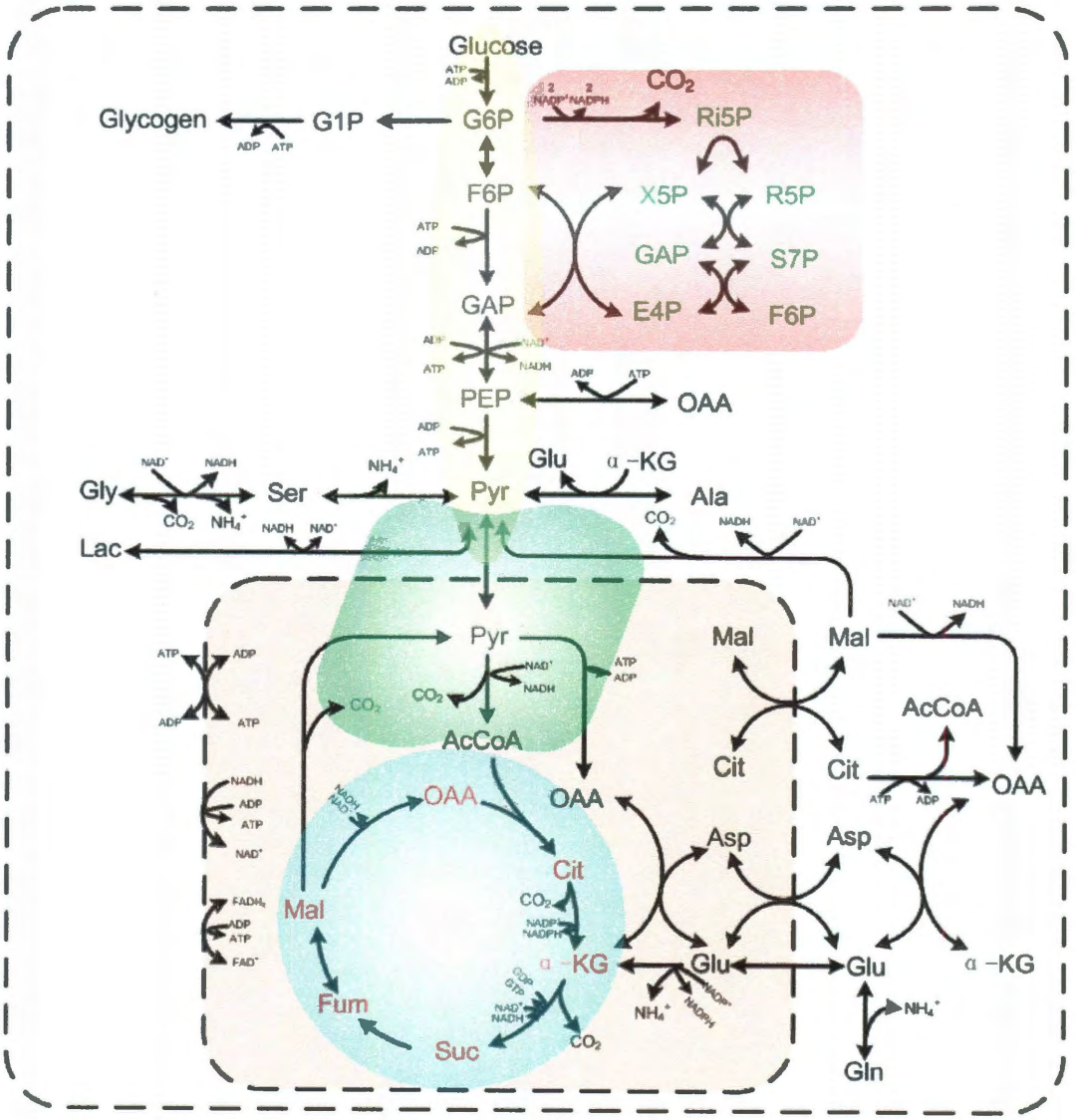

A

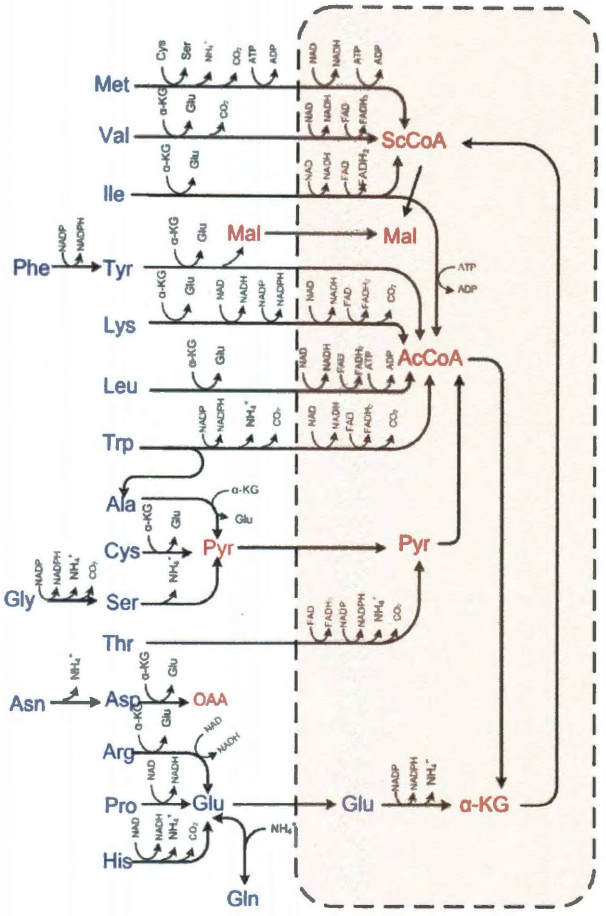

B

Figure 23 MFA Model A) Glucose metabolism and B) Amino acid metabolism

7.2. Results

7.2.1. Metabolic investigations on CHO cells between healthy and early apoptotic cells

Preliminary study showed that in the process of mammalian cell culture, apoptotic rate increases once glucose is exhausted. However, other nutrients like

amino acids are not depleted, which shows that during the initiation of apoptosis in cell culture, depletion of glucose is dominant. The result from combination of 2-NBDG and Annexin V-PE showed significant differences on glucose uptake rates for healthy and early apoptotic cells. The specific glucose uptake rate of healthy cells were found to follow Monod model, while the specific glucose uptake rate of early apoptotic cells did not follow the Monod model and instead exhibited a constant. The specific glucose uptake rate in healthy was approximate 10-fold higher than early apoptotic cells. The low activity of the glucose uptake of early apoptotic cells indicated that a possible steady state assumption for the extracellular condition could be applied for the metabolic flux analysis in early apoptotic cells. During the late exponential phase, most of the cells are from healthy to early apoptotic status and the metabolism of amino acids and glucose is assumed to serve this process. A metabolic steady state for early apoptotic cells is assumed that no matter what kind of phases cells are, exponential or stationary, the metabolic behaviors of early apoptotic are similar. Thus, the measurements of the consumption of amino acids and glucose, and the generation of lactate from the late exponential phase can be considered as the metabolic behavior of the early apoptotic cells and work for all cell phases throughout the course of a cell culture cycle.

The profiles of the consumption of glucose and the generation of lactate are presented in figure 24. Once glucose was depleted, cells entered death phase. Also at the same time, the level of lactate reached the maximum level. Although these data were simple, they showed the relationship between cell death and the environmental factors. In any case, when cells are grown at a high specific growth

rate (figure 11), sooner or later some limiting conditions would be reached and the culture would start the irreversible death phase. At physiological levels of glucose, most of them is converted to lactate and the higher the glucose level in the medium, the higher the rate of this conversion. On the other hand, under low glucose concentration, the glucose is preferentially used for biosynthesis[55]. When glucose was depleted, the lactate produced by the consumption of glucose in CHO cells seems to be converted back to pyruvate and then be channeled towards TCA cycle. Similar finding were reported by Altamirano et al[139], and Tsao et al[140] at low glucose concentrations. And Tsao also hypothesized that glucose and lactate were both considered as carbon sources. However, when the concentration of lactate decreased, cells were almost in late apoptotic stage, where they lose the ability of uptake nutrients, and nutrients could not be used. It should be noted that this unique behavior might be related to the cell line and culture conditions.

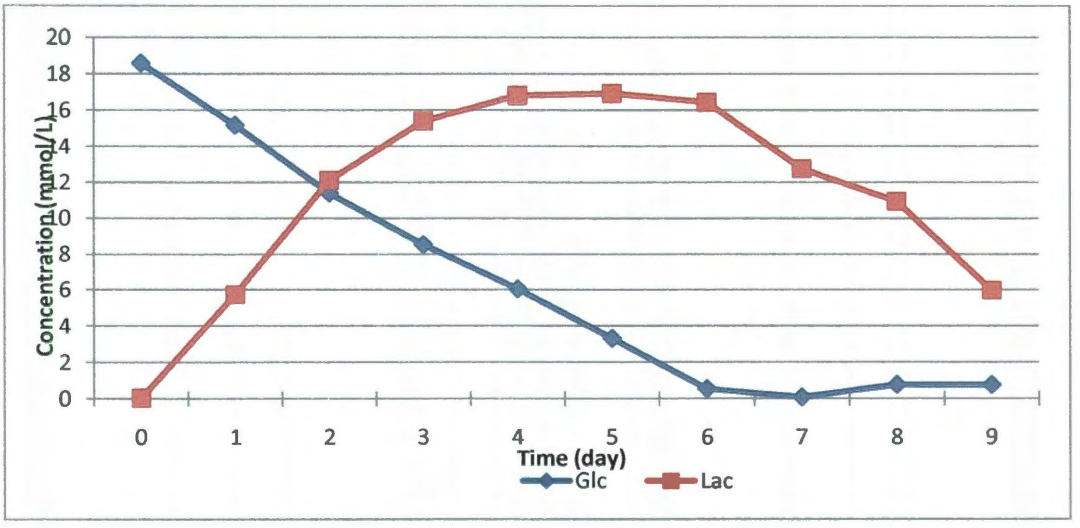

Figure 24 Profiles of glucose consumption and lactate formation

The metabolite concentrations were plotted against the corresponding glucose concentrations. Rates were determined from the plots using linear regression at two distinct growth phases, at exponential growth phase and at stationary phase. In the case of amino acids, most of them followed a linear relationship to glucose consumption during the exponential growth phase. However, few of them did not show linear relationship to glucose consumption very well, such as lysine, asparagines, and methionine. In the healthy cells, among the amino acids, aspartate, alanine and glycine showed production while all the others were consumed. On the other hand, in the apoptotic cells, only alanine was generated while all the others were consumed. During the exponential phase, the specific rates of metabolites formation were calculated using the equation [133]

$$[S] = [S_0] + \frac{q_S X_0}{\mu}(e^{\mu t} - 1)$$

where $q_S$is the specific rate, $[S]$is the measured metabolite concentration, $[S_0]$ is the initial metabolite concentration, $[S_0]$ is the initial biomass, μ is the specific cell growth rate and t is the time. While the specific rates of metabolites in early apoptotic were estimated using the measured metabolite concentrations at stationary phase with the equation

$$[S] = [S_0] + \frac{q_S X}{t - t_0}$$

where t_0 is the initial time point.

The data are shown in Table 8 for the cases studied for MFA.

Table 8 Calculated specific uptake rates in healthy and early apoptotic cells

Metabolite	q_S in healthy cells	q_S in early apoptotic cells	Unit
Glucose	-0.15	-0.0082	mmol 10^6 $cell^{-1}h^{-1}$
lactate	0.20	0.0012	mmol 10^6 $cell^{-1}h^{-1}$
ASP	0.43	-0.21	µmol 10^6 $cell^{-1}h^{-1}$
THR	-2.90	-0.14	µmol 10^6 $cell^{-1}h^{-1}$
SER	-11.22	-0.29	µmol 10^6 $cell^{-1}h^{-1}$
ASN	-14.79	-0.79	µmol 10^6 $cell^{-1}h^{-1}$
GLU	-9.38	-2.49	µmol 10^6 $cell^{-1}h^{-1}$
GLY	11.46	-0.27	µmol 10^6 $cell^{-1}h^{-1}$
ALA	4.30	0.36	µmol 10^6 $cell^{-1}h^{-1}$
VAL	-3.02	-0.19	µmol 10^6 $cell^{-1}h^{-1}$
CYS	-11.51	-0.26	µmol 10^6 $cell^{-1}h^{-1}$
MET	-7.26	-0.09	µmol 10^6 $cell^{-1}h^{-1}$
ILE	-4.85	-0.22	µmol 10^6 $cell^{-1}h^{-1}$
LEU	-3.34	-0.09	µmol 10^6 $cell^{-1}h^{-1}$
TYR	-2.91	-0.31	µmol 10^6 $cell^{-1}h^{-1}$
PHE	-3.44	-0.16	µmol 10^6 $cell^{-1}h^{-1}$
LYS	-2.95	-0.32	µmol 10^6 $cell^{-1}h^{-1}$
HIS	-1.13	-0.08	µmol 10^6 $cell^{-1}h^{-1}$
ARG	-3.88	-0.49	µmol 10^6 $cell^{-1}h^{-1}$
PRO	-3.83	-0.04	µmol 10^6 $cell^{-1}h^{-1}$

This basic study will help us understand the intracellular behavior of glucose and other metabolite concentrations on the whole cell culture span and the relationship between the level of glucose and apoptosis, and additional experiments are required to design for supporting this initial evidence.

7.2.2 Estimation of intracellular fluxes

MFA was conducted to obtain the intracellular fluxes using the extracellular measurements. The reaction network model for CHO cells is presented in Appendix A. This model was applied for estimation of intracellular fluxes using external measurements. The fluxes evaluated by stoichiometric modeling are listed in Table 9.

Table 9 Calculated intracellular fluxes via c-MFA

		Healthy	*Early apoptotic*
	Glycolysis		
24	GLC+ATP→ADP+G6P	150.01	8.2
25	G6P ↔F6P	146.95	8.2
26	F6P + ATP ↔ 2GAP+ADP	147.31	8.2
27	ADP+GAP+NAD+→ATP+H2O +NADH+PEP	293.52	16.4
28	ADP+PEP→ATP+PYR	293.52	16.4
29	NADH+PYR ↔LAC+NAD	200.00	2.2
	Pentose Phosphate pathway		
30	G6P + 2NADP+ → 2NADPH + CO2 + R5P	1.096	0
31	2R5P → GAP + S7P	0	0
32	GAP + S7P → E4P + F6P	0	0
33	X5P + E4P → F6P + GAP	0	0
	Mitochndrial Transport		
34	PYR ↔PYR(m)	120.04	14.74
35	MAL↔MAL(m)	101.19	16.29
36	AKG↔AKG(m)	-128.59	-18.39
37	MAL+CIT(m) ↔MAL(m)+CIT	-1.61	-0.94
38	ASP(m)+GLU ↔ASP+GLU(m)	-94.86	-15.30
39	GLU(c) →GLU(m)	45.17	6.19
	Anaplerotic reactions		
40	PYR(m)+NAD(m) →AcCoA(m) +CO2+NADH(m)	151.03	19.33
41	MAL+NADP→CO2+NADPH+PYR	11.40	0.48
42	MAL(m)+NADP(m) →CO2+NADPH(m)+PYR(m)	281.91	-6.19
43	OAA+ATP→PEP+ADP+CO2	0	0
44	PYR(m)+CO2+ATP(m)↔OAA(m)+ADP(m)	252.02	-10.78
	TCA cycle		
45	AcCoA (m)+ OAA(m)→CIT(m)	157.16	20.46
46	CIT(m)+NAD(m) →AKG(m)+ CO2+NADH(m)	158.77	21.40
47	AKG(m)+NAD(m) →SUCCoA(m)+CO2+NADH(m)	170.20	24.50
48	GDP(m)+SUCCoA(m)+FAD(m)→FUM(m)+FADH2(m)+GTP(m)	181.45	25.00

49	FUM(m)+H2O↔MAL(m)	182.33	25.00
50	MAL(m)+NAD(m) →OAA(m)+NADH(m)	184.05	46.53
51	MAL+NAD →OAA+NADH	--103.66	-15.36
	Amino acid metabolism		
52	ARG+AKG+NAD ↔2GLU(c)+NADH(c)+CO2+ NH4+	2.01	0.49
53	ASN↔ASP+NH4+	13.63	0.79
54	ASP+AKG ↔OAA+GLU	105.27	16.30
55	ASP(m)+AKG(m) ↔OAA(m)+GLU(m)	-94.86	-15.30
56	CYS+AKG→PYR+GLU+ NH4+	17.35	0.35
57	GLN↔GLU+ NH4+	-3.37	0.00
58	GLU(m)+NADP+(m) →AKG(m)+NADPH(m)+ NH4+	45.17	6.19
59	GLU+PYR ↔AKG+ALA	7.11	0.36
60	2GLY+NAD+→SER+NADH+CO2+ NH4+	4.30	-0.14
61	HIS+NAD+→GLU+CO2+NH4++NADH	0.49	0.08
62	ILE+AKG+ATP(m)+NAD+(m)+FAD+(m)→GLU+Ac CoA(m)+NADH(m)+FADH(m)+SUCCoA(m)+ADP(m)	3.31	0.22
63	LEU+AKG+ATP(m)+FAD+(c)→GLU+3AcCoA(m)+F ADH2(m)+ADP(m)	0.73	0.09
64	LYS+AKGNADPH+2NAD++2NAD+(m)+FAD(m)→2 GLU+2CO2+2AcCoA(m)+2NADH(m)+2NADH+FA DH2(m)+NADP+(m)	0.31	0.36
65	MET+SER+3ATP+ATP(m)+NAD+(m)→CYS+SUC CoA(m)+CO2+NH4++3ADP+ADP(m)+NADH(m)	6.67	0.09
66	PHE+NADPH→TYR+NADP+	2.81	0.16
67	PRO+2NAD+↔GLU+2NADH	3.00	0.04
68	SER→NH4+ +PYR	7.07	0.07
69	THR+NAD(m)+FAD(m)+NAD→PYR(m)+FADH2(m) +NH4++NADH(m)+CO2	1.09	0
70	TRP+2NAD+(m)+FAD+(m)+NADPH→ALA+4CO2+ 2AcCoA(m)+ NH4++2NADH(m)+FADH2(m)+NADP+	0	0
71	TYR+AKG→MAL+CO2+2AcCoA+GLU	5.14	0.47
72	VAL+AKG+ 2NAD+(m)+FAD+(m)→SUCCoA(m)+GLU+ 2NADH(m)+FADH2(m) +CO2	1.27	0.19

Both the TCA cycle and glycolysis provide most of the redox equivalents for cellular respiration. It is clearly shown that there is efficient utilization of glucose and amino acids from the results obtained via MFA by healthy and early apoptotic cells. As far as glucose, the limitation of glucose will decouple some modules in metabolic network, such as glycolysis and TCA cycle, leading to abnormal metabolic states. The glycolysis limitation will potentially trigger apoptosis[141]. Pyruvate is a key intermediate between glycolysis and TCA cycle. Pyruvate is a key metabolite in central metabolism since it is the end product of glycolysis, and most of the

fermentative products are derived from it. Pyruvate is also an important precursor metabolite for the biosynthetic building blocks. Therefore, it is important to analyze metabolic flux distribution around pyruvate. The pyruvate ratio (PR) is used to indicate the efficiency of pyruvate channeling to TCA cycle for energy generation. PR was calculated using the equation

$$PR = \frac{v_{34}}{v_{28} + v_{41} + v_{56} + v_{68}}$$

where the numerator represents the flux of pyruvate entering mitochondria for TCA cycle, while the denominator represents the fluxes of pyruvate generation. Thus the limit of PR is 1 and values close to 1 indicate high energy efficiency from glucose. The calculated values are presented in table 9. The significantly high value of PR in early apoptotic cells indicated that most of the flux from pyruvate was diverted towards the TCA cycle, whereas, in healthy cells under growth conditions, most of the pyruvate was channeled to lactate. Similar trends in pyruvate has been observed by Sengupta et al[142] in the study of metabolic flux analysis of CHO cells in the non-growth phase.

In the metabolism of mammalian cells, glutamate and α-ketoglutarate are also key metabolites and prominent intermediates. Once glutamate is transported into the cell, its fate is determined by glutamate dehydrogenase (GDH) or transaminases. GDH deaminates glutamate to α-ketoglutarate and channels it towards the TCA cycle. On the other hand, glutamate can be converted to α-ketoglutarate via the activities of glutamate dehydrogenase (GDH), alanine transaminase (AlaAT) or aspartate transaminase (AspAT). In the case of oxidation

by GDH, glutamate can be oxidized completely to CO_2 via TCA cycle and yield 27 molecules of ATP, whereas, in the transamination pathways by AlaAT or AspAT, only 6 to 9 molecules of ATP will be generated[134, 143]. Therefore, when more energy is required, glutamate is deviated towards the efficient oxidation pathway. Thus, the glutamate oxidation ratio (GOR) is used to indicate the efficiency of utilization of the main nitrogen source, glutamate, for energy generation. GOR was calculated using the equation

$$GOR = \frac{v_{58}}{v_{58} + v_{54} + v_{55} + v_{59}}$$

where the numerator represents the flux of glutamate oxidized to α-ketoglutarate, while the denominator represents the fluxes of all the fate of glutamate in central metabolism by GDH and transaminases. Thus the limit of GOR is 1 and values close to 1 indicate high energy efficiency from glutamate. The value of GOR in early apoptotic cells is higher in the healthy cells (Table 10), indicating that glutamate plays a major role in maintaining a high activity of TCA cycle during glucose limitation causing by low glucose uptake rate in early apoptotic cells. This result is similar to the metabolic shift observed in other cell lines at low glucose concentrations[23, 129, 134].

Taken together, the analysis of flux distribution around the TCA cycle indicated that in early apoptotic cells, the flux of pyruvate to TCA cycle was very high with very low or no lactic acid production, and TCA cycle was also compensated by higher incorporation of glutamate oxidation to recover the ATP level serving the apoptotic process.

Table 10 distribution of metabolic fluxes around pyruvate and glutamate-- α-ketoglutarate

parameter	Healthy	Early apoptotic
PR	0.36	0.85
GOR	0.72	0.81

In the case of amino acids, although most of the cell culture media contain all the twenty amino acids, only five of them, aspartate, glutamate, serine, glycine and alanine, are consumed for energy production[98] and, interestingly, only these five amino acids were reported to be biosynthetically labeled by [U-13C] glucose[144]. These five amino acids were compared together and showed significant difference between healthy and early apoptotic cells. A comparison of the normalized rates to uptake rate of glutamate (Table 11) reveals that the glutamate is the major amino acid consumed during early apoptotic stage. The negative values of fluxes of glysine and aspartate in healthy cells indicated that higher fluxes of transamination reaction in the metabolism of glutamate. These results agree with the conclusion derived from GOR values. Results from the fluxes of amino acid metabolism indicated that the contribution of other amino acids to TCA cycle intermediates was almost negligible in early apoptotic cells and they only contributed to the synthesis of some key enzymes involved in apoptotic process. Comparison to glutamate, the consumption rates of other amino acids were close to negligible. The dramatic high value of glutamate uptake also reveals that glutamate plays a key role in energy metabolism instead of glucose in the early apoptotic cells. However, in healthy cells,

the uptake rates of each amino acid were comparable, indicating that they are mostly utilized for biomass synthesis, including glutamate.

Table 11 extracellular fluxes (normalized to glutamate uptake, mol/mol glutamate)

	Healthy	Early apoptotic
GLU	1	1
SER	1.20	0.11
ALA	0.46	0.14
GLY	-1.22	0.18
ASP	-0.05	0.08

7.3. Discussion

Metabolic flux analysis shows the significant metabolic differences between healthy and early apoptotic cells. Our results indicate that early apoptotic state is not necessarily associated with a shutdown of metabolism. Early apoptotic cells are actually metabolically very active. A higher efficiency of glucose and glutamate utilization was observed during the apoptotic process. The general flux trends, normalized respect to glucose uptake, are compared in figure 25, which shows the decoupling of glycolysis and TCA cycle and the decoupling between glucose and glutamate utilization. This metabolic shift from healthy to early apoptotic cells with the high efficiency of major nutrient utilization indicates that apoptosis requires energy to fulfill the process.

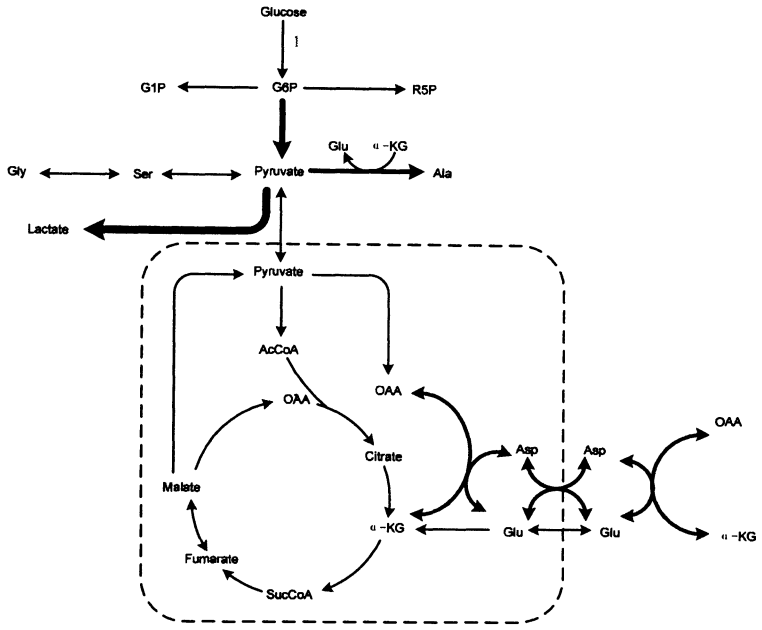

(A)

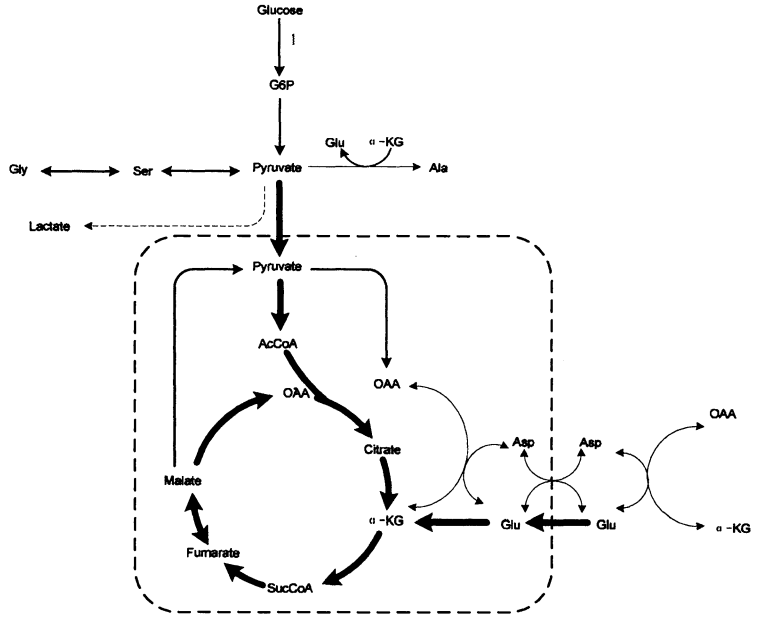

(B)

Figure 25 Comparison of flux trends in (A) healthy cells (B) early apoptotic cells

The c-MFA method utilizes a balance on stoichiometric matrix in order to resolve the intracellular fluxes. One of the first problems encountered in this approach is that the system is underdetermined. The pentose phosphate pathway (PPP) is an underdetermined network together with glycolysis and TCA cycle[95]. The PPP contains oxidative reactions with the generation of NADPH and non-oxidative reactions via transaldolase and transketolase. Both the oxidative and non-oxidative parts are considered in the proposed model (Figure 23). However, when the measured extracellular fluxes were applied on the stoichiometric matrix to calculated the fluxes of PPP, both results in healthy and early apoptotic had the exactly zero flux in oxidative branch and ribose-5-phosphate was formed through the transaldolases and transsketolases. And there was no significant difference between healthy and early apoptotic cells. Without more information, the PPP was lumped into one reaction just for both the generation of NADPH and the generation of ribose-5-phosphate for nucleotide synthesis in our c-MFA. However, the PPP operate in different modes depending on the cellular status and requirement, and there should be a balance between oxidative and non-oxidative branches. Figure 25 has shown the dicoupling of glycolysis, TCA cycle, and amino acids metabolism in early apoptotic cells. It should be similar to the PPP for the different demand for NADPH and PPP intermediates. The fluxes in PPP for healthy and early apoptotic cells need to be considered carefully due to the following observations:

1) For rapid growing healthy cells, oxidative branch is inhibited by high fructose-1,6-biphosphate[145-146], and non-oxidative branch is active.
2) Expression of apoptotic gene p53 leads to inhibit the non-oxidative and redirect

glucose to oxidative branch[147].

For the accurate quantification of the fluxes in PPP, it is necessary to compliment the stoichiometric balancing of metabolites with isotopic labeling analysis. The rate of oxidative branch of PPP can be estimated via [1,2-$^{13}C_2$] glucose[126, 145, 148]. $^{13}C_2$ lactate is directly derived from glycosis whereas $^{13}C_1$ lactate originates from glucose metabolized by oxidative PPP and then recycled to glycolysis by non-oxidative branch. This shows that labeling flux analysis is largely free from the drawbacks discussed for the c-MFA. It employs a balance on labeled carbon bonds, and since each isotopic isomer of a compound can be regarded as a separate metabolite, there are huge numbers of measurements available to get an estimate of fluxes with high degree of confidence.

In conclusion, in early apoptotic cells, metabolic profiling shows specific flux shifts in glycolysis and TCA cycle, and reveals major changes in glucose and glutamate utilization. A more comprehensive analysis using advanced techniques, such as labeling MFA, could bring more information in metabolic pathways like pentose phosphate pathway, aspartate-malate shuttle, fatty acid synthesis and so on to compare the metabolic shift in early apoptotic cells. Metabolic flux analysis provides vital information beyond the genetic and signaling pathways studies on apoptosis, indicating that a metabolic shift in carbon flow and amino acid metabolism is taking place in the transition from healthy to early apoptotic cells. Therefore, metabolic flux analysis is a powerful tool to identify crucial targets and can help elucidate the complex mechanisms mediating apoptosis in cultured mammalian cells.

Chapter 8

Conclusions and Future Work

The overall project aim of this work was to achieve an improved understanding of apoptotic behavior in cultured CHO cells. CHO cells are a powerful model system for studying mammalian cell culture. A major problem faced in culture is cell death. Apoptosis is a genetically controlled process but it is still recognized as an unclean in cell culture. The better understanding of metabolic behavior during the apoptosis, the better strategies will be devised to control the cell death during cell culture.

Fluorescence imaging of annexin V-FITC and PI staining taken for batch experiments indicated that death of the CHO cells is primarily via apoptosis. This observation is similar to the previous reports [17, 32, 55, 59, 149]. The condensation of chromatin and shape changes were both observed in bright field and fluorescent field. Fluorescence imaging captured the changes in cellular morphology along the course of cell culture. At the same time, to further confirm

this observation and quantitatively investigate the transition behavior, another kind of immunofluorescent technique, FACS, was applied to detect and monitor the transition of apoptotic cells and estimate subpopulations. The healthy, early apoptotic and late apoptotic cells were distinguished and samples collected under different culture time and conditions used to establish the link between metabolism and apoptosis using metabolic flux analysis. Significant morphology changes and dramatic high apoptotic rate were found at the end of the exponential growth phase, coinciding with the exhaustion of glucose, providing the evidence that glucose metabolism and apoptosis are coordinated and indicating the importance of MFA to better understand apoptotic processes in cultured CHO cells.

Considering the similarity between immunofluorescent technique and immunomaganetic technique, we used the results from FACS and fluorescence imaging to optimize the Magnetic Activated Cell Sorting (MACS) process to separate different samples on the order of 10^7 cells to detect proteins expressed and labeling carbon mapping in future work. In our study, one of the early features of apoptosis, which is the externalization of phosphatidylserine (PS) residues normally present on the inner leaflet of the plasma membrane, was used. Colloidal paramagnetic microbeads conjugated with annexin V binding to PS was applied to separate healthy and apoptotic cells by MACS. Apoptotic cells with externalized PS can bind to these microbeads while healthy cells cannot and hence the subpopulation are separated by magnetic field. MiniMACS column was considered as an affinity column and the amount of antibodies and the mobile phase were optimized to get rather good purity in both negative and positive selections. The results of MACS to

partition apoptotic and non-apoptotic cells have shown that the modified procedure also had a high throughput and the loading capacity is around 2×10^8 cells/ml. The advantages of the MACS method are

1) simple and short procedure that does not require complex and specialized equipments.
2) mild method during the fractionation, though some debris could be generated through the column.
3) suitable for obtaining large amount of purified apoptotic and healthy cells and therefore could be easily introduced in other biochemical studies, such as proteomics and isotopomer labeling MFA.

Most biochemical studies of apoptotic cells have been done on the whole cell populations treated with apoptotic inducers or inhibitors, and the results would be for the mixture of cells which are at various cellular stages. Using MACS has allowed us to examine the direct relationship between cells that are undergoing apoptosis and the metabolism or expression of apoptotic proteins.

The results of fluorescence imaging and apoptotic kinetics showed a significant apoptotic change on glucose depletion. It is well documented that the activity of BAD, a pro-apoptotic Bcl-2 family member also serves as the regulator of glucokinase activity to ensure that glucose metabolism and apoptosis are coordinated[150], which is the first evidence for an association between cellular metabolism and the apoptotic process. On the other hand, the most studies on metabolism and apoptosis are the effect of Bcl-2 family members, which are key

regulators of the apoptotic pathway. It has been reported that loss of glucose leads to a decreased level of anti-apoptosis proteins from Bcl-2 family[151]. In our research by combination of 2-NBDG and Annexin V-PE, the initial difference in glucose metabolism between healthy and early apoptotic cells is glucose uptake and this difference shows that early apoptotic cells have rather low uptake rate and the constant rate indicate that environment has low or no effect on early apoptotic cells.

After glucose uptake, the difference between healthy and early apoptotic cells identified via metabolic flux analysis is a promising strategy, which can effectively link apoptosis and the metabolic shift. Under high density conditions in bioreactors, the mechanism behind the metabolic regulation of apoptosis in mammalian cells is still like a grey box because the whole process of apoptosis is too complex and many causes can trigger apoptosis in cell culture. Most recent experiments have focused on the inhibition of apoptosis by the over-expression of Bcl-2 family members. The major problem in the elucidation of apoptosis mechanisms in all cell culture system is the fact that there is no single parameter responsible for its initiation, nor a specific assay distinguishing between the apoptotic modalities. However, essential cellular and metabolic events are demonstrating the key processes throughout the whole life of cells. The use of metabolic flux analysis as model for apoptosis research to investigate the functions and interactions may be a powerful tool. We assumed late apoptotic cells did not have much of metabolic activity. The metabolism is activated in the early apoptotic stage, controlled by the active degraded proteases[16, 44, 47]. Flux maps of cultured CHO cells between apoptotic and healthy phase of batch culture were generated

using stoichiometric modeling. MFA indicated that most of flux from pyruvate was channeled towards the TCA cycle, only with little lactate production. Moreover, the utilization of glutamate was significantly high. In early apoptotic cells, the glucose uptake rate becomes lower than in healthy cells. We monitored the rate of glutamate consumption. The increase in glutamate uptake rate and oxidative rate has demonstrated that the glutamate is a necessary energy and carbon source for early apoptotic cells. Glutamate is the preferred anaplerotic source for carbon skeletons and energy generation. These results are in agreement with literature. Zwingmann et al[152] studied glucose metabolism in hepatocellular apoptosis and proposed a metabolic model for the whole process of apoptosis. They suggested that metabolic events of increased mitochondrial glucose oxidation and de novo synthesis of glutathione occur in very early apoptotic stages and they are possibly to mantain adequate energy levels in order for apoptosis to proceed.

In addition, isotomer labeling MFA, enzyme activity tests and proteomic approaches are performed to further explain the metabolic network and apoptotic process. The c-MFA analysis is based on the assumed metabolic network with all the assumptions from the reported findings. This conventional technique will not only validate the existing pathways for the apoptotic and healthy CHO cells, but will also help determine conditions and approaches required for the implementation of system-wide techniques. Labeling based experiments are powerful techniques to investigate metabolism. They not only have the capability to estimate intracellular fluxes to a high degree of resolution, but also provide information for refining the reaction network under consideration. Labeling based experiments provides us

with the capability to assess which reactions are active and which reactions are inactive between apoptotic and healthy cells. An important part of the future work will examine metabolism and estimate the flux in different cell phases. For this, we would use labeled 13C glucose or 13C glutamic acid for cell culture and analyze the labeling pattern of metabolites in different metabolic pathway using NMR spectroscopy. The labeling pattern we obtain can bring more information to investigate into the metabolism of apoptotic and non-apoptotic cells.

For the analysis of 13C-based metabolic flux, most of them use GC/MS, because MS is significantly more sensitive than NMR[153]. Miccheli et al [154]. That is the reason why most of the lab which focused on 13C labeling MFA used GC/MS to measure labeled metabolites. Recently, the sensitivity of NMR analysis has significantly improved. [155], but the sample amount is rather high. For 1H-NMR, 3×107 cells per sample are collected, while for 1-D 13C-NMR or 2-D [13C, 1H] HSQC, $1.8\sim3\times 108$ cells per sample are required [56, 89, 156-157]. When proliferating mammalian cells are at metabolic steady state, labeled glucose can achieve isotopic steady state within glycolysis, the pentose phosphate pathway and the TCA cycle within 6 hours of application [56, 89, 156-157]. Among those tracers, [U-13C6]glucose and [1,2-13C2]glucose are commonly used in mammalian cells.

The methodology for estimation of fluxes using labeling pattern of amino acids is discussed in section 2.4. The reaction network model and carbon rearrangement model are constructed for the purpose of intracellular flux estimation, further for the difference between apoptotic and non-apoptotic phases

according to the intracellular flux estimations. In our reaction network model, we have lumped most of amino acids metabolism. All of these amino acids can be connected by TCA cycle (figure 3). So, the amounts of these amino acids must be appropriately balanced. Amino acids must be supplied form the media to ensure the metabolic functions of mammalian cells and supply the required amounts in a balanced state. The absence of any of these amino acids would trigger the onset of cell death.[7, 11, 17]. So we will consider the data obtained from the culture of cell with [U-13C] glucose and [U-13C] glutamic acid. The final carbon fractional labeling in amino acids would give more information into the changes in amino acid utilization during apoptosis.

On the other hand, system-level analysis can be used to enhance the understanding of complex biological processes. With the estimated parameters, it becomes possible to reproduce the observed system behavior and to predict important system properties of apoptosis in mammalian cell culture. Based on classical analysis of the correlation of apoptosis and culture conditions, metabolic characterization and proteomics are powerful approaches for global study. We would try to analyze the difference in biological data between apoptotic and non-apoptotic cells and unravel the functions and interactions during CHO cell culture. Depending on the results from the conventional analysis, the conditions of system-level comparison will be identified. Then according to the comparison, the study of system-wide responses to different stages of cell behavior should consider the identification of proteins and reactions or pathways involved in cell apoptosis. Although the metabolic and apoptosis pathways are distinctly different, they

converge on a shared set of proteins. Proteomics is then a promising approach to investigate biochemical processes on the protein level. Therefore, the investigation of the phenomenon of apoptosis will use proteome research in our study. Much of the evidence for the link between environmental stimuli, cellular metabolism and anti-apoptosis comes from the study of cancer cells[141]. This work will be designed in accordance with the culture condition and proteomics results, which in turn will help us find the pathways of apoptosis in CHO cell cultures. In this study, we will use the proteomic approach for the identification of proteins that are regulated according to the degree of apoptotic behaviors. Proteomics is the study of the expressed protein complement of a genome at a specific time and as a study of proteins expressed in a cell. Proteomics will facilitate the systematic analysis of protein molecules related to such a complicated biological system. Protein expression profiles including information about protein signatures, localization and their quantitative changes with extracellular stimulations are extremely useful to construct intracellular pathway models resulting in the apoptotic cell death.

Hence the samples chosen by the preliminary work in different culture stages will be investigated with 2-D gel electrophoresis. In the two different collections, 2-D gel electrophoresis-mass spectrometry approach will be applied to cellular protein samples for the identification of apoptosis associated proteins. As the samples are collected from the same culture condition, the effects from a vast number of extracellular factors are minimized, but the intracellular behaviors leading to the anti- or pro-apoptotic protein expression patterns in different cell stage need to be investigated. It is interesting to notice that although many new

apoptosis actors were identified, there are many of the proteins involved in apoptosis were not detected. Thus, the observations of samples collected from the same condition would overcome this limitation, and our proteomics approach could realize the real globe analysis. The behaviors of viable and apoptotic cells are rapidly bringing either up-regulation or down-regulation of proteins in both the central energy metabolic and apoptotic pathways. Some gel replicates can be carried out for apoptotic and non-apoptotic states, respectively, which will used for differential analysis. In this study, comparison of the protein profiling between different conditions can lead to ascribing genes related to cell apoptosis or growth. Furthermore, the functional analysis of proteins modified during apoptosis would be an important work. As soon as some proteins are identified and validated in the proteome mapping, the underlying molecular mechanism and the correlation between cellular growth and apoptosis become more straightforward.

Overall, the results from functional genomics approaches will greatly improve the fundamental knowledge of apoptosis in mammalian cell culture. Apoptotic stimuli are inherent in the high cell density at the late cell growth exponential phase due to the nutrient depletion in our CHO cell in batch culture. Such evidence suggests the hypothesis that the effects of environmental factors that switch CHO cells from healthy status to apoptotic status are reflected by metabolic phenotype changes. Depletion of the energy supply will decouple the link between each module in metabolic network, such as glycolysis, the pentose phosphate pathway and the TCA cycle. The unbalance of metabolic will limit the function of some enzymes and trigger apoptosis. The changes of metabolism can be detected to

analyze their effect on apoptosis programs, especially glucose metabolism can be monitored to provide information on metabolic changes in response to cell stresses. So in order to bring novel strategies to understand apoptosis in mammalian cell cultures, our study will focus not only at the apoptotic pathway but will also expand to metabolic network to set up a link between cell growth and apoptosis. These studies maybe validate our models to further characterize the apoptotic response and behavior in mammalian cell culture. These micro scale data can bring us some meaningful information to understand the biological phenomena: from inside of cell to the outside of medium environment, and in setting up the bridge to the relationship between cell proliferation and apoptosis transition.

References

1. Freshney, R.I., *Culture of Animal Cell* Fifth ed. 2005: wiley.

2. G.Harrison, R., *Observations on the riving developing nerve fiber.* . Anat. Rec., 1907. **1**: p. 116-118.

3. Walsh, G., *Biopharmaceuticals benchmarks—2003.* Nat Biotechnol 2003. **21**: p. 865-887.

4. Walsh, G., *Biopharmaceuticals benchmarks—2006.* Nat Biotechnol 2006. **24**: p. 769-778.

5. DT Molowa, R.M., *The state of biopharmaceutical manufacturing.* Biotechnol Annu Rev 2003. **9**: p. 285-302.

6. T. T. Puck, S.J.C.a.A.R., *Genetics of somatic mammalian cells III. Long-term cultivation of euploid cells from human and animal subjects.* J. Exptl. Med., 1958. **108**: p. 945-956.

7. Sadettin S. Ozturk, W.-s.H., *Cell culture Technology for Pharmaceutical and Cell-based Therapies.* 2005: Taylor &Francis.

8. Bulter, M., *Animal cell culture: recent achievements and perspectives in the production of biopharmaceuticals.* Appl Microbiol Biotechnol, 2005. **68**: p. 283-291.

9. Mastrangelo, A.J., Zou, S., Hardwick, J.M., Betenbaugh, M.J., *Antiapoptosis chemicals prolong productive lifetimes of mammalian cells upon Sindbis virus vector infection.* Biotechnol. Bioeng, 1999. **65**(3): p. 298-305.

10. Mastrangelo, A.J., Hardwick, J.M., Bex, F., Betenbaugh, M.J, *Part I. Bcl-2 and Bcl-xL limit apoptosis upon infection with alphavirus vectors.* Biotechnol. Bioeng., 2000. **67**(5).

11. Hansjorg Hauser, R.W., *Mammalian Cell Biotechnology in Protein Production.* 1997: Walter de Gruyter.

12. Builder, S., van Reis, R., Paoni, N., Ogez, J, *Process development and regulatory approval of tissue-type plasminogen activator*, in *8th International Biotechnology Symposium*. 1988, Societe Franscaise de Microbiologie: Paris.

13. M-D. Wang, M.Y., N. Huzel, M. Butler, *Erythropoietin production from CHO cells grown by continuous culture in a fluidized-bed bioreactor.* Biotechnology and Bioengineering, 2002. **77**(2): p. 194-203.

14. R J Kaufman, L.C.W., A J Dorner, *Synthesis, processing and secretion of recombinant human factor VIII expressed in mammalian cells.* The Journal of biological chemistry, 1988. **263**: p. 6352-6362.

15. Walsh, G., *Biopharmaceuticals benchmarks—2006.* Nat Biotechnol, 2006. **24**: p. 769-778.

16. Nilou Arden, M.J.B., *Life and death in mammalian cell culture: strategies for apoptosis inhibition.* TRENDS in Biotechnology, 2004. **22**: p. 174-180.

17. Freshney, R.I., *Culture of Animal Cell.* Fifth ed. 2005: Wiley.

18. Jonathan Bogan, A.M., *Insulin-Responsive Compartments Containing GLUT4 in 3T3-L1 and CHO Cells: Regulation by Amino Acid Concentrations.* Molecular and Cellular Biology, 2001. **21**(14): p. 4785-4806.

19. JE Pessin, G.B., *Mammalian facilitative glucose transporter family: Structure and molecular regulation.* Annu. Rev. Physiol., 1992. **54**: p. 911-930.

20. Pareds, C., Sanifeliu A, Cardenas F. , *Estimation of the intracellular fluxes for a hybridoma cell line by material balances.* Enzyme and microbial technology, 1998. **23**: p. 187-198.

21. Fitzpatrick L, J.H., Butler M. , *Glucose and glutamine metabolism of a B-lymphocyte hybridoma grown in batch culture.* Appl Biochem Biotechnol, 1993. **43**(2): p. 93-116.

22. Mancuso A, S.S., *Examination of primary metabolic pathways in a murine hybridoma with carbon-13 nuclear magnetic resonance spectroscope.* Biotechnol Bioeng, 1994. **44**: p. 563-585

23. Bode, B.P., *Recent Molecular Advances in Mammalian Glutamine Transport.* Journal of Nutrition, 2001. **131**: p. 2475-2485.

24. R. Wagner, T.R., H. Krafft and J. Lehmann, *Variation of amino acid concentrations in the medium of HU β-IFN and HU IL-2 producing cell lines.* Cytotechnology, 1988. **1**: p. 145-150.

25. W. M. Miller, C.R.W.a.H.W.B., *Transient responses of hybridoma cells to lactate and ammonia pulse and step changes in continuous culture* Bioprocess and Biosystems Engineering, 1988. **3**: p. 113-122.

26. Glacken, M.W., *Catabolic Control of Mammalian Cell Culture.* Bio/Technology, 1988. **6**: p. 1041-1050.

27. Anne McQueen, J.E.B., *Effect of ammonium ion and extracellular pH on hybridoma cell metabolism and antibody production.* 1990. **35**(11): p. 1067-1077.

28. Ryll T, V.U., Wagner R, *Biochemistry of growth inhibition by ammonium ions in mammalian cells.* Biotechnol Bioeng, 1994. **44**: p. 184-193.

29. R., G.M.V.U.W., *Ammonium ion and glucosamine dependent increases of oligosaccharide complexity in recombinant glycoproteins secreted from*

cultivated BHK-21 cells. Biotechnology and Bioengineering, 1998. **55**: p. 518-528.

30. Polverni, P.J., *Apoptosis and predisposition to oral cancer.* Crit Rev Oral Biol Med, 1999. **10**: p. 139-152.

31. Tina M. Sauerwald, B.F.J., J. Marie Hardwick , George A. Oyler , Michael J. Betenbaugh, *Combining caspase and mitochondrial dysfunction inhibitors of apoptosis to limit cell death in mammalian cell cultures.* Biotechnology and Bioengineering, 2006. **94**(2): p. 362-272.

32. Cotter, T., Al-Rubeai, M, *Cell death (apoptosis) in cell culture systems.* TIBTECH, 1995. **13**: p. 150.

33. Haley A Laken, M.W.L., *Understanding and modulating apoptosis in industrial cell culture* Current Opinion in Biotechnology, 2001. **12**: p. 175-179.

34. C Du, F.M., Li Y, Li L, Wang X., *Smac, a mitochondrial protein that promotes cytochrome c-dependent caspase activation by eliminating IAP inhibition.* Cell, 2000. **102**: p. 33-42.

35. SB Bratton, G.W., Srinivasula SM, Sun X-M, Butterworth M, Alnemri ES, GM Cohen, *Recruitment, activation and retention of caspases-9 and -3 by Apaf-1 apoptosome and associated XIAP complexes.* EMBO J, 2001. **20**: p. 998-1009.

36. Cory, J.M.A.a.S., *The Bcl-2 Protein Family: Arbiters of Cell Survival* Science, 1998. **28**: p. 1322-1326.

37. Brown, R., *The bcl-2 family of proteins* British Medical Bulletin, 1997. **53**: p. 466-477.

38. Danny Chee Furng Wong , K.T.K.W., Yih Yean Lee , Peter Nissom Morin , Chew Kiat Heng , Miranda Gek Sim Yap, *Transcriptional profiling of apoptotic pathways in batch and fed-batch CHO cell cultures.* Biotechnology and Bioengineering, 2006. **94**(2): p. 373-282.

39. Aaron D. Schimmer, I.M.P., Shinichi Kitada, Emel Eksioglu-Demiralp, Mark D. Minden, Ryan Pinto, Ken Mah, Michael Andreeff, Youngsoo Kim, Won Suk Suh and John C. Reed, *Functional Blocks in Caspase Activation Pathways Are Common in Leukemia and Predict Patient Response to Induction Chemotherapy.* Cancer Research, 2003. **63**: p. 1242-1248.

40. G. Kroemer, B.D.a.M.R.-R., *The mitochondrial death/life regulator in apoptosis and necrosis.* Annu. Rev. Physiol., 1998. **60**: p. 619-642.

41. Elemore, S., *Apoptosis: A review of programmed cell death* TOXICOLOGIC PATHOLOGY 2007. **35**(4): p. 495-516.

42. Salvesen GS, d.V., *Caspases: intracellular signaling by proteolysis.* Cell, 1997. **91**(4): p. 443-446.

43. Pickens, C.O., *Cell apoptotic signalling pathways* 2007, New York: Nova Biomedical Books.

44. Valentino, R.G., *New cell apoptosis research* 2007, New York: Nova Biomedical Books.

45. S Fulda, K.D., *Extrinsic versus intrinsic apoptosis pathways in anticancer chemotherapy.* Oncogene, 2006. **25**: p. 4798-4811.

46. Sheikh, M., *Death and decoy receptors and p53-mediated apoptosis.* Leukemia, 2000. **14**(8): p. 1509-1513.

47. Kettleworth, C.R., *Cell apoptosis research advances.* 2007, New York: Nova Science Publishers.

48. Scaffidi C, F.S., Srinivasan A, Friesen C, Li F, Tomaselli KJ, Debatin KM, Krammer PH, Peter ME., *Two CD95 (APO-1/Fas) signaling pathways.* The EMBO journal, 1998. **17**(6): p. 675-1687.

49. Darzynkiewicz Z, B.S., Del Bino G, Gorczyca W, Hotz MA, Lassota P, Traganos F, *Features of apoptotic cells measured by flow cytometry. Cytometry.* Cytometry, 1992. **13**: p. 795-808.

50. Clavien PA, R.H.a.S.M., *Mechanism of hepatocyte death after ischemia: apoptosis versus necrosis.* Int J Oncol, 2000. **17**: p. 869-879.

51. Nicoletti, I., Migliorati, G., Pagliacci, M. C., Grignani, F., and Riccardi, C, *A rapid and simple method for measuring thymocyte apoptosis by propidium iodide staining and flow cytometry.* J Immunol Methods, 1991. **139**(2): p. 271-279.

52. Dive C, G.C., Phipps DJ, Evans DL, Milner AE, Wyllie AH., *Analysis and discrimination of necrosis and apoptosis (programmed cell death) by multiparameter flow cytometry.* Bioch Biophysica Acta, 1992. **1133**(3): p. 275-285.

53. Van Cruchten S., V.D.B.W., *Morphological and biochemical aspects of apoptosis, oncosis and necrosis.* Anat. Histol. Embryol, 2002. **31**: p. 174-180.

54. R. P. Singh, M.A.-R., C. D. Gregory, A. N. Emery, *Cell death in bioreactors: A role for apoptosis.* Biotechnology and Bioengineering, 1994. **44**(6): p. 720-726.

55. Barnes, J.P.M.D., *Methods in Cell Biology Volume 57* Animal Cell Culture Methods. 1998: AP.

56. Chen yang, a.d.R., Andrei Osterman, Jeffrey W Smith, *Profiling of central metabolism in human cancer cells by two-dimensional NMR, GC-MS analysis, and isotopomer modeling* Metabolomics, 2008. **4**(1): p. 13-29.

57. Toshiko Atsumi, K.T., Seiichiro Fujisawa, *Induction of early apoptosis and ROS-generation activity in human gingival fibroblasts (HGF) and human submandibular gland carcinoma (HSG) cells treated with curcumin.* Archives of Oral Biology, 2006. **51**(10): p. 913-921.

58. Yasushi Noguchi, J.D.Y., Jose O. Aleman, Michael E. Hansen, Joanne K. Kelleher, Gregory Stephanopoulos, *Effect of Anaplerotic Fluxes and Amino Acid Availability on Hepatic Lipoapoptosis.* Jounral of Biological Chemistry, 2009. **284**(38): p. 33425-33436.

59. Goswami J, S.A., Steller H, Stephanopoulos GN, Wang DI., *Apoptosis in batch cultures of Chinese hamster ovary cells.* Biotechnol Bioeng, 1999. **62**: p. 632-640.

60. Richard A. Billington, C.T., Emanuela Ercolano, Ubaldina Galli, Cintia Blasi Roman, Ambra A. Grolla, Pier Luigi Canonico, Fabrizio Condorelli and Armando A. Genazzani, *Characterization of NAD Uptake in Mammalian Cells.* The Journal of biological chemistry, 2008. **283**(10): p. 6367-6374.

61. Weihai Ying ; Conrad alano, P.G.R.S., *NAD+ as a metabolic link between DNA damage and cell death.* Journal of Neuroscience Research, 2005. **79**: p. 216-223.

62. Zanghi JA, F.M., Bailey JE, *Serum protects protein-free competent Chinese hamster ovary cells against apoptosis induced by nutrient deprivation in batch culture.* Biotechnology and Bioengineering, 1999. **64**: p. 108-119.

63. James A. Zanghi, W.A.R., James E. Bailey, Martin Fussenegger, *The growth factor inhibitor suramin reduces apoptosis and cell aggregation in protein-free CHO cell Batch cultures.* Biotechnol. Prog., 2000. **16**: p. 319-325.

64. Yan-Ling Zhang, Y.-F.K., Yu Zhao, Li Wu, and Zhong-Yin Zhang, *Suramin Is an Active Site-directed, Reversible, and Tight-binding Inhibitor of Protein-tyrosine Phosphatases.* J Biol Chem., 1998. **273**(20): p. 12281-12287.

65. Shin Sik Choi, W.J.R., and Tai Hyun Park, *Inhibition of Human Cell Apoptosis by Silkworm Hemolymph* Biotechnol. Prog., 2002. **18**(4): p. 874-878.

66. Elena B. Lasunskaia, I.I.F., Zoulfia A. Darieva, Mariele S.R. Da Silva, Milton M. Kanashiro, Boris A. Margulis, *Transfection of NS0 myeloma fusion partner cells with hsp70 gene results in higher hybridoma yield by improving cellular response to apoptosis.* Biotechnology and Bioengineering, 2003. **81**(4): p. 496-504.

67. Francesc, T.A.G.C.V.J.P.E.C.J.J.C.L.G., *The protection of hybridoma cells from apoptosis by caspase inhibition allows culture recovery when exposed to non-inducing conditions.* Jounral of Biotechnology, 2002. **95**(3): p. 205-214.

68. Jean-Luc Perfettini, G.K., *Caspase activation is not death.* Nature Immunology, 2003. **4**: p. 308-310.

69. Noelle-Anne S. Sunstrom, R.D.G., Danny C. Wong, Neil A. Kitchen, Leonore DeBoer, and Peter P. Gray *Insulin-like growth factor-I and transferrin mediate growth and survival of Chinese Hamster Ovary Cells.* Biotechnol. Prog., 2000. **16**(5): p. 698-702.

70. Brian D. Follstad, D.I.C.W., and Gregory Stephanopoulos, *Mitochondrial membrane potential selects hybridomas yielding high viability in fed-batch cultures. Biotechnol. Prog.* Biotechnol. Prog., 2002. **18**(1): p. 1-5.

71. R. Robert Balcarcel, G.S., *Rapamycin reduces hybridoma cell death and enhances monoclonal antibody production.* Biotechnology and Bioengineering, 2001. **76**(1): p. 1-10.

72. Singh, R.P., *Enhancement of Survivability of Mammalian Cells by Overexpression of the apoptosis-Suppressor Gene bcl-2.* Biotechnology and Bioengineering 1996. **52**: p. 166-175.

73. B J Stähelin, U.M., M Solioz, H Zimmermann, and J Reichen, *False positive staining in the TUNEL assay to detect apoptosis in liver and intestine is caused*

by endogenous nucleases and inhibited by diethyl pyrocarbonate. Molecular Pathology, 1998. **51**(4): p. 204-208.

74. Chen, Y.A.I.a.F.W., *Quantitation of DNA fragmentation in apoptosis.* Nucleic Acids Research, 1996. **24**(5): p. 992-993.

75. Akira Komoriya, B.Z.P., Martin J. Brown, Ming-Lei Wu, and Pierre A. Henkart, *Assessment of Caspase Activities in Intact Apoptotic Thymocytes Using Cell-permeable Fluorogenic Caspase Substrates* The Journal of Experimental Medicine, 2000. **191**(11): p. 1819-1828.

76. Falcieri E, Z.L., Santi S, Cinti C, Gobbi P, Bosco D, Cataldi A, Betts C, Vitale M., *The behaviour of nuclear domains in the course of apoptosis.* Histochemistry, 1994. **102**(3): p. 221-231.

77. Mercille, S., *Induction of apoptosis in nutrient-deprived cultures of hybridoma and myeloma cells.* Biotechnology and Bioengineering, 1994. **44**(9): p. 1140-1154.

78. Dana Kylarová, J.P., Jana Mad'arová, Jan Bartoš and Václav Lichnovský, *Comparison of the TUNEL, lamin B and annexin V methods for the detection of apoptosis by flow cytometry.* Acta Histochemica, 2002. **104**(4): p. 367-370.

79. Manon van Engeland, L.J.W.N., Frans C. S. Ramaekers, Bert Schutte, Chris P. M. Reutelingsperger *Annexin V-Affinity assay: A review on an apoptosis detection system based on phosphatidylserine exposure.* Cytometry, 1998. **31**(1): p. 1-9.

80. Studzinski, G.P., *Apoptosis: a Practical Approach*, ed. B.D. Hames. 1999: Oxford University Press.

81. D Recktenwald, A.R., *cell Separation Methods and Applications.* 1997, New York: Dekker.

82. Milica Radisic, R.K.I., Shashi K Murthy *Micro- and nanotechnology in cell separation.* International Journal of Nanomedicine, 2006. **1**(1): p. 3-14.

83. TAMER M. SAID, A.A.M.Z., SONJA GRUNEWALD, HANS-JUERGEN GLANDER, UWE PAASCH, *Utility of Magnetic Cell Separation as a Molecular Sperm Preparation Technique.* Journal of Andrology, 2008. **29**(2): p. 134.

84. Hatti-Kaul, R., *Aqueous Two-Phase Systems: Methods and Protocols.* 2000, Totowa, New Jersey: Humana Press.

85. A Kumar, I.G., B Mattiasson, *Advances in Biochemical engineering/ Biotechnology.* Cell Separation, ed. T. scheper. 2007: Springer.

86. Ashok Kumar, I.Y.G., Bo Mattiasson, *Cell Separation Fundamentals, Analytical and Preparative Methods.* Advances in Biochemical Engineering / Biotechnology, ed. T. Scheper. 2007, berlin Heidelberg: Springer.

87. Harry Walter, E.J.K., *Membrane surface properties reflected by cell partition in two-polymer aqueous phases Classes of beef erythrocytes having different membrane lipid, charge and affinity for a ligand.* FEBS Letters, 1977. **78**(1): p. 105-108.

88. Ki-Hwan Nam, W.-J.C., Hyejin Hong, Sang-Min Lim, Dong-Il Kim, Yoon-Mo Koo *Continuous-Flow Fractionation of Animal Cells in Microfluidic Device Using Aqueous Two-Phase Extraction.* Biomedical Microdevices, 2005. **7**(3): p. 189-195.

89. Masatoshi Tsukamoto, S.T., Shohei Yamamura,Yasutaka Morita, Naoki Nagatani,Yuzuru Takamura and Eiichi Tamiya, *Cell separation by an aqueous two-phase system in a microfluidic device.* Analyst, 2009. **134**: p. 1994-1998.

90. J. T. Kemsheadl, J.U., *Magnetic separation techniques: their application to medicine* Molecular and Cellular Biochemistry, 1985. **67**(1): p. 11-18.

91. Stefan Miltenyi, W.M., Walter Weichel, Andreas Radbruch, *High gradient magnetic cell separation with MACS.* Cytometry Part A, 1990. **11**(2): p. 231-238.

92. Masaru Okabe , S.M., Morio Nagira, Xing Ying, Yasuhiro Kohama, Tsutomu Mimura, *Collection of acrosome-reacted human sperm using monoclonal antibody-coated paramagnetic beads.* Molecular Reproduction and Development, 1992. **32**(4): p. 389-393.

93. Jürgen Weitz, M.K., Peter Kienle, Andrea Schrödel, Frank Willeke, Axel Benner, Thomas Lehnert, Christian Herfarth, Magnus von Knebel Doeberitz, *Detection of Hematogenic Tumor Cell Dissemination in Patients Undergoing Resection of Liver Metastases of Colorectal Cancer.* Annals of Surgery, 2000. **232**(1): p. 66-72.

94. Kjersti Flatmark, K.B., Hans Olaf Johannessen,Elisabeth Hegstad, Rocio Rosales, Lisbeth Hårklau, Jan Helge Solhaug, Ragnar S. Faye, *Immunomagnetic Detection of Micrometastatic Cells in Bone Marrow of Colorectal Cancer Patients.* Clinical Cancer research, 2002. **8**: p. 444-449.

95. Mohamed Al-Rubeai, M.F., *Cell Engineering*. Systems Biology. Vol. 5. 2007: Springer.

96. Stemphanopoulou, G., *Metabolic fluxes and metabolic engineering.* Met. Engg., 1999. **1**: p. 1-11.

97. G. Stemphanopoulos, A.A.A., J. Nielsen, *Metabolic engineering: pringciples and methodology*. 1998: Academic Press.

98. Liangzhi Xie, D.I.C.W., *Stoichiometric analysis of animal cell growth and its application in medium design.* Biotechnology and Bioengineering, 2004. **43**(11): p. 1164-1174.

99. Kathleen M. Champion , D.A., William J. Henzel, Sam Hermes, Stefanie Weikert , John Stults, Martin Vanderlaan, Lynne Krummen, *A two-dimensional protein map of Chinese hamster ovary cells.* Electrophoresis, 1999. **20**(4-5): p. 994-1000.

100. Paula Meleady, M.H., Patrick Gammell, Padraig Doolan, Martin Sinacore, Mark Melville, Linda Francullo, Mark Leonard , Timothy Charlebois , Martin Clynes, *Proteomic profiling of CHO cells with enhanced rhBMP-2 productivity following co-expression of PACEsol.* Proteomics, 2008. **8**: p. 1-14.

101. Hayduk, E.C., LH; Lee, KH, *A two-dimensional electrophoresis map of Chinese hamster ovary cell proteins based on fluorescence staining.* ELECTROPHORESIS, 2004. **25**(15): p. 2545-2556.

102. Joon Chong Yee, M.d.L.G., Robin J. Philp, Miranda Yap, Wei-Shou Hu, *Genomic and proteomic exploration of CHO and hybridoma cells under sodium butyrate treatment.* Biotechnology and Bioengineering, 2007. **99**(5): p. 1186-1204.

103. Meleady P, H.M., Gammell P, Doolan P, Sinacore M, Melville M, Francullo L, Leonard M, Charlebois T, & Clynes M., *Proteomic profiling of CHO cells with enhanced rhBMP-2 productivity following co-expression of PACEsol.* Proteomics, 2008. **8**(13): p. 2611-2624.

104. Christine Stadelmann, H.L., *Detection of apoptosis in tissue sections.* Cell Tissue Res., 2000. **301**(1): p. 19-31.

105. death, M.f.o.c., *Morphological features of cell death.* News in Physiological Scienses, 2004. **19**: p. 124-128.

106. K.H. Moley, M.M.M., *Glocose transport and apoptosis.* Apoptosis, 2000. **5**: p. 99-105.

107. S. Grunewald, M.R., V. Blumenauer, A. F. Hmeidan, H.-J. Glander, U. Paasch, *Effects of post-density gradient swim-up on apoptosis signalling in human spermatozoa.* andrologia, 2010. **42**(2): p. 127-131.

108. treatment, H.-i.c.d.P.a.p.o.t.u.a.a.g., *Hormone-induced cell death. Purification ad properties of thymocytes undergoing apoptosis after glucocorticoid treatment.* The American Journal of Pathology, 1982. **109**(1): p. 78-87.

109. Chosy EJ, N.M., Melnik K, Comella K, Lasky LC, Zborowski M, Chalmers JJ, *Characterization of antibody binding to three cancer-related antigens using flow cytometry and cell tracking velocimetry.* Biotechnology and Bioengineering, 2003. **82**(3): p. 340-351.

110. Lee GM, S.J., Palsson BO., *Serum can act as a shear protecting agent in agitated hybridoma cell cultures.* Hybridoma, 1989. **8**(6): p. 639-645.

111. D. A. Schiemann, M.R.C., Pamela J. Swanz, *Surface properties of Yersinia species and epithelial cell interactions in vitro by a method measuring total associated, attached and intracellular bacteria.* Journal of Medical Microbiology, 1987. **24**: p. 205-218.

112. James Searles, P.T., Dhinakar Kompala, *Viable Cell Recycle with an Inclined Settler in the Perfusion Culture of Suspended Recombinant Chinese Hamster Ovary Cells.* Biotechnology Progress, 1994. **10**(2): p. 198-206.

113. A. A. Vereninov, V.E.Y.a.A.A.R., *The Role of Potassium, Potassium Channels, and Symporters in the Apoptotic Cell Volume Decrease: Experiment and Theory* Biomedical and Life Sciences. Vol. 398. 2004.

114. Glander HJ, S.J., Süss R, Paasch U, Grunewald S, Arnhold J., *Deterioration of spermatozoal plasma membrane is associated with an increase of sperm lyso-phosphatidylcholines.* Andrologia, 2002. **34**(6): p. 360-366.

115. Wu CH, H.Y., Tsai CY, Wang YJ, Tseng H, Wei PL, Lee CH, Liu RS, and Lin SY *In vitro and in vivo study of phloretin-induced apoptosis in human liver cancer cells involving inhibition of type II glucose transporter.* International Journal of Cancer, 2009. **124**(9): p. 2210.

116. Maggie M-Y Chi, J.P., Mary Carayannopoulos and Kelle H. Moley, *Decreased Glucose Transporter Expression Triggers BAX-dependent Apoptosis in the*

Murine Blastocyst. The Journal of biological chemistry, 2000. **275**: p. 40252-40257.

117. Chenhui Zoua, Y.W., Zhufang Shen, *2-NBDG as a fluorescent indicator for direct glucose uptake measurement* Journal of Biochemical and Biophysical Methods, 2005. **64**(3): p. 207-215.

118. Dimitriadis G, M.E., Boutati E, Psarra K, Papasteriades C, Raptis SA., *Evaluation of glucose transport and its regulation by insulin in human monocytes using flow cytometry.* Cytometry A, 2005. **64**(1): p. 27-33.

119. Sheth RA, J.L., Mahmood U., *Evaluation and clinically relevant applications of a fluorescent imaging analog to fluorodeoxyglucose positron emission tomography.* Journal of Biomedical Optics, 2009. **14**(6): p. 064014.

120. Arvind Natarajan, F.S., *Dynamics of Glucose Uptake by Single Escherichia coli Cells.* Metabolic Engeering, 1999. **1**(4): p. 320-333.

121. Katsuya Yamada, M.S., Hideaki Matsuoka & Nobuya Inagaki, *A real-time method of imaging glucose uptake in single, living mammalian cells.* Nature Protocols, 2007. **2**: p. 753-762.

122. Barros LF, B.C., Loaiza A, Ruminot I, Larenas V, Moldenhauer H, Oyarzún C, Alvarez M., *Kinetic validation of 6-NBDG as a probe for the glucose transporter GLUT1 in astrocytes.* Journal of Neurochemistry, 2009. **109**(Suppl 1): p. 94-100.

123. Ki-Bong Oh, H.M., *Rapid viability assessment of yeast cells using vital staining with 2-NBDG, a fluorescent derivative of glucose.* International Journal of Food Microbiology, 2002. **76**(1-2): p. 47-53.

124. Ursula Banning, H.B., Christine Mauz-Körholz, Regine Kluge, Dieter Körholz, Osama Sabri, *Effect of drug-induced cytotoxicity on glucose uptake in*

Hodgkin's lymphoma cells. European Journal of haematology, 2006. **77**(2): p. 102-108.

125. Chi-hsien liu, L.-H.C., *Enhanced recombinant M-CSF production in CHO cells by glycerol addition: model and validation* Cytotechnology, 2007. **54**(2): p. 89-96.

126. Stephen R. Fox, U.A.P., Miranda G. S. Yap, Daniel I. C. Wang, *Maximizing interferon-gamma production by Chinese hamster ovary cells through temperature shift optimization: experimental and modeling.* Biotechnology and Bioengineering, 2004. **85**(2): p. 177-184.

127. C. Altamirano, C.P., *Improvement of CHO Cell Culture Medium Formulation: Simultaneous Substitution of Glucose and Glutamine.* Biotechnology Progress, 2000. **16**: p. 69-75.

128. Savinell JM, P.B., *Network analysis of intermediary metabolism using linear optimization. I. Development of mathematical formalism.* Journal of Theorertical Biology 1992. **154**(4): p. 421.

129. Savinell JM, P.B., *Network analysis of intermediary metabolism using linear optimization. II. Interpretation of hybridoma cell metabolism.* Journal of Theorertical Biology 1992. **154**(4): p. 455-473.

130. Zupke C, S.A., Stephanopoulos G., *Intracellular flux analysis applied to the effect of dissolved oxygen on hybridomas.* Applied Mocrobiology and Biotechnology, 1995. **44**(1-2): p. 27-36.

131. Altamirano C, I.A., Casablancas A, Gámez X, Cairó JJ, Gòdia C., *Analysis of CHO cells metabolic redistribution in a glutamate-based defined medium in continuous culture.* Biotechnology Progress, 2001. **17**(6): p. 1032-1041.

132. Europa AF, G.A., Fu PC, Hu WS., *Multiple steady states with distinct cellular metabolism in continuous culture of mammalian cells.* Biotechnology and Bioengineering, 2000. **67**(1): p. 25-34.

133. Altamirano C, C.J., Gòdia F., *Decoupling cell growth and product formation in Chinese hamster ovary cells through metabolic control.* Biotechnology and Bioengineering, 2001. **76**(4): p. 351-360.

134. Agnes Provost, G.B., S. N. Agathos, Y. -J. Schneider, *Metabolic design of macroscopic bioreaction models: application to Chinese hamster ovary cells.* Bioprocess And Biosystem Engineering, 2006. **29**(5): p. 349-366.

135. Salway, J., *Metabolism at a glance*. 1999, Oxford: Blackwell Publishers.

136. Altamirano C, P.C., Illanes A, Cairó JJ, Gòdia F, *Strategies for fed-batch cultivation of t-PA producing CHO cells: substitution of glucose and glutamine and rational design of culture medium.* Journal of Biotechnology, 2004. **110**(2): p. 171-179.

137. Tsao YS, C.A., Condon RG, Voloch M, Lio P, Lagos JC, Kearns BG, Liu Z., *Monitoring Chinese hamster ovary cell culture by the analysis of glucose and lactate metabolism.* Journal of Biotechnology, 2005. **118**(3): p. 316-327.

138. Brian S. Majors, M.J.B., and Gisela G. Chiang, *Links between metabolism and apoptosis in mammalian cells: Applications for anti-apoptosis engineering* Metabolic Engineering, 2007. **9**(4): p. 317-326.

139. Neelanjan Sengupta, S.T.R., John A. Morgan, *Metabolic flux analysis of CHO cell metabolism in the late non-growth phase.* Biotechnology and Bioengineering, 2010. **108**(1): p. 82-92.

140. Teixeira A, C.A., Clemente JJ, Moreira JL, Cruz HJ, Alves PM, Carrondo MJ, Oliveira R., *Modelling and optimization of a recombinant BHK-21 cultivation process using hybrid grey-box systems.* Journal of Biotechnology, 2005. **118**: p. 290-303.

141. Deshpande, R.R., *Mammalian Cell Culture: High Throughput applications of Oxygen Sensor Plates and Cellular Physiological Studies Using 13C-Labeling*, in

Biochemical Engineering Institute. 2007, Saarland University: Saarbrücken,Germany.

142. László G. Boros, M.C., Wai-Nang Paul Lee, *Metabolic profiling of cell growth and death in cancer: applications in drug discovery.* Drug Discovery Today, 2002. **7**(6): p. 364-372.

143. Sybille Mazurek , C.B.B., Ferdinand Hugo, Erich Eigenbrodt, *Pyruvate kinase type M2 and its role in tumor growth and spreading.* Seminars in Cancer Biology 2005. **15**: p. 300-308.

144. Matthew G. Vander Heiden, L.C.C., and Craig B. Thompson, *Understanding the Warburg Effect: The Metabolic Requirements of Cell Proliferation.* Science, 2009. **324**: p. 1029-1033.

145. László G. Boros, N.J.S., Marta S. Cascante,Wai-Nang Paul Lee, *Use of metabolic pathway flux information in targeted cancer drug design* Drug Discovery Today: Therapeutic Strategies, 2004. **1**(4): p. 435-443.

146. Laurent Simon, M.N.K., *Control of starvation-induced apoptosis in Chinese hamster ovary cell cultures.* Biotechnology and Bioengineering, 2002. **78**(6): p. 645-657.

147. Nika N. Danial, C.F.G., Luca Scorrano, Chen-Yu Zhang, Stefan Krauss, Ann M. Ranger, Sandeep Robert Datta, Michael E. Greenberg, Lawrence J. Licklider, Bradford B. Lowell, Steven P. Gygi, Stanley J. Korsmeyer, *BAD and glucokinase reside in a mitochondrial complex that integrates glycolysis and apoptosis.* Nature Biotechnology, 2003. **424**: p. 952-956.

148. Yuxing Zhao, B.J.A., Jonathan L. Coloff, Catherine E. Herman, Sarah R. Jacobs, Heather L. Wieman, Jessica A. Wofford, Leah N. Dimascio, Olga Ilkayeva, Ameeta Kelekar, Tannishtha Reya, Jeffrey C. Rathmell, *Glycogen Synthase Kinase 3{alpha} and 3ß Mediate a Glucose-Sensitive Antiapoptotic Signaling*

Pathway To Stabilize Mcl-1. Molecular and Cellular Biology, 2007. **27**(2): p. 4328-4339.

149. Claudia Zwingmann, M.B., *Metabolic insights into the hepatoprotective role of N-acetylcysteine.* Hepatology, 2006. **43**(3): p. 454-463.

150. Weckwerth, W., *Metabolomics: Methods and Protocols.* Methods in molecular biology, ed. J.M. Walker. 2007: Humana Press.

151. A. Miccheli, A.T., C. Puccetti, M. Valerio, G. Peluso, F. Tuccillo, M. Calvani, C. Manetti, F. Conti,, *Metabolic profiling by 13C-NMR spectroscopy: [1,2-13C2]glucose reveals a heterogeneous metabolism in human leukemia T cells.* Biochimie, 2006. **88**(5): p. 437-448.

152. Lake-Ee Quek, S.D., Jens O. Kröme, Lars K. Nielsen, *Metabolic flux analysis in mammalian cell culture* Metabolic Engineering, 2009. **article in press**.

153. Christian M. Metallo, J.L.W., Gregory Stephanopoulos, *Evaluation of 13C isotopic tracers for metabolic flux analysis in mammalian cells.* Journal of Biotechnology, 2009. **144**(3): p. 167-174.

154. Chetan Goudar, Richard Biener, C. Boisart, Rüdiger Heidemann, James Piret, Albert de Graaf, Konstantin Konstantinov, *Metabolic flux analysis of CHO cells in perfusion culture by metabolite balancing and 2D [13C, 1H] COSY NMR spectroscopy* Metabolic Engeering, 2009. **Article in press**.

Appendix A. Model Development for Flux Analysis

The metabolic reaction network was constructed as described in section7.2. In the case of healthy cells, cell growth reaction was used. However, in the case of apoptotic cells, cells don't grow and some of DNA will be damaged during the process of apoptosis. Subsequently, apoptotic bodies will be formed. A reaction of apoptotic complex was induced. Only one reaction $v_{78(a)}$ or $v_{78(b)}$ was used at a time. Biomass $v_{78(a)}$ was used in healthy model and apoptotic complex $v_{78(b)}$ was used in apoptotic model. v_{79} and intermediate Damaged DNA were used only in apoptotic model. In both cases, the degrees of freedom were 27.

Cytosol Membrane Transport

1 GLC(ex) →GLC
2 ALA(ex)+1/3 ATP↔ALA
3 ARG(ex) +1/3 ATP ↔ARG +1/3 ADP
4 ASN(ex) +1/3 ATP ↔ASN+1/3 ADP
5 ASP(ex) +ATP ↔ASP+ ADP
6 CYS(ex) +1/3 ATP ↔CYS+1/3 ADP
7 GLU(ex)+ATP↔GLU+ADP
8 GLY(ex) ↔GLY
9 HIS(ex) +1/3 ATP ↔HIS+1/3 ADP
10 ILE(ex) +1/3 ATP ↔ILE+1/3 ADP
11 LEU(ex) +1/3 ATP ↔LEU+1/3 ADP
12 LYS(ex) +1/3 ATP ↔LYS+1/3 ADP
13 MET(ex) +1/3 ATP ↔MET+1/3 ADP
14 PHE(ex) +1/3 ATP ↔PHE+1/3 ADP
15 PRO(ex) +1/3 ATP ↔PRO+1/3 ADP
16 SER(ex) +1/3 ATP ↔SER+1/3 ADP
17 THR(ex) +1/3 ATP ↔THR+1/3 ADP
18 TRP(ex) +1/3 ATP ↔TRP+1/3 ADP
19 TYR(ex) +1/3 ATP ↔TYR+1/3 ADP
20 VAL(ex) +1/3 ATP ↔VAL+1/3 ADP
21 LAC→LAC(ex)
22 NH3→NH3(ex)
23 CO2→CO2(ex)

Glycolysis

24 GLC+ATP→ADP+G6P
25 G6P ↔F6P
26 F6P + ATP ↔ 2GAP+ADP
27 ADP+GAP+NAD+→ATP+H2O +NADH+PEP
28 ADP+PEP→ATP+PYR
29 NADH+PYR ↔LAC+NAD

Pentose Phosphate pathway

30 G6P + 2NADP+ → 2NADPH + CO2 + R5P
31 2R5P → GAP + S7P
32 GAP + S7P → E4P + F6P
33 X5P + E4P → F6P + GAP

Mitochndrial Transport

34 PYR ↔PYR(m)
35 MAL↔MAL(m)
36 AKG↔AKG(m)
37 MAL+CIT(m) ↔MAL(m)+CIT
38 ASP(m)+GLU ↔ASP+GLU(m)
39 GLU(c) →GLU(m)

Anaplerotic reactions

40 PYR(m)+NAD(m) →AcCoA(m) +CO2+NADH(m)
41 MAL+NADP→CO2+NADPH+PYR
42 MAL(m)+NADP(m) →CO2+NADPH(m)+PYR(m)
43 OAA+ATP→PEP+ADP+CO2
44 PYR(m)+CO2+ATP(m)↔OAA(m)+ADP(m)

TCA cycle

45 AcCoA (m)+ OAA(m)→CIT(m)
46 CIT(m)+NAD(m) →AKG(m)+ CO2+NADH(m)
47 AKG(m)+NAD(m) →SUCCoA(m)+CO2+NADH(m)
48 GDP(m)+SUCCoA(m)+FAD(m)→FUM(m)+FADH2(m)+GTP(m)
49 FUM(m)+H2O↔MAL(m)
50 MAL(m)+NAD(m) →OAA(m)+NADH(m)
51 MAL+NAD →OAA+NADH

Amino acid metabolism

52 ARG+AKG+NAD ↔2GLU(c)+NADH(c)+CO2+ NH4+
53 ASN↔ASP+NH4+
54 ASP+AKG ↔OAA+GLU
55 ASP(m)+AKG(m) ↔OAA(m)+GLU(m)
56 CYS+AKG→PYR+GLU+ NH4+
57 GLN↔GLU+ NH4+
58 GLU(m)+NADP+(m) →AKG(m)+NADPH(m)+ NH4+
59 GLU+PYR ↔AKG+ALA
60 2GLY+NAD+→SER+NADH+CO2+ NH4+
61 HIS+NAD+→GLU+CO2+NH4++NADH
62 ILE+AKG+ATP(m)+NAD+(m)+FAD+(m)→GLU+AcCoA(m)+NADH(m)+FADH(m)+SUCCoA(m)+ADP(m)
63 LEU+AKG+ATP(m)+FAD+(c)→GLU+3AcCoA(m)+FADH2(m)+ADP(m)
64 LYS+AKGNADPH+2NAD++2NAD+(m)+FAD(m)→2GLU+2CO2+2AcCoA(m)+2NADH(m)+2NADH+FADH2(m)+NADP+(m)
65 MET+SER+3ATP+ATP(m)+NAD+(m)→CYS+SUCCoA(m)+CO2+NH4++3ADP+ADP(m)+NADH(m)
66 PHE+NADPH→TYR+NADP+
67 PRO+2NAD+↔GLU+2NADH

68 SER→NH4+ +PYR

69 THR+NAD(m)+FAD(m)+NAD→PYR(m)+FADH2(m)+NH4++NADH(m)+CO2

70 TRP+2NAD+(m)+FAD+(m)+NADPH→ALA+4CO2+2AcCoA(m)+ NH4++2NADH(m)+FADH2(m)+NADP+

71 TYR+AKG→MAL+CO2+2AcCoA+GLU

72 VAL+AKG+ 2NAD+(m)+FAD+(m)→SUCCoA(m)+GLU+ 2NADH(m)+FADH2(m) +CO2

Other reactions

73 CIT+ATP↔AcCoA+OAA+ADP

Synthesis of Macromolecules(DNA, RNA, carbohydrates,lipid and Protein)

74 R5P+1.295 ASP + 0.5 GLY+1.41 GLN+4.7 ATP→ 1.41 GLU+ DNA +0.205 FUM(m) + 4.7ADP

75 R5P+1.24 ASP+0.5 GLY+1.76 GLN+4.67 ATP→ RNA+1.76 GLU + FUM(m)+4.67 ADP

76 G6P+3.5 ATP→TC+3.5 ADP

77 0.75 GAP + 0.193 SER + 17 ATP + 9 NADH + 17 NADPH + 17.8 AcCoA→ lipid + 17 ADP + 9 NAD + 17 NADP
0.095 ALA + 0.063 ARG + 0.039 ASN + 0.048 ASP + 0.028 CYS + 0.052 GLN + 0.064 GLU + 0.078 GLY + 0.022 HIS + 0.052 ILE + 0.088 LEU + 0.089 LYS + 0.02 MET + 0.021 PHE + 0.028 PRO + 0.057 SER + 0.061 THR + 0.006 TRP + 0.02 TYR + 0.059 VAL + 4 ATP → protein + 4 ADP

Synthesis of biomass

78 0.00844 DNA + 0.0246 RNA + 0.8932 protein + 0.01467 lipid + 0.059 TC → CELL

Internal balanced metabolites

No.	Internal metabolite	No.	Internal metabolite	No.	Internal metabolite
1	AcCoA	19	GAP	37	PEP
2	AcCoA(m)	20	GLC	38	PHE
3	AKG	21	GLN	39	PRO
4	AKG(m)	22	GLU	40	Protein
5	ALA	23	GLU(m)	41	PYR
6	ARG	24	GLY	42	PYR(m)
7	ASN	25	GLY(m)	43	R5P
8	ASP	26	HIS	44	RNA
9	ASP(m)	27	ILE	45	S7P
10	CIT	28	LEU	46	SER
11	CIT (m)	29	Lipid	47	SER(m)
12	CO2	30	LYS	48	SucCoA(m)
13	CYS	31	MAL	49	TC
14	DNA	32	MAL(m)	50	HHR
15	E4P	33	MET	51	TRP
16	F6P	34	NH4	52	TYR
17	FUM(m)	35	OAA	53	VAL

18	G6P	36	OAA(m)	54	X5P

Balance of energetic cofactors

As is it documented in the literature, energetic cofactors ATP, NAD(P)H and FADH2 cannot be regarded as internal balanced metabolites. Assuming that 1 mol of NAD(P)H yields 2.5 mol of ATP, 1 mol of FADH2 yields 1.5 mol of ATP and 1 mol GTP equals 1 mol of ATP , the respiration reactions are considered as:

$$2.5ADP(m)+NADH(m)\rightarrow 2.5ATP(m)+NAD(m)$$
$$1.5ADP(m)+FADH2(m)\rightarrow 1.5ATP(m)+FAD(m)$$

Healthy Model

The metabolism of CHO cells considered in the healthy condition has 78 reactions and 54 balanced intermediates. The 20 extracellular metabolites present in the medium which are either nutrients or byproducts of excretion were measured. However, the system of flux analysis is underdetermined, with commonly available measurements in our research. Linear programming was used to reduce the range of solution. The objective function is maximization of cell growth rate.

Apoptotic Model

In this case, 77 reactions and 54 balanced intermediates were used. In order to reduce degrees of freedom and to characterize the feasible set of solutions using the extracellular measurements only, some additional constraints and assumptions were used.

1) No catabolism of threonine, that is v_{69} is 0. Zamorano et al[1]applied this assumption to study metabolic flux analysis of an

underdetermined network of CHO cells. Since threonin catabolism utilizes serine hydroxymethtrasferase (SHMT) to generate Acetyl-CoA and glycine. In apoptotic condition, glycine shows negative uptake behavior indicating that threonine catabolism is not active and the uptake of threonine works for the cellular macromolecule synthesis.

2) No Phospoenolpyruvate carboxkinase (PEPCK) activity. FBA result in healthy cells shows that reaction v_{43} is 0. Also as is it reported in literature, the short or lack of PEPCK exists in various mammalian cell lines, such as CHO, hybridoma, and BHK cell lines[2-4]. In apoptotic condition, v_{43} is imposed as 0.

3) Zamaraeva et al argued that cell undergoing apoptosis exhibit an increase in cytosolic ATP with little increase in total cellular ATP[5]. ATP/ADP exchange allows ATP to move out of the mitochondria and ADP to move in. Vander et al reported that an early event in apoptosis is a defect in mitochondrial ATP/ADP exchange and growth factor withdrawal leads to a decline in cellular ATP stores and a concomitant increase in cytosolic ADP[6]. The mitochondrial ATP/ADP exchange reaction: ATP(m)+ADP ←→ATP+ADP(m) was selected as objection function. Minimizing this will reduce the total cellular ATP and increase the ratio of cytosolic ATP to cellular ATP, having a good agreement with literature mentioned above. Also the minimum of the mitochondrial ATP/ADP exchange also describes mitochondrial dysfunction.

Abbreviation	Description
(c)	Cytosolic
(m)	Mitochondrial
AcCoA	Acetyl Coenzyme A
ADP	Adenosine diphosphate
AKG	-Ketoglutarate
ALA	Alanine
AMP	Adenosine monophosphate
ARG	Arginine
ASN	Asparagine
ASP	Aspartate
ATP	Adenosine triphosphate
CIT	Citrate
CoA	Coenzyhme A
CO2	Carbondioxide
CYS	Cysteine
E4P	Erythrose-4-phosphate
F6P	Fructose-6-phosphate
F1,6P	Fructose-1, 6-biphosphate
FAD(H2)	Falvine adenosine dinucleotide (reduced)
FUM	Fumarate
G6P	Glucose 6-phosphate
GLC	Glucose
GLN	Glutamine
GLU	Glutamate
GLY	Glycine
HIS	Histidine
LAC	Lactate
ILE	Isoleucine
LEU	Leucine
LYS	Lysine
MAL	Malate
MET	Methionine
NAD(H)	Nicotinamide adenine dinucleotide (reduced)
NADP(H)	Nicotinamide adenine dinucleotide phosphate (reduced)
NH4+	Ammonium
OAA	Oxaloacetate
PEP	Phosphoenolpyruvate
PHE	Phenylalanine
Pi	Orthophosphate
PRO	Proline
PYR	Pyruvate
R5P	Ribose 5-phosphate
RNA	Average RNA bound nucleic acid (mol. wt. 325.39)

S7P	Sedoheptulose-7-phosphate
SER	Serine
SUC	Succinate
SucCoA	Succinyhl coenzyme A
THR	Threonine
TRP	Tryptophan
TYR	Tyrosine
VAL	Valine
X5P	Xylulose 5-phosphate

1. Zamorano F, W.A., Bastin G., *A detailed metabolic flux analysis of an underdetermined network of CHO cells.* Journal of Biotechnology, 2010. **150**(4): p. 497-508.
2. Sadettin S. Ozturk, W.-s.H., *Cell culture Technology for Pharmaceutical and Cell-based Therapies.* 2005: Taylor &Francis.
3. Fitzpatrick L, J.H., Butler M. , *Glucose and glutamine metabolism of a B-lymphocyte hybridoma grown in batch culture.* Appl Biochem Biotechnol, 1993. **43**(2): p. 93-116.
4. Zupke C, S.A., Stephanopoulos G., *Intracellular flux analysis applied to the effect of dissolved oxygen on hybridomas.* Applied Mocrobiology and Biotechnology, 1995. **44**(1-2): p. 27-36.
5. M V Zamaraeva, R.Z.S., E Maeno, Y Ando-Akatsuk, S V Bessonova, Y Okada, *Cells die with increased cytosolic ATP during apoptosis: a bioluminescence study with intracellular luciferase.* Cell Death and Differentiation, 2005. **12**(1390-1397).
6. Vander Heiden MG, C.N., Schumacker PT, Thompson CB., *Bcl-xL prevents cell death following growth factor withdrawal by facilitating mitochondrial ATP/ADP exchange.* Molecular Cell, 1999. **3**(2): p. 159-167.

Appendix B Biomass Composition

The biomass composition of the CHO TF 70R cells was taken from resource of [1], and is given as follows. The dry weight of cell was 320μg/10^6 cells

Macromolecules	Molar Fraction	Average MW
Proteins	70.6%	108[1]
Lipids	7.7%	717[2]
DNA	1.9%	307.5[3]
RNA	5.8%	321.6[3]
carbohydrates	7.0%	162[2]

The amino acid composition of cellular proteins

The average molecular weight was calculated to be 108 from the molar fraction of amino acids

Amino Acid	Molar Fraction	Amino Acid	Molar Fraction
ALA	0.95%	LEU	0.88%
ARG	0.63%	LYS	0.89%
ASP	0.48%	MET	0.20%
ASN	0.39%	PHE	0.21%
CYS	0.28%	PRO	0.28%
GLN	0.52%	SER	0.57%
GLU	0.64%	THR	0.61%
GLY	0.78%	TRP	0.06%
HIS	0.22%	TYR	0.20%
ILE	0.52%	VAL	0.59%

1. Altamirano C, I.A., Casablancas A, Gámez X, Cairó JJ, Gòdia C., *Analysis of CHO cells metabolic redistribution in a glutamate-based defined medium in continuous culture.* Biotechnology Progress, 2001. **17**(6): p. 1032-1041.

2. Deshpande, R.R., *Mammalian Cell Culture: High Throughput applications of Oxygen Sensor Plates and Cellular Physiological Studies Using 13C-Labeling*, in *Biochemical Engineering Institute.* 2007, Saarland University: Saarbrücken,Germany.

3. Lander ES, L.L., Birren B, Nusbaum C, Zody MC, Baldwin J, Devon K, Dewar K, Doyle M, FitzHugh W, Funke R, Gage D, Harris K, Heaford A, Howland J, Kann L, Lehoczky J, LeVine R, McEwan P, McKernan K, Meldrim J, Mesirov JP, Miranda C, Morris W, Naylor J, Raymond C, Rosetti M, Santos R, Sheridan A, Sougnez C, Stange-Thomann N, Stojanovic N, Subramanian A, Wyman D, Rogers J, Sulston J, Ainscough R, Beck S, Bentley D, Burton J, Clee C, Carter N, Coulson A, Deadman R, Deloukas P, Dunham A, Dunham I, Durbin R, French L, Grafham D, Gregory S, Hubbard T, Humphray S, Hunt A, Jones M, Lloyd C, McMurray A, Matthews L, Mercer S, Milne S, Mullikin JC, Mungall A, Plumb R, Ross M, Shownkeen R, Sims S, Waterston RH, Wilson RK, Hillier LW, McPherson JD, Marra MA, Mardis ER, Fulton LA, Chinwalla AT, Pepin KH, Gish WR, Chissoe SL, Wendl MC, Delehaunty KD, Miner TL, Delehaunty A, Kramer JB, Cook LL, Fulton RS, Johnson DL, Minx PJ, Clifton SW, Hawkins T, Branscomb E, Predki P, Richardson P, Wenning S, Slezak T, Doggett N, Cheng JF, Olsen A, Lucas S, Elkin C, Uberbacher E, Frazier M, Gibbs RA, Muzny DM, Scherer SE, Bouck JB, Sodergren EJ, Worley KC, Rives CM, Gorrell JH, Metzker ML, Naylor SL, Kucherlapati RS, Nelson DL, Weinstock GM, Sakaki Y, Fujiyama A, Hattori M, Yada T, Toyoda A, Itoh T, Kawagoe C, Watanabe H, Totoki Y, Taylor T, Weissenbach J, Heilig R, Saurin W, Artiguenave F, Brottier P, Bruls T, Pelletier E, Robert C, Wincker P, Smith DR, Doucette-Stamm L, Rubenfield M, Weinstock K, Lee HM, Dubois J, Rosenthal A, Platzer M, Nyakatura G, Taudien S, Rump A, Yang H, Yu J, Wang J, Huang G, Gu J, Hood L, Rowen L,

Madan A, Qin S, Davis RW, Federspiel NA, Abola AP, Proctor MJ, Myers RM, Schmutz J, Dickson M, Grimwood J, Cox DR, Olson MV, Kaul R, Raymond C, Shimizu N, Kawasaki K, Minoshima S, Evans GA, Athanasiou M, Schultz R, Roe BA, Chen F, Pan H, Ramser J, Lehrach H, Reinhardt R, McCombie WR, de la Bastide M, Dedhia N, Blöcker H, Hornischer K, Nordsiek G, Agarwala R, Aravind L, Bailey JA, Bateman A, Batzoglou S, Birney E, Bork P, Brown DG, Burge CB, Cerutti L, Chen HC, Church D, Clamp M, Copley RR, Doerks T, Eddy SR, Eichler EE, Furey TS, Galagan J, Gilbert JG, Harmon C, Hayashizaki Y, Haussler D, Hermjakob H, Hokamp K, Jang W, Johnson LS, Jones TA, Kasif S, Kaspryzk A, Kennedy S, Kent WJ, Kitts P, Koonin EV, Korf I, Kulp D, Lancet D, Lowe TM, McLysaght A, Mikkelsen T, Moran JV, Mulder N, Pollara VJ, Ponting CP, Schuler G, Schultz J, Slater G, Smit AF, Stupka E, Szustakowski J, Thierry-Mieg D, Thierry-Mieg J, Wagner L, Wallis J, Wheeler R, Williams A, Wolf YI, Wolfe KH, Yang SP, Yeh RF, Collins F, Guyer MS, Peterson J, Felsenfeld A, Wetterstrand KA, Patrinos A, Morgan MJ, de Jong P, Catanese JJ, Osoegawa K, Shizuya H, Choi S, Chen YJ; International Human Genome Sequencing Consortium., *Initial sequencing and analysis of the human genome.* Nature, 2001. **409**: p. 860-921.